

MODULATION OF MEDIAL ENTORHINAL CORTEX LAYER II  
CELL CIRCUITRY BY STRESS HORMONES

AN ABSTRACT

SUBMITTED ON THE TWENTY FIFTH DAY OF OCTOBER 2017

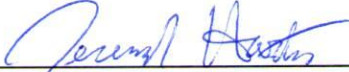
TO THE TULANE UNIVERSITY BRAIN INSTITUTE  
IN PARTIAL FULFILLMENT OF THE REQUIREMENTS  
OF THE SCHOOL OF SCIENCE AND ENGINEERING  
OF TULANE UNIVERSITY

FOR THE DEGREE

OF

DOCTOR OF PHILOSOPHY

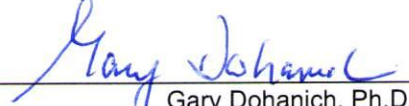
BY

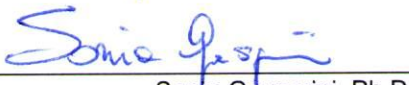
  
JEREMIAH HARTNER

Approved:

  
Laura Schrader, Ph.D., Advisor

  
Jeffrey Tasker, Ph.D.

  
Gary Dohanich, Ph.D.

  
Sonja Gasparini, Ph.D.

## ABSTRACT

Stress can cause spatial memory deficits in males, but the underlying mechanisms affecting the known memory pathways remain unclear. Spatial memory processing requires functional interaction between the hippocampus and the medial entorhinal cortex (MEC). The grid cells of the MEC are most abundant in layer II and rely on a complex network of local inhibitory interneurons to generate spatial firing properties, but the effects of stress on this region have not been studied. Stress activates both the autonomic nervous system and the hypothalamic-pituitary-adrenal axis to release norepinephrine (NE) and glucocorticoids respectively. Given that glucocorticoid receptor (GR) and adrenergic receptor (AR) expression is abundant in the MEC, both glucocorticoids and NE released in response to stress may have rapid effects on MEC-LII networks.

We used whole-cell patch clamp electrophysiology in MEC slice preparations from male mice to test the effects of glucocorticoids and NE on synaptic inputs of MEC-LII principal cells. Glucocorticoids rapidly decreased the frequency of spontaneous inhibitory postsynaptic currents (IPSCs), but not miniature IPSCs in MEC-LII principal cells. Unlike glucocorticoids, NE dramatically increased both the frequency and amplitude of spontaneous IPSCs as well as frequency of miniature IPSCs in a majority of MEC-LII principal cells. Application of NE alone increased the frequency and amplitude of sIPSCs in most principal cells of MEC-LII, but failed to modulate frequency of inhibitory signaling in ~25% of cells tested. Interestingly, pre-treatment with

dexamethasone prior to NE application led to an NE-induced increase in sIPSC frequency in all cells. This effect was mediated by the  $\alpha$ 1-AR, as application of an  $\alpha$ 1-AR agonist, phenylephrine (PHE) yielded the same results, suggesting that there is a subset of cells in MEC-LII that are unresponsive to  $\alpha$ 1-AR activation without prior activation of GR. We conclude that activation of GR primes a subset of cells that were previously insensitive to NE to become responsive to  $\alpha$ 1-AR activation in a transcription-independent manner. These findings demonstrate the ability of stress hormones to markedly alter inhibitory signaling within MEC-LII circuits and suggest the intriguing possibility of modulation of network processing upstream of the hippocampus.

MODULATION OF MEDIAL ENTORHINAL CORTEX LAYER II  
CELL CIRCUITRY BY STRESS HORMONES

A DISSERTATION

SUBMITTED ON THE TWENTY FIFTH DAY OF OCTOBER 2017

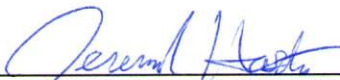
TO THE TULANE UNIVERSITY BRAIN INSTITUTE  
IN PARTIAL FULFILLMENT OF THE REQUIREMENTS  
OF THE SCHOOL OF SCIENCE AND ENGINEERING  
OF TULANE UNIVERSITY

FOR THE DEGREE

OF

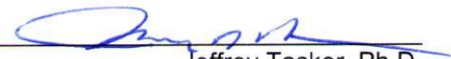
DOCTOR OF PHILOSOPHY

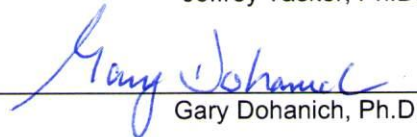
BY

  
JEREMIAH HARTNER

Approved:

  
Laura Schrader, Ph.D., Advisor

  
Jeffrey Tasker, Ph.D.

  
Gary Dohanich, Ph.D.

  
Sonia Gasparini, Ph.D.

**© Copyright by Jeremiah Hartner, 2017**

**All Rights Reserved**

## **ACKNOWLEDGMENTS**

This thesis is the result of more than six years of work, which was only made possible by an incredible amount of support. First, I'd like to express my sincere gratitude to Dr. Laura Schrader. I'm especially appreciative that she allowed me to explore my own ideas and venture into the medial entorhinal cortex. I'm not only grateful for her continuous support and mentoring throughout my time in her lab, but also for the excitement with which she approached my projects.

I'd also like to thank the members on my committee: Dr. Jeffrey Tasker, Dr. Gary Dohanich, and Dr. Sonia Gasparini for their insight and guidance during my qualifying exam and prospectus. Dr. Tasker's questions at each of my presentations over the past six years brought to light perspectives that have been extremely helpful for my work. And a special thanks to Dr. Dohanich for his help during my search for a postdoctoral position.

I owe an incredible debt to my colleague Allan Diankun Yu, who was a source of daily support whether it was troubleshooting problems with recordings, data analysis, or future directions. Going through this process with such a kind and helpful friend who expressed great interest in my work has made this an incredible experience. I'd also like to thank the other members of my lab,

especially Damek Homiack, Ted Sawyer, Steven Springer, and Matthieu Maroteaux, who have not only been a great help in my research, but provided a great lab environment in which to work.

The love and support from my family over the course of my education has been invaluable and given me the courage to pursue a career in science. Most importantly, I'd like to thank my wife, Lynaya, for her endless support, patience, and confidence in me throughout this process. Without her, this work would not have been possible.

## TABLE OF CONTENTS

ACKNOWLEDGMENTS.....	ii
LIST OF TABLES AND FIGURES.....	vi

### CHAPTER 1: INTRODUCTION

Introduction.....	2
Stress Overview.....	3
Sympathetic Nervous System Overview.....	4
HPA Axis.....	5
Activation and Modulation of HPA Axis During Stress.....	6
Corticosteroid Receptors.....	7
Navigation and Spatial Memory.....	9
Spatial Processing in Individual Cells.....	10
Implication of MEC Dysfunction in Disease.....	12
Connectivity of Spatial Memory Processing Regions.....	13
Lateral versus Medial Entorhinal Cortex.....	19
MEC – LII Principal Cell Types and Electrophysiological Properties.....	20
Layer II Afferents and Efferents.....	23
Network Models.....	23
Theta Oscillation in Spatial Processing Regions.....	24
Theta and Gamma Encoding of Space.....	26
Layer II Inhibitory Cells.....	28
Layer II Networks and Connectivity.....	28
Effect of Stress on Hippocampal-Dependent Memory.....	30
Effect of Stress on Hippocampal Pyramidal Cell Signaling.....	31
Adrenergic Receptor Activation in the Hippocampus.....	33
Adrenergic Receptor Activation in the Rodent Medial Entorhinal Cortex.....	35
Effect of Stress on Medial Entorhinal Cortex Circuitry.....	37

CHAPTER 2: RAPID EFFECTS OF GLUCOCORTICOIDS ON SYNAPTIC SIGNALING IN MEDIAL ENTORHINAL CORTEX LAYER II PRINCIPAL CELLS

Introduction ..... 40  
Methods ..... 43  
Results ..... 47  
Discussion ..... 60

CHAPTER 3: ACTIVATION OF GLUCOCORTICOID RECEPTORS IN LAYER II OF THE MEDIAL ENTORHINAL CORTEX REVEALS ENHANCED NOREPINEPHRINE-MEDIATED INHIBITORY SIGNALING

Introduction ..... 63  
Methods ..... 69  
Results ..... 74  
Discussion ..... 102

CHAPTER 4: CONCLUSIONS

Conclusions ..... 108

LIST OF REFERENCES ..... 120

## LIST OF TABLES AND FIGURES

Figure 1.1: Excitatory Connectivity between the Entorhinal Cortex and Hippocampus. Pg.18

Figure 1.2: Chronic stress altered dendritic architecture in MEC – LII principal cells. Pg.38

Figure 2.1: Whole-cell patch clamp recording protocol in MEC – LII. Pg.46

Figure 2.2: Dexamethasone application had no effect on spontaneous excitatory signaling in MEC – LII principal cells. Pg.48

Figure 2.3: Dexamethasone had no effect on mEPSCs in MEC – LII principal cells. Pg. 49

Figure 2.4: Dexamethasone significantly decreased frequency, but not amplitude, of spontaneous inhibitory signaling in MEC – LII principal cells. Pg.52

Figure 2.5: Dexamethasone did not affect sIPSC burst behavior. Pg.53

Figure 2.6: Dose-dependent effects of dexamethasone on spontaneous IPSCs. Pg.54

Figure 2.7: Dexamethasone had no effect on terminal-specific inhibitory signaling in MEC – LII principal cells. Pg.55

Figure 2.8: Corticosterone significantly decreased frequency, but not amplitude, of spontaneous inhibitory signaling in MEC – LII principal cells. Pg.57

Table 1: Effect of glucocorticoids on frequency of excitatory and inhibitory synaptic transmission. Pg.58

Table 2: Effect of glucocorticoids on amplitude of excitatory and inhibitory synaptic transmission. Pg.58

Table 3: Effect of glucocorticoids on decay time of excitatory and inhibitory synaptic transmission. Pg.59

Figure 3.1: Experimental design timeline. Pg.73

Figure 3.2: Norepinephrine significantly increased spontaneous IPSC frequency and amplitude, but not decay time, in MEC – LII principal cells. Pg.77

Figure 3.3: Norepinephrine-sensitive cells had different intrinsic characteristics than norepinephrine-insensitive cells. Pg.78

Figure 3.4: Norepinephrine significantly increased spontaneous IPSC frequency and amplitude, but not decay time, in MEC – LII principal cells. Pg.79

Figure 3.5: Norepinephrine significantly increased miniature IPSC frequency and decay time, but not amplitude, in MEC – LII principal cells. Pg.80

Figure 3.6: Phenylephrine increased spontaneous IPSC frequency in a subset of neurons, and had no effect on amplitude or decay time. Pg.82

Figure 3.7: Phenylephrine had no effect on miniature IPSC frequency, amplitude, or decay time in MEC – LII principal cells. Pg.83

Figure 3.8: UK14304 had no effect on sIPSC frequency, amplitude, or decay time in MEC – LII principal cells. Pg.85

Figure 3.9: UK14304 had no effect on IPSC frequency or amplitude, but significantly increased miniature IPSC decay time in MEC – LII principal cells. Pg.86

Figure 3.10: Isoprenaline had no effect on sIPSC frequency, amplitude, or decay time in MEC-LII principal cells. Pg.88

Table 4: Effect of adrenergic receptor activation on IPSC frequency. Pg.89

Table 5: Effect of adrenergic receptor activation on IPSC amplitude. Pg.89

Table 6: Effect of adrenergic receptor activation on IPSC decay time. Pg.90

Figure 3.11: Effects of co-administration of dexamethasone and norepinephrine. Pg.93

Figure 3.12: Dexamethasone pre-treatment increased the proportion of MEC-LII principal cells affected by NE. Pg.94

Figure 3.13: Effects of co-administration of dexamethasone and phenylephrine. Pg.97

Table 7: Effect of PHE on sIPSC frequency. Pg.98

Table 8: Effect of PHE on sIPSC amplitude. Pg.98

Table 9: Effect of PHE on sIPSC decay time. Pg.98

Figure 3.14: Dexamethasone pre-treatment increased the proportion of MEC-LII principal cells affected by phenylephrine. Pg.99

Table 10: Effect of adrenergic receptor activation on IPSC frequency with and without Dex pre-treatment. Pg.100

Table 11: Effect of adrenergic receptor activation on IPSC amplitude with and without Dex pre-treatment. Pg.100

Table 12: Effect of adrenergic receptor activation on IPSC decay time with and without Dex pre-treatment. Pg.101

Table 13: Chi-square comparison of NE-alone versus Dex-primed NE. Pg. 101

Table 14: Chi-square comparison of PHE-alone versus Dex-primed PHE. Pg. 101

Figure 3.14: Effect of AR activation on IPSCs in MEC-LII principal cells. Pg.106

Figure 4.1: Comparison of effects of NE and PHE on sIPSC frequency, amplitude, and decay with and without Dex pre-treatment. Pg.117

Table 15: 2-way ANOVA table for normalized sIPSC frequency effect of NE and PHE with or without Dex. Pg.118

Table 16: 2-way ANOVA table for normalized sIPSC amplitude effect of NE and PHE with or without Dex. Pg.118

Table 17: 2-way ANOVA table for normalized sIPSC decay time effect of NE and PHE with or without Dex. Pg.118

Figure 4.2: Functional hypothesis for Dex-induced sensitization of NE/PHE-insensitive cells. Pg. 119

# CHAPTER 1

## INTRODUCTION

## CHAPTER 1: INTRODUCTION

### Introduction

An organism's ability to navigate through its environment is crucial for survival. Navigation in mammals requires the ability to learn, remember, and identify spatial relationships between self and other organisms or objects. Many different brain regions are responsible for processing internal, or egocentric, and distal, or allocentric, cues. Disruption of an organism's homeostasis, or stressors, can cause biological and physiological changes that lead to deficits in the processing of spatial memory cues.

A multitude of evidence has shown that both chronic and acute stress can impair a male rodent's performance on spatial memory tasks (Bowman et al., 1994; Conrad et al., 1996; Park et al., 2001; Conrad et al., 2004; Diamond et al., 1996), but the underlying mechanisms affecting the known memory pathways remain unclear. To this point, much of the research on spatial memory processing has focused on the hippocampus (HC), and research on how stress affects spatial memory processing has focused exclusively on effects of stress in the HC. In 2005, the discovery of space-encoding cells, known as grid cells, within a region of the entorhinal cortex (EC) dramatically altered the understanding of how an organism processes spatial information. This discovery has also opened an opportunity to investigate how stress could affect spatial

memory processing in an area other than the hippocampus that is now known to be an important component of spatial memory processing: layer II of the medial entorhinal cortex (MEC – LII). A better understanding of the biological underpinnings of spatial memory processing deficits due to stress is necessary to understand mechanisms that lead to neuropathologies and to identify targets for intervention in afflicted populations. A comprehensive understanding of these effects requires investigation into how stress can modulate signaling particularly within MEC – LII; however, the effects of stress on network functionality of MEC-based spatial memory systems remain unstudied.

### **Stress Overview**

Until recently, stress has been defined as any stimulus that disrupts an organism's homeostasis, while the stress response is the organism's physiological reaction to return to homeostasis (Chrousos, 2009). The stress response is considered either adaptive or maladaptive in nature, where maladaptive responses tend to occur only after prolonged exposure to stress; however, defining the stress responses as either adaptive or maladaptive has proved difficult (Koolhaas et al., 2011). It has been more recently argued that stress itself is better defined by an organism's perception that an event is either unpredictable or uncontrollable (Koolhaas et al., 2011).

Stressful stimuli simultaneously activate the hypothalamo-pituitary-adrenal (HPA) axis and the sympathetic nervous system, which act to mobilize energy

and resources in order to allow the organism to attend to the stressful event (Miller and O'Callaghan, 2002; Tsigos and Chrousos, 2002). Stress-induced activation of the autonomic nervous system is immediate and works through neural innervation of organs, resulting in rapid alterations of physiological states (Ulrich-Lai and Herman, 2009). Activation of the HPA axis is the organism's means of a sustained response following a stressor, and it causes release of glucocorticoids which can take more than ten minutes to reach peak concentration in the bloodstream and hours to return to basal levels (Droste et al, 2008; Ulrich-Lai and Herman, 2009).

### **Sympathetic Nervous System Overview**

Stress-induced activation of the sympathetic nervous system is often referred to as an organism's "fight or flight" response. The sympathetic nervous system is part of the autonomic nervous system, which is an unconscious peripheral system regulated by the hypothalamus. Activation of the sympathetic nervous system causes postganglionic neurons in the spinal cord to release a catecholamine, epinephrine/adrenaline, which acts on adrenergic receptors in the associated target organs (Malpas, 2010). Adrenergic receptors can be one of three types:  $\alpha$ -1,  $\alpha$ -2, or  $\beta$ . Each type of adrenergic receptor is G-protein coupled. The  $\alpha$ -1 receptor is coupled to  $G_q$  and activates phospholipase C to increase intracellular calcium,  $\alpha$ -2 is coupled to  $G_i$  and inhibits adenylyl cyclase production resulting in decreased levels of cyclic-AMP, and all three  $\beta$  receptors are coupled

to  $G_s$  and activate adenylyl cyclase to increase cyclic-AMP (Strosberg, 1993; O'Dell et al., 2015).

Activation of the sympathetic nervous system induces a peripheral “fight or flight” response to prepare an organism to attend to the stressor. Activation of adrenergic receptors in the target organs prepare the organism to attend to the stressor and cause a variety of responses including pupil dilation, increased blood glucose, increased heart rate, and elevated blood pressure (Tank and Lee Wong, 2015). This systemic activation causes an increase in peripheral catecholamine levels; however, epinephrine and norepinephrine do not readily cross the blood-brain barrier (Weil-Malherbe and Bone, 1957; Gold, 2014), so central nervous system activation must be achieved through vagal nerve activation. The peripheral catecholamine signal activates  $\beta$  –adrenergic receptors of the vagus nerve, which in turn activate brainstem solitary tract nuclei (NTS), and locus coeruleus (LC), to cause central norepinephrine release (Rooszendaal and McGaugh, 2011; Timmermans et al., 2013; Gold, 2014). Noradrenergic efferents from the LC and NTS regulate neuronal function in a variety of areas including those that are crucial to learning and memory: the hippocampus, prefrontal cortex, and amygdala (Gibbs and Summers, 2002; Rooszendaal et al., 2009).

### **HPA Axis**

The hypothalamic-pituitary-adrenal (HPA) axis is composed of three endocrine glands: the hypothalamus, pituitary gland, and adrenal glands. The

hypothalamus is made up of distinct nuclei including the paraventricular nucleus (PVN), which consists of parvocellular neurons that produce corticotropin-releasing hormone (CRH) and vasopressin (AVP) that can activate the pituitary gland. In response to this peptide signal from the hypothalamus, the anterior pituitary gland releases adrenocorticotropic hormone (ACTH) into the bloodstream. ACTH stimulates the adrenal cortex of the adrenal glands to produce and release corticosteroids: glucocorticoids and mineralocorticoids (de Kloet et al., 2005; Timmermans et al., 2013; Hanukoglu et al., 1990; Herman et al., 2016; Engelmann et al., 2004).

### **Activation and Modulation of HPA Axis During Stress**

Stress activates the hypothalamic-pituitary-adrenal (HPA) axis and causes release of the corticosteroid stress hormone cortisol or corticosterone, a species-specific glucocorticoid from the adrenal cortex (Miller and O'Callaghan, 2002; Engelmann, Landgraf, and Wotjak, 2004). Structural differences and alternative splicing causes species-specific differences in glucocorticoid receptor isoform expression, resulting in differential sensitivity to cortisol and corticosterone (Reul and de Kloet, 1985; Reul et al., 1990; Otto, Reichardt, and Schutz, 1997; de Kloet et al., 1998). Humans produce cortisol, while rodents produce corticosterone.

Glucocorticoid release follows a diurnal rhythm whereby the highest levels are achieved during the active phase of the light cycle (during high light for humans and darkness for rodents) and the lowest during the inactive phase

(Kalsbeek et al., 2012). Both physiological and psychological stressors drive HPA axis activation through different neural substrates. Physiological stressors activate CRH neurons in the PVN directly through relayed sensory input from visceral afferents, nociceptors, and circumventricular organs; however, limbic-associated structures can indirectly activate the CRH neurons through disinhibition of the bed nucleus of the stria terminalis (BNST) (Herman et al., 2003). Interestingly though, stress is not the only modulator of the HPA axis.

Stress-induced activation of the HPA axis causes rapid increases in circulating glucocorticoid levels, and maximum adrenal output occurs within fifteen minutes (de Kloet et al., 1998). The HPA axis, in normal circumstances, incorporates a negative feedback loop to tightly regulate the release of glucocorticoids. Almost immediately, glucocorticoids acting in the PVN cause retrograde release of endocannabinoids to inhibit pre-synaptic glutamate release and thereby decrease the excitability of CRH neurons (Di et al., 2003; Evanson et al., 2010). The BNST is rich with inhibitory relays that translate excitatory output from the prelimbic cortex and hippocampus into inhibition of the PVN, which can also cause cessation of the HPA response (Cullinan, Herman, and Watson, 1993; Herman, Dolgas, and Carlson, 1998; Herman et al., 2003; Ulrich-Lai and Herman, 2009).

### **Corticosteroid Receptors**

Glucocorticoids are a class of corticosteroids excreted from the adrenal medulla that act on target receptors in nearly all types of neural tissue.

Glucocorticoids are steroid hormones that readily cross cell membranes and act primarily on two receptor types: the glucocorticoid receptor (GR) and the mineralocorticoid receptor (MR) (de Kloet, 1991; McEwen, de Kloet, and Rostene, 1986). Activation of corticosteroid receptors can result in many different cellular effects, including energy mobilization and inhibition of the inflammatory response (Herman et al., 2016). GR expression is abundant almost everywhere in the brain, with the highest density in pituitary and CRH neurons (de Kloet et al., 1998). MRs are highly receptive to the mineralocorticoid hormone, aldosterone, and are highly expressed in the hypothalamus where they regulate salt appetite (McEwen et al., 1986; Gomez-Sanchez, 1997; Ma et al., 1997); however, they also have high affinity for corticosterone and are found in many other brain regions including the hippocampus, where interestingly, the MR receptor does not readily bind its natural ligand aldosterone (Veldhuis et al., 1982; Krozowski and Funder, 1983). It is also important to note that even though MRs have a high affinity for both glucocorticoids and mineralocorticoids, glucocorticoids are found in concentrations in the bloodstream that are nearly 100-fold higher than aldosterone (Funder, 2017).

GRs and MRs can mediate the traditional role of steroid receptors and transcription factors that are capable of modulating a large number of genes (de Kloet et al., 1998). MRs have a 10-fold higher affinity than GRs for corticosterone binding (Timmermans et al., 2013; de Kloet et al., 1998). At normal levels of glucocorticoid circulation, a basal activity level of the HPA axis is maintained through MR activation, but the physiological response to stress increases the

release of glucocorticoids to allow for the binding of GRs to mobilize the body to respond to the stressor (de Kloet et al., 1998). Aldosterone signaling through MRs is regulated by the enzyme 11- $\beta$  hydroxysteroid dehydrogenase (11- $\beta$ HSD), which exists in two forms: type I and II. In the kidney for example, 11- $\beta$ HSD type I inactivates glucocorticoids and allows MR sensitivity to aldosterone; however, in the brain 11- $\beta$ HSD enhances MR sensitivity to glucocorticoids (Seckl, 1993; Seckl and Walker, 2001).

Activation of the corticosteroid receptors can have both rapid and long-term effects. Rapid effects are non-genomic and can alter cell structure, energy metabolism, or signal transduction, while long-term effects are achieved through transcriptional alterations (de Kloet et al., 1998; Haller, Mikics, and Makara, 2008; Venero and Borrell, 1999). Structures critical for memory processing including the hippocampus, amygdala, and prefrontal cortex express both MR and GR (de Kloet, Joels, and Holsboer, 2005). Corticosteroids together with noradrenaline, CRH, and endocannabinoids can cause behavioral adaptations to stress and regulate learning and memory processing (Joels et al., 2006; Joels, Fernandez, and Roozendaal, 2011), but the specific mechanisms are not well-understood.

### **Navigation and Spatial Memory**

Navigation through an environment requires interpretation of information about environmental stimuli and the location of an animal within an environment independent of the stimuli (O'Keefe, 1976). Representation of environmental

stimuli in a spatial framework requires both static positional information as well as egocentric positioning based on integration of information obtained through motion within an environment (Buzsaki and Moser, 2013; O'Keefe and Nadel, 1979; McNaughton et al., 1996). Static positional cues obtained from the environment that help an organism determine its own position are termed "allocentric" cues while "egocentric" is relative to the animal (O'Keefe and Burgess, 1996). Egocentric positioning based on cues from movement through an environment is termed "path integration" and allows an organism to estimate distances between objects (Buzsaki and Moser, 2013). Path integration incorporates information of speed, time, head direction, and starting point (McNaughton et al., 2006). Together, allocentric and egocentric strategies require two neural systems that can work simultaneously, though depending on available cues within the environment, one system may be more heavily relied upon (Knierim et al., 1998; Derdikman et al., 2009; Gothard et al., 1996). Allocentric navigation bears many similarities to semantic memory, while egocentric navigation uses systems that are thought to support episodic memory, and both types of memory are capable of encoding by the hippocampus and entorhinal cortex (Buzsaki and Moser, 2013).

### **Spatial Processing in Individual Cells**

The hippocampus plays a crucial role in spatial memory processing (Scoville and Milner, 1957; Squire, Stark, and Clark, 2004; Jarrard, 1993; McClelland and Goddard, 1996), but the discovery of "place cells" provided the

first evidence of individual cells capable of encoding spatial information. Place cells are found in all hippocampal regions but are most prominent in CA1 and CA3 (Barnes et al., 1990). Place cells become active only when an organism enters a specific area within the environment and are otherwise silent, thus encoding a single egocentric point within a given space (O'Keefe and Dostrovsky, 1971). Layer II of the medial entorhinal cortex (MEC – LII) contains “grid cells” that are active during spatial memory processing and fire in a hexagonal pattern across the entire applicable space, thus encoding a larger representation of the environment (Hafting et al., 2005). This recent discovery has led to an increase in focus on the MEC as a necessary component of the memory-processing loop. In fact, it has been shown that input from grid cells is necessary for place cell firing properties (Brun et al., 2002).

Place and grid cells are not the only cells in the brain to encode spatial information, however. Border cells encode the edges of the spatial field (Solstad et al., 2008), head direction cells encode the animal's head orientation (Taube, Muller, and Ranck, 1990), band cells encode planar periodic representations of space (similar to grid cells but firing in band-like patterns instead of hexagonal) (Krupic et al., 2012), and speed cells encode the animal's speed independent of visual input (Kropff et al, 2015). Interestingly, the medial entorhinal cortex contains grid cells, border cells, head directions cells, and speed cells, and unlike place cells of the hippocampus that are only active in a single region within a given environment, each of these cell types is active in all types of spatial fields (Solstad et al., 2008), indicating that the brain uses these cells as a means of

universal spatial encoding no matter the type of environment encountered (Moser, Kropf, and Moser, 2008; Hafting et al., 2005). Rodents begin to develop spatial processing abilities very early in life. In fact, rodent pups have adult-like head-direction cells when they first leave the nest at two weeks of age, and though place and grid cells are also active at this age, they do not fully mature until four weeks (Langston et al., 2010). Grid cell activity is not unique to rodents and has also been recorded from the MEC in bats (Yartsev et al., 2011), and importantly, primates performing a visual exploration task without locomotion (Killian et al., 2012), as well as in humans (Doeller et al., 2010; Jacobs et al., 2013).

### **Implication of MEC Dysfunction in Disease**

There is evidence associating the MEC with temporal lobe epilepsy as well as memory deficiencies tied to aging, Alzheimer's disease, and chronically stressed populations. These disease states may implicate MEC – LII circuit dysfunction as the cause. Spatial memory declines with normal aging in both humans (Iachini et al., 2009) and animals (Sharma et al., 2010). Furthermore, the entorhinal cortex is one of the most heavily damaged and first affected areas in Alzheimer's disease (Braak and Braak 1991; Van Hoesen et al. 1991). In fact, patients with Alzheimer's disease show a marked decrease in number of MEC – LII cells, and it has been shown that the MEC, CA1 of the hippocampus, and subiculum are the areas most affected by the disease (Pavlopoulos et al., 2013). There is also strong evidence of spatial memory deficiencies in male mice that have been chronically stressed (Bowman et al., 1994; Conrad et al., 1996; Park

et al., 2001) or acutely stressed (Conrad et al., 2004; Diamond et al., 1996; Shors and Thompson, 1992). The mechanisms leading to these memory deficits are not fully understood, and a better understanding of the circuitry within MEC – LII could reveal a target for better treatment and/or prevention of these disease states.

Like the hippocampus, the EC is highly plastic and displays long-term potentiation mechanisms that are able to trigger epileptic behavior (Alonso et al., 1990). Furthermore, cells in the EC have intrinsic characteristics and synaptic properties that make them susceptible to generation of epileptiform discharges and sustained seizure activity that causes temporal lobe epilepsy in rodents, guinea pigs, and humans (Jones and Heinemann 1988; Jones and Lambert 1990; Pare et al. 1992; Rutecki et al. 1989; Stanton et al. 1987). Interestingly, the dentate gyrus (DG) of the HC does not show spontaneous seizure-like activity in acute brain slices with reduced magnesium concentrations, but spontaneous seizure-like activity in the EC can induce epileptiform activity in the DG (Stanton et al, 1987). Application of NE can block epileptiform activity via  $\alpha$ -1 AR activation, while activation of  $\beta$  ARs prolongs epileptiform activity (Stanton et al., 1987). These findings highlight the potential importance of EC function in triggering seizures.

### **Connectivity of Spatial Memory Processing Regions**

The trisynaptic pathway (TSP) is a feed-forward excitatory pathway connecting the entorhinal cortex to the hippocampus: layer II of the EC projects

to the dentate gyrus via the perforant path, the DG projects to CA3 via the mossy fibers, CA3 projects to CA1 via the schaffer collaterals, and finally CA1 projects back to the deeper layers of the EC through the subiculum (Witter et al., 2000; Nakashiba et al., 2008; Aimone et al., 2011; Fanselow and Dong, 2010). EC – LV sends projections out to cortical areas as well as back to the superficial layers of the EC (Kohler, 1985; Dolorfo and Amaral, 1998; van Haeften et al., 2000). Another loop between the EC and HC can bypass the DG and CA3 via the monosynaptic pathway (MSP) or temporoammonic pathway (TA): EC – LIII projects directly to CA1, bypassing the DG and CA3 regions (Steward, 1976; Nakashiba et al., 2008) (Fig. 1.1). Nearly all of the associative areas of the neocortex send inputs to the HC through the EC (Nakashiba et al., 2008).

Different portions of these loops are thought to contribute to various types of memory. The DG contains principal cells called granule cells that are tightly packed together and receive unidirectional inputs directly from the EC via the perforant path (Amaral et al., 2007). Interestingly, adult neurogenesis occurring in the DG causes a range of granule cell ages and maturation levels that mediate differences in excitability and thresholds for induction of long-term potentiation (Ge et al., 2007). Excitability of granule cells decreases over time (Ge et al., 2007), with newly born cells being hyper-excitable compared to mature granule cells (Li et al., 2009; Aimone et al., 2011). Cells in the DG with different levels of excitability as well as increased inhibition are thought to act as a gating mechanism for the information flowing from the MEC through the HC (Aimone et al., 2011). The connection of the EC to the DG and CA3 regions, because of the

gating of information by the DG granule cells, is thought to contribute to pattern separation (Ge et al., 2007; McHugh et al., 2007; Nakashiba et al., 2008; O'Reilly and McClelland, 1994), while recurrent collaterals within CA3 are thought to be responsible for pattern completion (Nakazawa et al., 2002; Nakazawa et al., 2004; Nakashiba et al., 2008; Rolls and Kesner, 2006), and CA1 is thought to be involved in recognition of novel contexts and pattern associations (Kesner et al., 2000; Nakashiba et al., 2008).

Studies looking at the effects of damage or lesions to the hippocampus or fornix (output of HC) in macaques and humans have shown the necessity of these regions for completion of object-place memory tasks (Burgess et al., 2002; Crane and Milner, 2005; Gaffan, 1994; Parkinson et al., 1988; Smith and Milner, 1981). Selective lesioning of the primate hippocampus impairs spatial scene learning (Murray et al., 1998). Selective hippocampal lesions in rats cause spatial memory deficits in terms of remembering specific places (Cassaday and Rawlins, 1997; Jarrard, 1993; Martin et al., 2000; O'Keefe and Nadel, 1978), or when using spatial cues to complete a task (Eichenbaum et al., 1990; Kesner and Rolls, 2001). Furthermore, saturation of long-term potentiation impairs spatial learning (Moser et al., 1998). And finally, selective inhibition of the MSP causes deficits in temporal association learning (Suh et al., 2011).

Recent studies show that spatial memory processing is not confined to the hippocampus, and it requires functional interaction between the hippocampus and the entorhinal cortex (Nakashiba et al., 2008). In rodents the EC was initially divided into two regions based on morphological differences: lateral entorhinal

area (LEA) and medial entorhinal area (MEA) (Krieg, 1946a,b; Blackstad, 1956). The EC contains three distinctly separate bands of neurons with projections to different areas of the DG: the lateral band afferents connect to the dorsal half, the intermediate band projects to the third quarter, and the medial band sends afferents to the ventral quarter (Dolorfo and Amaral, 1998). These bands are functionally distinct, and lesioning the ventral or temporal area of the rat hippocampus causes no spatial impairments while lesioning the dorsal or septal area causes marked impairment of spatial learning in the Morris water maze (Moser et al., 1995). The lateral band of the MEA, which projects to the septal HC, contains cells that are active in many different place-specific fields and are capable of predicting a rat's location within an environment (Fyhn et al., 2004). These cells were later determined to be grid cells with firing fields that are not disrupted by lesions of the HC (Hafting et al., 2005).

The EC is composed of six layers: four cellular layers and two acellular (I and IV). As previously mentioned, layers II and III provide the major input to the HC, and receive the major output from other cortical areas (Witter et al., 2000a). Layers V and VI receive the major outputs from CA1 and the subiculum and relay this information to association cortices, the superficial layers of the MEC, and subcortical areas including the basal ganglia, amygdala, and thalamus (Witter et al., 2000a). Importantly, the different layers of the MEC contain different types of spatially-sensitive cells. Layer II contains grid cells (Hafting et al., 2005), head direction cells (Ranck, 1985; Taube, 1995), band cells (Krupic et al., 2012), and border cells (Solstad et al., 2008). Layer III and V contain border cells (Solstad et

al., 2008), grid cells, as well as conjunctive cells capable of encoding both position and head direction information (Sargolini et al., 2006). All layers contain speed cells (Kropff et al., 2015) as well as grid cells, though layer II contains the highest proportion of grid cells (Sargolini et al., 2006).

Global ablation of the MEC impairs rodent performance on spatial maze tasks (Parron et al., 2004; Steffenach et al., 2005; Eichenbaum, 2007; Esclassan et al., 2009). Lesions of the dorsolateral EC cause spatial memory deficits, while lesions of the ventromedial EC fail to affect performance on a spatial memory task (Steffenach et al., 2005). Furthermore, lesions of the cholinergic inputs to MEC – LII disrupted the “gridness” of stellate cells (Koenig et al., 2011; Newman, Climer, and Hasselmo, 2014), and blocking theta oscillation input to the MEC by lesioning the medial septum also disrupted stellate cell gridness without affecting firing of place, band, border, or head direction cells (Koenig et al., 2011; Brandon et al., 2011). Furthermore, pharmacological inactivation of the HC disrupted grid cell firing patterns in the MEC without affecting border and head direction cells, and surprisingly, grid cell firing was altered to then provide head direction information (Bonnievie et al., 2013). Each of these studies reiterates the necessity of the MEC for functional spatial memory processing.

**Figure 1.1 – Excitatory Connectivity between the Entorhinal Cortex and Hippocampus**

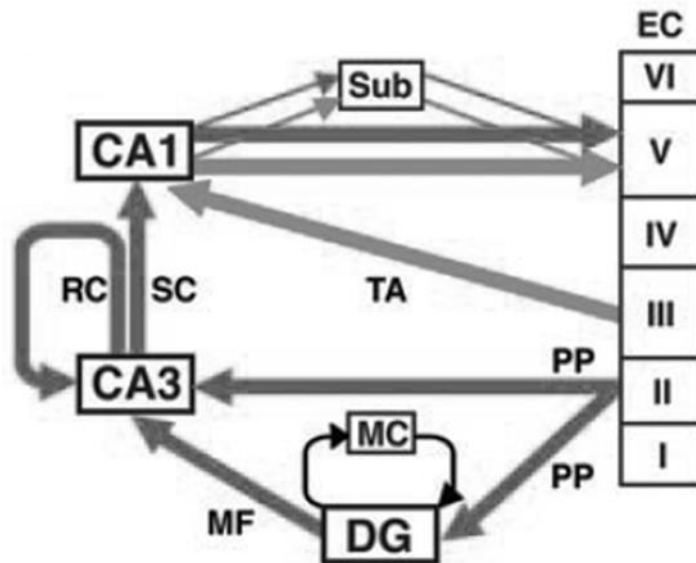


**Fig. 1.1:** Schematic of connectivity between the entorhinal cortex (EC) and the various hippocampal subregions. Dark gray arrows = trisynaptic pathway (TSP). Light grey arrows = monosynaptic/temporoammonic (TA) pathway. Sub, subiculum; PP, perforant path, MF, mossy fibers, SC, schaffer collaterals; RC, recurrent collaterals. Adapted from Nakashiba et al., 2008.

### **Lateral versus Medial Entorhinal Cortex**

The circuitry of the EC has been described in rodents. The LEA receives inputs from brain regions such as the amygdala, olfactory structures, piriform cortex, and insular regions, which are thought to provide non-spatial information about context and emotional significance (Kerr et al., 2007). The perirhinal cortex, which processes sensory information, is reciprocally connected with the LEA (Kerr et al., 2007). The lateral band of the MEA receives more input than the LEA from the visual, posterior parietal, and retrosplenial and cingulate cortices (Kerr et al., 2007). The lateral and intermediate bands of the MEA are targeted by the dorsal thalamus, which contains head-direction cells (Mizumori and Williams, 1993; Taube, 1995). The presubiculum, parasubiculum, and postrhinal cortices (parahippocampal structures), as well as visuospatial information from cortical and subcortical areas most heavily target these same bands (Kerr et al., 2007). Thus, the MEA is strongly connected to areas that are involved in providing spatial information (Kerr et al., 2007). It is also important to note that the dorsocaudal area of the MEA contains grid cells, and receives considerable input from dorsal thalamic, posterior parietal, and visual association areas (Kerr et al., 2007). Together, the lateral and intermediate bands of the EC are targeted by both non-spatial and spatial inputs, with the non-spatial information being carried to the LEA and the spatial information to the MEA before projecting to the HC (Kerr et al., 2007). Furthermore, recordings from cells within the dorsolateral band of the MEC that are connected to the dorsal hippocampus show strong spatial specificity while cells from the LEC do not (Hargreaves et al., 2005).

A division between lateral and medial processing of spatial memory also occurs in species other than rodents. There is evidence that the MEA in monkeys is primarily used for spatial processing while the LEA is used for object and context processing (Bellgowan et al., 2009). In humans, however, there is strong evidence for lateralization of spatial processing, where fMRI studies have shown that the perirhinal and entorhinal cortices, in the right hemisphere in particular, are necessary for spatial encoding (Bellgowan et al., 2009; Burgess et al., 2002; Crane and Milner, 2005).

### **MEC – LII Principal Cell Types and Electrophysiological Properties**

MEC – LII sends its afferents to the DG of the HC as the first part of the trisynaptic pathway that is crucial for spatial memory processing. Initially, MEC – LII was thought to have two principal cell types based on their electrical membrane properties: the stellate cells (SCs) and pyramidal cells (PCs), each of which has distinctly different dendritic branching (Alonso and Klink, 1993). MEC – LII is primarily composed of stellate cells (Alonso and Klink, 1993) that are spatially tuned and show grid-like firing properties necessary to establish a big picture grid-like representation of the environment (Hafting et al., 2005). SCs have unique firing characteristics as well as a complex network of inhibitory inputs. Stellate cells show sub-threshold rhythmic theta (4-12Hz) oscillations, membrane properties that cause a sag response following depolarizing or hyperpolarizing sub-threshold current pulses, have lower spike thresholds than PCs, shorter spike duration than PCs, strong spike frequency adaptation, and

repetitive and minimally adapting bursting patterns when held near threshold (Alonso and Klink, 1993; Pastoll et al., 2012). Conversely, PCs do not show sub-threshold oscillations, have minimal sag compared to SCs, have higher spike thresholds and longer spike durations, and show moderate spike frequency adaptation (Alonso and Klink, 1993; Pastoll et al., 2012). Furthermore, stellate cells recorded more dorsally display stronger stellate cell characteristics, while stellate cells positioned more ventrally show intermediate values between stellate and pyramidal characteristics (Pastoll et al., 2012; Hafting et al., 2005; Sargolini et al., 2006; Giocomo et al., 2007). Pyramidal cells are anatomically interlaced in grid-like fashion around stellate cells within MEC – LII (Varga, Lee, and Soltesz, 2010). Because pyramidal cells are found in clustered patches throughout MEC – LII they have been termed “island cells”, whereas stellate cells are more evenly distributed and have been termed “ocean cells” (Kitamura et al., 2015; Ray et al., 2014).

More recently, principal cell types in MEC – LII have been subdivided into four classes: stellate cells, intermediate stellate cells, pyramidal cells, and intermediate pyramidal cells based on connectivity and electrophysiological properties (Fuchs et al., 2016). Even though MEC – LII may contain four types of excitatory cells based on distinct electrophysiological properties, these properties alone have not been able to fully account for the generation of grid-like firing behaviors. Grid cells of the MEC have long been thought to be the stellate cells in MEC – LII. Surprisingly, grid cells can be either stellate or pyramidal neurons (Domnisoru et al., 2013; Tang et al., 2014), and based on known connectivity

between grid cells and fast-spiking interneurons it has been suggested that grid cells can be stellate cells, intermediate stellate cells, and intermediate pyramidal cells, but not pyramidal cells (Fuchs et al., 2016). Furthermore, grid cells representing space are discretized, meaning grid cells across the dorsal-ventral axis fit into distinct modules that code for different grid orientations and scales with little overlap or interaction (Stensola et al., 2012).

The majority of grid cells in MEC – LII were found to be calbindin<sup>+</sup> pyramidal cells (Tang et al., 2014), but based on the recent division of principal cell types into four classes, these calbindin<sup>+</sup> cells are more likely to be intermediate pyramidal cells than pyramidal cells (Fuchs et al., 2016). Border cells of MEC – LII were predominately calbindin<sup>-</sup> (stellate cells) (Tang et al., 2014). Furthermore, it has been shown that only calbindin<sup>-</sup> cells in MEC – LII project to the DG of the HC, while calbindin<sup>+</sup> cells can project to CA1 of the HC as well as the contralateral MEC (Varga et al, 2010). There is also evidence that pyramidal cells in MEC – LII do not project to the DG (Kitamura et al, 2014; Ray et al., 2014; Kitamura et al., 2015). This implies that the majority of information received by the DG from MEC – LII is information about environmental borders from ocean cells, which may contribute to path-integration processing in the DG. In fact, evidence has shown that island cells (calbindin<sup>+</sup>) are not activated in a context-specific manner, whereas ocean cells (reelin<sup>+</sup>) are activated by novel contexts and encode contextual information by activating granule cells in the DG (Kitamura et al., 2015).

## **Layer II Afferents and Efferents**

Interestingly, the pyramidal cells within MEC-LII receive more connections than stellate cells from the deeper layers of MEC (Beed et al., 2010; Buralossi and Brecht, 2014), which are known to provide information about position, direction, and speed (Sargolini et al., 2006). Pyramidal cells also receive a larger number of the cholinergic inputs from the PaS (Ray et al., 2014). Stellate cells are the only cell type within MEC – LII that project to the ipsilateral DG, while pyramidal cells project only to the contralateral MEC (Varga et al., 2010; Ray et al., 2014; Kitamura et al., 2014). LII and LIII are the only MEC layers that project to the hippocampus (Schwartz and Coleman, 1981; Nakashiba et al., 2008), and the hippocampal CA1 region sends projections back to the deeper layers of MEC to complete the loop between the two structures (Nakashiba et al., 2008). This evidence suggests that the pyramidal cells receive the majority of information from the contralateral MEC and ipsilateral hippocampus through the deeper layers of the ipsilateral MEC. Since stellate cells are the only cell type within MEC – LII to send spatial information to the hippocampus, it is likely that pyramidal cells are able to influence stellate cell signaling to the hippocampus.

## **Network Models**

Since the discovery of grid cells, the mechanism to explain generation of hexagonal firing patterns in single cells in the MEC has been elusive. Many network models have been developed as a means of explaining these firing patterns, but the two most promising models are the attractor model which posits

that grid cell activity is generated in concert by the network, and the oscillatory interference model in which the grid activity is generated by single cells as a result of interference between network signaling and intrinsic oscillatory properties of the cell (Fuchs et al., 2016; Burak and Fiete, 2009). Particularly relevant to this dissertation is the attractor model. In this model, it has been demonstrated that strong inhibitory input from the local network is sufficient to generate hexagonal firing in a single cell if general feed-forward excitation is applied to the whole network and if the local inhibitory inputs surround that cell (Burak and Fiete, 2009). The implication that grid cell firing behavior can be generated solely by local inhibitory interneurons emphasizes the importance of the MEC – LII local inhibitory networks for spatial memory processing. Thus, it is important to understand how hormones and neurotransmitters involved in stress may modulate inhibitory signaling in MEC-LII in order to understand the effects of stress on spatial processing.

### **Theta Oscillations in Spatial Processing Regions**

The oscillatory interference models previously mentioned require interference between network theta and single cell membrane rhythmicity (Burgess et al., 2007; Hasselmo et al., 2007). Theta rhythm oscillations are a common network occurrence in memory processing regions, and require a pacemaker to generate and sustain these rhythms (Mitchell et al., 1982). Hippocampal theta is generated by the medial septal area (MSA), which includes the medial septal nucleus and the nucleus of the diagonal band (Mitchell et al.,

1982). The MSA sends projections via the fimbria and fornix to all cell fields of the hippocampus (Raisman, 1966; Meibach and Siegel, 1977; Swanson and Cowan, 1977). Lesions of the MSA's projections through the fimbria and fornix in rodents are sufficient to block theta in the hippocampus (Rawlins et al., 1979) while lesions of the dorsal fornix eliminate theta in the entorhinal cortex and impair male rodents' performance on the radial arm maze (Mitchell et al., 1982). Lesions of the medial septum cause a loss of theta in the HC and MEC (Mizumori et al., 1990; Mitchell et al., 1982; Jeffery and Donnett, 1995) and abolish grid cells' periodic spatial firing pattern, termed 'gridness' (Koenig et al., 2011; Brandon et al., 2011). Accordingly, loss of theta from the MSA causes spatial memory processing deficits in male rodents (Givens and Olton, 1994; Mizumori et al., 1990; Winson, 1978; Mitchell et al., 1982; Chrobak et al., 1989; Martin et al., 2007). Interestingly, inactivation of theta only in the MEC and loss of grid cell gridness does not affect place cell firing in male rodents exploring familiar contexts (Brandon et al., 2011).

Movement velocity and direction modulate oscillatory behavior (Burgess et al., 2007; Hasselmo et al., 2007; O'Keefe and Burgess, 2005), and could be the basis for generation of spatially-tuned firing seen in single cells in the MEC (Koenig et al., 2011). Interestingly, stellate cells in MEC – LII express high levels of HCN1 and a correspondingly large h-current (Nolan et al., 2007), which enables them to generate sub-threshold theta oscillations (Alonso and Klink, 1993; Dickson et al., 2000; Nolan et al., 2007). The ability of these cells to generate theta oscillations coupled with the theta oscillation inputs sent by the

MSA creates an interaction that could generate the firing patterns seen in grid cells, and forms the basis for the oscillatory interference models.

### **Theta and Gamma Encoding of Space**

In the hippocampus, spatial coding by place cells occurs through theta phase precession, whereby pyramidal cell firing is locked to phases of theta (O'Keefe and Recce, 1993). MEC – LII grid cells also coordinate firing with theta phase, whereby the neuron fires at advancing portions of the theta phase as a rat runs through the neuron's receptive field (Hafting et al., 2008; Mizuseki et al., 2009). Furthermore, inactivation of the hippocampus does not interfere with phase precession in the MEC, and interestingly, nearly all principal cells in MEC – LII exhibit phase precession while very few of MEC – LIII principal cells show phase precession (Hafting et al., 2008). It is thereby proposed that in order to achieve path integration for encoding of space, theta network oscillations must provide a temporal coding system for pairing spatial information from the MEC, including speed, head direction, and other identifiers, with spatial information from the HC (Hasselmo et al., 2007; O'Keefe and Burgess, 2005).

The use of phases of theta as a way to time-lock information is further supported by the discovery of the incorporation of gamma frequencies, in the range of 60-120Hz, nested within theta (Chrobak and Buzsaki, 1998; Colgin et al., 2009). As previously mentioned, firing of individual cells time-locked to phases of rhythmic oscillations is considered a means of connecting the MEC and HC, and high-frequency gamma nested within theta may further demonstrate the near-

simultaneous cooperation between the hippocampal and entorhinal networks encoding spatial information (Buzsaki and Draughn, 2004; Colgin et al., 2009). Theta in the MEC has been shown to alter the power of locally-generated gamma oscillations as a means of coordinating the encoding of information from each MEC layer (Chrobak and Buzsaki, 1998; Cunningham et al., 2003; Dickson et al., 2003; Mormann et al., 2005; Steinvorth et al., 2010). Furthermore, collective firing of MEC neurons phase-locked to gamma-nested theta can more efficiently activate hippocampal neurons (Buzsaki and Wang, 2012; Fries, 2009).

Gamma frequencies in the hippocampus are generated by perisomatic inhibition via fast-spiking interneurons (parvalbumin<sup>+</sup> basket cells) (Hajos and Paulsen, 2009; Freund and Katona, 2007; Hasenstaub et al., 2005; Bragin et al., 1995; Buzsaki and Wang, 2012). Considering the dense inhibitory network present in MEC – LII, it is not surprising that theta-nested gamma frequencies are generated by feedback inhibition (Pastoll et al., 2013) and are crucial for spatial memory processing (Colgin et al., 2009; Buzsaki and Wang, 2012). Importantly, grid cell function, and generation of grid fields, can be achieved through recurrent inhibition (Couey et al., 2013), and PV<sup>+</sup> interneurons can provide grid cell-driven recurrent inhibition in MEC – LII (Buetfering et al., 2014). Because stellate cells in MEC – LII are known to communicate through feedback inhibition, this suggests a need for precise coordination between excitation of stellate cells and inhibition from local parvalbumin<sup>+</sup> inhibitory interneurons in order to time-lock the processing of spatial information between the HC and EC (Pastoll et al., 2013).

## **Layer II Inhibitory Cells**

There is ample evidence that MEC – LII principal cells receive relatively strong inputs from inhibitory networks located locally within MEC – LII (Jones and Buhl, 1993; Pastoll et al., 2013), and that this inhibitory network is significantly larger and comparatively stronger than the inhibitory network of the LEC – LII region (Varga et al., 2010; Beed et al., 2013). MEC – LII contains multiple inhibitory networks composed primarily of three types of inhibitory interneurons: parvalbumin<sup>+</sup> (PV<sup>+</sup>) fast-spiking interneurons (FSIs), cholecystinin (CCK) and cannabinoid type 1 receptor (CB1R)-expressing basket cells (CCKBCs), and somatostatin-positive (SOM<sup>+</sup>) interneurons (Miettinen et al., 1996; Varga et al., 2010; Lee et al., 2010). Recently it has been suggested that the CCKBCs in MEC – LII should be considered a sub-class of the 5HT3A receptor-containing interneuron (Fuchs et al., 2016; Lee et al., 2010; Morales and Bloom, 1997). The 5HT3AR-containing interneurons include the four commonly used neuropeptide markers: SST, CCK, VIP, and NPY (Lee et al., 2010); however, the majority of the research on inhibitory interneurons in MEC – LII uses FSIs, CCKBCs, and SOM<sup>+</sup> as the three classes.

## **Layer II Networks and Connectivity**

There is little evidence thus far showing that MEC – LII excitatory networks are directly linked, and no evidence that pyramidal cell activation can influence stellate cell signaling. Previous studies doing simultaneous recordings

have shown that stimulation of stellate cells in MEC – LII causes inhibition of neighboring stellate cells through fast-spiking interneurons, and that stellate cells are connected to each other exclusively through inhibitory interneurons (Couey et al., 2013; Pastoll et al., 2013); however, there is some evidence of excitatory connections between principal cells of MEC – LII (Fuchs et al., 2016; Beed et al., 2010; Burgalossi and Brecht, 2014). Prior to the classification of MEC-LII excitatory cells into four groups (pyramidal, stellate, intermediate pyramidal, and intermediate stellate), there was evidence that stimulation of pyramidal cells resulted in neither excitatory nor inhibitory responses in any stellate cells (Couey et al., 2013), while stimulation of stellate cells rarely (less than 10 percent of the time) caused excitatory responses in pyramidal cells (Couey et al., 2013). More recently it has been shown that connections between pyramidal cells are extremely rare (~1%), while ~10% of intermediate pyramidal cells send inputs to pyramidal and stellate cells (Fuchs et al., 2016). Stellate cells, on the other hand, do not send projections to other stellate cells or to intermediate pyramidal cells, but less than 5-10% of stellate cells send inputs to intermediate stellate cells and vice versa (Fuchs et al., 2016).

About fifty percent of the GABAergic cells in MEC – LII are PV<sup>+</sup> cells (Wouterlood et al., 1995; Miettinen et al., 1996) that send inhibitory inputs to both excitatory and inhibitory cells within both MEC – LII and LIII (Wouterlood et al., 1995; Varga et al., 2010; Canto et al., 2008; Soriano et al., 1993), including all principal cell types in MEC – LII (Buetfering et al., 2014). Notably, PV<sup>+</sup> interneurons provide the majority of inhibition in MEC – LII, and spontaneous

inhibitory post-synaptic current (sIPSC) frequency, but not amplitude, measured in principal cells in the dorsal portions of MEC – LII is higher than sIPSC frequency in more ventral principal cells (Beed et al., 2013). Interestingly, stellate cells receive inhibitory input primarily from fast-spiking PV<sup>+</sup> interneurons (Buetfering et al., 2014; Couey et al., 2013; Pastoll et al., 2013), while pyramidal cells receive inhibitory input primarily from CCKBCs (5HT3A<sup>+</sup>), but no inputs from PV<sup>+</sup> interneurons (Fuchs et al., 2016; Varga et al., 2010). Intermediate stellate and intermediate pyramidal cells receive inputs from, and send excitatory inputs to, the PV<sup>+</sup> interneurons (Fuchs et al., 2016).

### **Effect of Stress on Hippocampal-Dependent Memory**

In both humans and animal models, stress and glucocorticoids target receptors in the HC (McEwen, 2007; Gibbs et al., 2010; O'Dell et al., 2015) and cause reversible deficits in spatial memory and episodic memory (Lupien and McEwen, 1997). In order to elucidate these effects, rodents have been stressed in a variety of ways: forced swimming, restraint, predator exposure, electrical shock, and social defeat stress. Both chronic (Bowman et al., 2002; Conrad et al., 1996; Park et al., 2001; Luine et al., 1994; Venero et al., 2002; Sandi et al., 2003) and acute (Conrad et al., 2004; Diamond et al., 1996, 2006; Woodson et al., 2003; Sandi et al., 2005, Sandi and Pinelo-Nava, 2007) stress can impair a male rodent's performance on spatial memory tasks. Furthermore, chronic glucocorticoid elevation (Sandi, 2004; Cerqueira et al., 2005) or deactivation of GR (Oitzl et al., 1997) is sufficient to impair performance on spatial memory tasks

in male rodents. The negative impact of stress on spatial memory processing in male rodents is clear, but the underlying mechanisms affecting the known memory pathways remain unclear.

### **Effect of Stress on Hippocampal Pyramidal Cell Signaling**

The hippocampus is known to be crucial to spatial memory processing, but also can modulate neuroendocrine responses (Ulrich-Lai and Herman, 2009). In addition, the hippocampus receives projections from the locus coeruleus (LC) (Gibbs et al., 2010) and contains a high level of GR and MR receptors (McEwen, 2007). Thus, the HC has been the main target of study for stress and spatial memory research. In the hippocampus, corticosterone can alter spatial memory processing by modulating network signaling in a number of ways, and the magnitude of the effects follow a dose-dependent inverted-U pattern as glucocorticoid levels increase (Diamond et al., 1992). Specifically, corticosterone application at intermediate levels promotes synaptic strengthening and long-term potentiation (LTP) (Wiegart et al., 2006; Pavlides et al., 1996; Kerr et al., 1994), increases the frequency of mini excitatory post-synaptic currents (mEPSCs) (Karst et al., 2005), and increases glutamate release probability (Olijslagers et al., 2008). Glucocorticoids in high concentrations, following the inverted-U pattern of glucocorticoid dosage effects on behavior, can also have suppressive effects. Long-term depression (LTD) is a reduction of excitatory transmission, and high levels of glucocorticoids in the HC facilitate LTD achieved by low frequency stimulation (Pavlides et al., 1995; Kerr et al., 1994). Furthermore, acute and

chronic stress can both facilitate LTD in the hippocampus (Yang et al., 2005; Holderbach et al., 2007), and LTD induced by acute stress has been correlated with spatial memory deficits in male rodents (Wong et al., 2007).

Because of the wealth of evidence that adrenal steroids can alter signaling in hippocampal networks, it's not surprising that glucocorticoids can also alter dendritic architecture. Chronic restraint stress has been shown to cause atrophy in the apical dendrites of CA3 pyramidal neurons in which length of the dendrites is shortened while branching patterns decrease in complexity (Watanabe et al., 1992; Conrad et al., 1999; Vyas et al., 2004; McEwen, 2016). Dendritic atrophy has also been shown to occur in CA1 and granule cells of the DG following chronic stress, and these animals show impaired spatial memory processing (Sousa et al., 2000). Furthermore, prolonged elevation of glucocorticoid levels is sufficient to cause dendritic atrophy in CA1 and CA3 of the HC (Woolley et al., 1990; Magarinos et al., 1998). Interestingly, acute restraint stress and shortened intervals of chronic restraint stress do not cause hippocampal dendritic atrophy (Magarinos and McEwen, 1995; Pham et al., 2003). However, a decrease in density of dendritic spines in apical branches of both CA1 and CA3 neurons has been shown following both chronic and acute stressors (Sunanda et al., 1995; Pawlak et al., 2005; Castaneda et al., 2015; Huang et al., 2015), indicating that male rodents experiencing any form of stress undergo hippocampal dendritic remodeling that could potentially lead to signaling changes within spatial processing circuits. Also, in human disease states resulting from prolonged, chronic, or severe stress, the structure and volume of the hippocampus is known

to change whereby patients show a loss of grey matter potentially due to structural changes in neurons and glial cells (Rajkowska and Miguel-Hidalgo, 2007; Kassem et al., 2013; Malykhin and Coupland, 2015). These structural changes could also be an underlying mechanism for stress-induced deficits in spatial memory processing.

### **Adrenergic Receptor Activation in the Hippocampus**

The locus coeruleus sends projections to the ventral and dorsal HC (Gibbs et al., 2010) where the pyramidal cells of the HC and granule cells of the DG express  $\alpha_1$ ,  $\alpha_2$ ,  $\beta_1$ , and  $\beta_2$ -ARs (Nicholas et al., 1993; Hillman et al., 2005; Guo and Li, 2007). Inhibitory interneurons also express both  $\alpha_1$  and  $\beta$ -ARs, but  $\beta_1$  and  $\beta_2$  levels vary widely depending on interneuron type (Papay et al., 2006; Cox et al., 2008). AR activation in the hippocampus has been shown to both enhance and impair performance on memory tasks, and is receptor sub-type dependent (O'Dell et al., 2015). Injection of NE into the HC, or stimulation of the locus coeruleus (LC) inputs into the HC, promotes spatial and associative memory retrieval that requires activation of  $\beta$ -ARs (Devauges and Sara, 1991; Przybylski et al., 1999; Sara et al., 1999).  $\beta$ -AR activation has been shown to facilitate induction of LTP in all regions of the HC (O'Dell et al., 2010) and can even induce LTP from weaker stimulus patterns that would not normally be sufficient to induce LTP (Gelinias and Nguyen, 2005; Gelinias et al., 2007; Ma et al., 2011).  $\beta$ -AR antagonists in the HC do not block LTP induction (Swanson-Park et al., 1999), but do impair spatial memory in male rodents (Ji et al., 2003).

There is evidence that somatostatin-expressing interneurons in CA1 of the HC express functional  $\alpha$ 1-ARs (Hillman et al., 2005; Hillman et al., 2007). Activation of  $\alpha$ 1-ARs in CA1 of the HC causes depolarization of inhibitory interneurons and a subsequent increase in frequency and amplitude of spontaneous IPSCs in CA1 pyramidal cells (Bergles et al., 1996). Interestingly, this depolarization is not dependent on the excitatory inputs onto the interneurons, as blocking these inputs does not block the depolarization or subsequent increase in spontaneous IPSC frequency in CA1 pyramidal neurons (Doze et al., 1991). Importantly, low concentrations of NE increase excitability of CA1 pyramidal cells, while high concentrations ( $>50\mu\text{M}$ ) depolarize inhibitory interneurons, which is mimicked by  $\alpha$ 1 agonism (Mueller et al., 1981; Mynlieff and Dunwiddie, 1988).

Agonists of  $\alpha$ 1-AR in general are known to facilitate locomotion and arousal (Sirvio and MacDonald, 1999). Infusion of  $\alpha$ 1-AR antagonists into CA1 of the HC impairs male rodent performance on a spatial memory task (MWM) (Torkaman-Boutorabi et al., 2014). In contrast, infusions of  $\alpha$ 2-AR antagonists into CA1 of the HC facilitated spatial learning in male rats (Torkaman-Boutorabi et al., 2014). Interestingly, peripheral injection of the  $\alpha$ 1-AR antagonist, prazosin, was not sufficient to impair male rats' ability to complete an object-position recognition task (Levcik et al., 2013). In CA3,  $\alpha$ 1-AR agonism reduces glutamate release at the pre-synaptic terminal and decrease excitability in pyramidal cells (Scanziani et al., 1993), which can modulate the synchronous firing in CA3 caused by its recurrent collaterals, which are known to be important for spatial

memory processing (Sirvio and MacDonald, 1999). These studies highlight a striking ability of NE to modulate spatial memory processing networks through a variety of mechanisms that depend on region and local AR expression.

### **Adrenergic Receptor Activation in the Rodent Medial Entorhinal Cortex**

In general,  $\alpha$ -AR activation is inhibitory, causing a decrease in glutamatergic transmission in the HC (Scanziani et al., 1993) or hyperpolarization in the LC (Aghajanian and VanderMaelen, 1982). Like the HC, the entorhinal cortex also expresses  $\alpha 1$  (Stanton et al., 1987),  $\alpha 2$  (Boyajian et al., 1987; Unnerstall et al., 1984, 1985; Mitrovic et al., 1992), and  $\beta$ -ARs (Booze et al., 1993). In two to three week old male rodents, NE application increases sIPSC frequency and amplitude as well as mIPSC frequency, but not mIPSC amplitude, and this increase is not dependent on calcium, PLC, PKC, or tyrosine kinases, and can be completely blocked by the  $\alpha 1$ -AR antagonist corynanthine (Lei et al., 2007). The effect on mIPSC frequency suggests that NE increases presynaptic GABA release without affecting GABA<sub>A</sub> receptors, and that this increase in GABA release is unlikely to be dependent on cation channels (Lei et al., 2007). Furthermore, NE application does not affect excitability in MEC-LIII inhibitory interneurons (Lei et al., 2007), but MEC-LII inhibitory interneurons were not tested. Also, NE application decreases action potential firing in more than 50% of cells, thereby significantly decreasing excitability of principal cells (Lei et al., 2007). It is important to note that this group recorded from principal cells within both layer II and III indiscriminately, and it is known that the principal cells within

layer II differ from layer III in terms of cell type, projection destination, and firing properties (Steward and Scoville, 1976; Witter et al., 2000a,b; Sargolini et al., 2006; Xiao et al., 2009). It is also important to note that these findings were in animals less than four weeks old, and it is known that grid cells in MEC – LII in rodents are not fully mature until four weeks of age (Langston et al., 2010). Furthermore, in rodents less than three weeks of age there is evidence that stellate cell stimulation is able to cause excitatory responses in neighboring stellate cells in MEC – LII. Importantly, this stellate cell connectivity decays with age and only occurs prior to stellate cells reaching full maturity, at which point no evidence of excitatory connections between stellate cells has been found (Couey et al., 2013).

Similar to  $\alpha$ 1-ARs,  $\alpha$ 2 AR activation via norepinephrine application in the EC decreases glutamatergic transmission and hyperpolarizes approximately 50% of MEC – LII principal cells (Pralong and Magistretti, 1994) by increasing potassium conductance (Pralong and Magistretti, 1995). Interestingly,  $\alpha$ 2-induced hyperpolarization occurs in a higher proportion of MEC – LIII cells than MEC – LII, and this  $\alpha$ 2 activation does not alter cell excitability in MEC – LV and MEC – LVI (Xiao et al., 2009), further highlighting the importance of recording from one discrete layer.

Unlike  $\alpha$ -ARs,  $\beta$ -AR activation is generally excitatory and can block spike frequency adaptation in hippocampal CA1 pyramidal cells and dramatically increase number of spikes per stimulus (Madison and Nicoll, 1982). In the EC,  $\beta$ -AR activation facilitates evoked glutamatergic transmission (Lacaille and Harley,

1985). Taken together, the effects of NE on ARs in the MEC may prove just as important as the effects of NE on the hippocampus, and further, may demonstrate a crucial role of the connection between sympathetic nervous system activation and spatial memory processing deficits.

### **Effect of Stress on Medial Entorhinal Cortex Circuitry**

Within the MEC, layer II houses a complex network of principal cells and inhibitory interneurons, including several cell types that possess unique intrinsic characteristics capable of encoding spatial information. Preliminary evidence has shown that chronic stress causes a decrease in total dendritic arbor (Fig. 1.2 A) and number of dendritic segments (Fig. 1.2 B) of MEC – LII principal cells (Homiack and Mahnke, unpublished). The fact that stress can alter dendritic architecture indicates a potential mechanism for stress-induced signaling changes in MEC-LII circuits.

**Figure 1.2 – Chronic stress altered dendritic architecture in MEC – LII principal cells.**

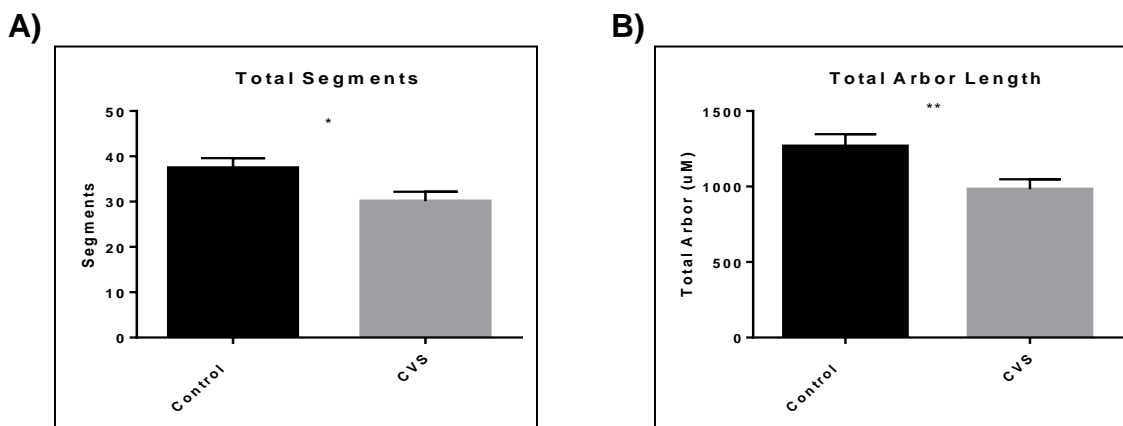


**Fig. 1.2:** Preliminary results from a sholl analysis of MEC – LII principal cell dendrites in golgi-stained brain slices from rats exposed to two weeks of a chronic variable stress (CVS) paradigm. **A)** Rats exposed to the CVS paradigm showed a significant decrease in total number of dendritic segments ( $30.09 \pm 2.08$ ,  $n=33$ ) in MEC – LII principal cells when compared to the control group ( $37.44 \pm 2.14$ ,  $n=36$ ,  $p=0.02$ ). **B)** Rats exposed to the CVS paradigm showed a significant decrease in total arbor length ( $982.16 \pm 65.53 \mu\text{M}$ ,  $n= 33$ ) in MEC – LII principal cells when compared to the control group ( $1267.22 \pm 79.41 \mu\text{M}$ ,  $n=36$ ,  $p<0.01$ ) (Figure adapted from results obtained by Homiack and Mahnke).

## **CHAPTER 2**

# **RAPID EFFECTS OF GLUCOCORTICOIDS ON SYNAPTIC SIGNALING IN MEDIAL ENTORHINAL CORTEX LAYER II PRINCIPAL CELLS**

## **CHAPTER 2: RAPID EFFECTS OF GLUCOCORTICOIDS ON SYNAPTIC SIGNALING IN MEDIAL ENTORHINAL CORTEX LAYER II PRINCIPAL CELLS**

### **Introduction**

Perceived challenges and uncontrollable events, better known as stressors, activate the HPA axis and cause release of glucocorticoids into the organism's bloodstream. This process is thought to be the adaptive physiological response to allow an organism to respond to the stressful stimuli (Miller and O'Callaghan, 2002; Tsigos and Chrousos, 2002). Glucocorticoids are important for metabolic responses, and after a stressor, glucocorticoids are released from the adrenal cortex and take ten or more minutes to reach peak circulating levels. Once peak circulating levels are reached in response to stress, it may take hours for glucocorticoid levels to return to baseline (Droste et al, 2008; Ulrich-Lai and Herman, 2009).

Glucocorticoids readily cross the blood-brain barrier and can act on both glucocorticoid receptors (GR) and mineralocorticoid receptors (MR), causing a range of effects. Glucocorticoids target receptors in the HC (McEwen, 2007; Gibbs et al., 2010; O'Dell et al., 2015) to alter local dendritic architecture and modulate hippocampal pyramidal cell signaling. Prolonged elevation of glucocorticoid levels is sufficient to cause dendritic atrophy in the HC (Woolley et al., 1990; Magarinos et al., 1998), which can lead to signaling changes within spatial processing circuits. The magnitude of glucocorticoids' effects on

pyramidal cell signaling follows a dose-dependent inverted-U pattern as glucocorticoid levels increase (Diamond et al., 1992). At intermediate levels, corticosterone has been shown to promote synaptic strengthening and long-term potentiation (LTP) (Wiegart et al., 2006; Pavlides et al., 1996; Kerr et al., 1994), increase the frequency of mini excitatory post-synaptic currents (mEPSCs) (Karst et al., 2005), and increase glutamate release probability (Olijslagers et al., 2008). At high concentrations, glucocorticoids facilitate LTD achieved by low frequency stimulation in the HC (Pavlides et al., 1995; Kerr et al., 1994).

Evidence that glucocorticoids can alter both dendritic architecture and signaling in the HC provides a possible mechanism for how chronic glucocorticoid elevation (Sandi, 2004; Cerqueira et al., 2005), or blockade of GR (Oitzl et al., 1997) can impair male rodents' performance on spatial memory tasks. Importantly, though the effects of glucocorticoids on both the hippocampus and spatial memory have been well studied, spatial memory processing requires functional interaction between the hippocampus and the entorhinal cortex (Nakashiba et al., 2008). Given the overwhelming evidence of the importance of the MEC networks for spatial memory processing, it is likely that glucocorticoids can act on these networks to contribute to spatial memory processing disruptions.

MEC-LII contains four principal cell classes: stellate, pyramidal, intermediate stellate, and intermediate pyramidal (Fuchs et al., 2016). Both types of stellate cell send projections to the DG of the hippocampus, while neither of the two pyramidal cell classes have direct connectivity to the DG, and instead project directly to CA1 and the contralateral MEC (Varga et al., 2010). MEC-LII

also contains multiple inhibitory cell classes including PV<sup>+</sup> FSIs, CCKBCs, and SOM<sup>+</sup> interneurons (Miettinen et al., 1996; Varga et al., 2010; Lee et al., 2010). The connectivity between the principal cells and inhibitory interneurons form a dense and complex network, but the role of these networks in generating and sustaining spatial characteristics in individual cells, along with their contributions to spatial memory processing, are not yet fully understood.

Given that both stellate and pyramidal cell classes are connected directly to hippocampal subregions (Varga et al., 2010) and possess intrinsic properties demonstrating the ability encode spatial information (Alonso and Klink, 1993; Hafting et al., 2005; Domnisoru et al., 2013; Tang et al., 2014), any disruption of spatial memory processing could affect both stellate and pyramidal cell signaling. Because stellate cells are connected to each other exclusively through inhibitory interneurons and do not form excitatory connections with other LII principal cells (Couey et al., 2013; Pastoll et al., 2013), along with the fact that MEC-LII has an extensive and relatively strong inhibitory network interwoven with four principal cell types, alterations to signaling between principal cells and local inhibitory interneurons is the most likely mechanism for spatial processing disruption underlying the link between stress and spatial memory deficits. In the present study, we test the effect of glucocorticoids on signaling inputs, both excitatory and inhibitory, in MEC – LII principal cells. Our results demonstrate that glucocorticoids do not affect excitatory transmission, but significantly reduce the frequency of spontaneous inhibitory post-synaptic currents (sIPSCs), and that the

decreased frequency of inhibitory inputs onto MEC – LII principal cells is spike-dependent.

### **Brain Slice Preparation**

The Tulane University Institutional Animal Care and Use Committee (IACUC) approved all procedures. C57Bl/6 male mice were obtained from Charles River and anesthetized with isoflurane (VetOne) inhalation and decapitated using a rodent guillotine. The mouse brains were immersed in 0-1°C NMDG-containing artificial cerebrospinal fluid (ACSF) composed of (in mM): 110 NMDG, 110 HCl, 3KCl, 10 MgCl<sub>2</sub>, 1.1 NaH<sub>2</sub>PO<sub>4</sub>, 0.5 CaCl<sub>2</sub>, 25 glucose, 3 pyruvic acid, 10 ascorbic acid, and 25 NaHCO<sub>3</sub>, with an osmolarity of 305-315 mOsm/L and a pH of 7.2-7.3. Sagittal slice preparations of 300 μm thickness were prepared and transferred to a storage chamber where they were maintained at room temperature in carboxygen-bubbled physiological artificial cerebrospinal fluid (ACSF) containing (in mM): 124 NaCl, 2.5 KCl, 25 NaHCO<sub>3</sub>, 1.2 NaH<sub>2</sub>PO<sub>4</sub>, 20 Glucose, 1 MgCl<sub>2</sub>, 2 CaCl<sub>2</sub>, with an osmolarity of 290-300 mOsm/L and a pH of 7.2-7.3.

### **Electrophysiological Recordings**

MEC slices were transferred to submersion recording chamber continuously perfused with 34-37°C ACSF. Whole-cell patch clamp recordings of principal cells were achieved in dorsal MEC – LII (Fig. 2.1 A) using a MultiClamp

700B amplifier (Molecular Devices) at a holding potential of -65 mV. Patch pipettes were formed on a horizontal puller (P97; Sutter Instruments) with a tip resistance of 2-6 M $\Omega$ .

For excitatory post-synaptic current (EPSC) recordings, patch electrodes were filled with an intracellular solution containing (in mM): 120 K $\text{Glu}$ , 20 KCl, 0.2 EGTA, 10 HEPES, 4 NaCl, 4 ATP-Mg, 14 Phosphocreatine, 0.3 TrisGTP, with an osmolarity of 300-310 mOsm/L and a pH adjusted to 7.2-7.3 with KOH.

Tetrodotoxin (TTX, 1 $\mu\text{M}$ ) was added to the bath when recording miniature EPSCs. For inhibitory post-synaptic current (IPSC) recordings, patch electrodes were filled with a high chloride intracellular solution containing (in mM): 120 CsCl, 30 HEPES, 2 MgCl<sub>2</sub>, 1 CaCl<sub>2</sub>, 11 EGTA, 4 ATP-Mg, with an osmolarity of 300-310 mOsm/L and a pH adjusted to 7.2-7.3 with CsOH. Excitatory glutamate receptor-mediated transmission was blocked by adding APV (50 $\mu\text{M}$ ) and DNQX (20 $\mu\text{M}$ ) to the bath. Tetrodotoxin (TTX, 1 $\mu\text{M}$ ) was added to the bath when recording miniature IPSCs.

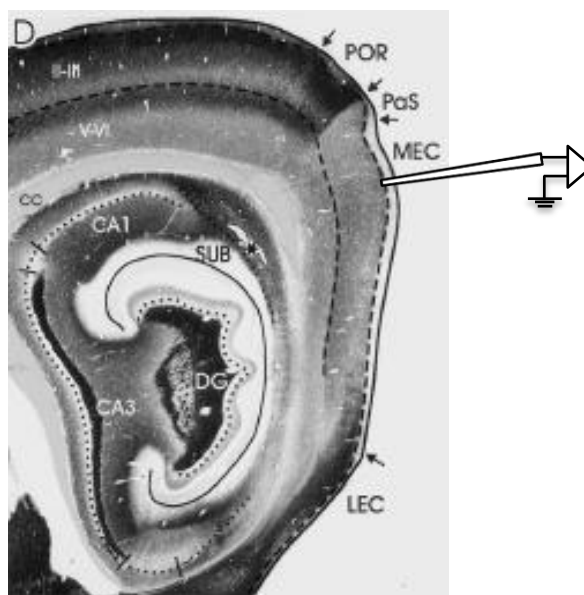
Following seal rupture, the cell was allowed to stabilize for five minutes prior to recording. Only cells with an access resistance of less than 20 M $\Omega$  and less than 20% change in access resistance over the course of the recording were used. All experimental recording conditions were performed with either dexamethasone (1  $\mu\text{M}$ ) or corticosterone (1  $\mu\text{M}$ ) perfused into the bath. EPSCs and IPSCs were recorded in voltage clamp at a holding potential of -65 mV for a minimum of two minutes in control condition prior to infusion of ACSF containing dexamethasone (Dex) or corticosterone (Cort). Voltage clamp recordings were

obtained periodically over time following perfusion of the drug. Experimental conditions were achieved for a minimum of 10 minutes to ensure maximal drug effect (Fig. 2.1 B).

Recordings of synaptic activity were analyzed using MiniAnalysis. Comparisons of one-minute averages representative of the control and maximum drug effect for synaptic activity frequency, inter-event interval, amplitude, and decay time between control and drug-treated cells were calculated using a repeated measures paired t-test. All statistical tests were performed in GraphPad Prism using paired t-tests between control and drug conditions. P-values  $<0.05$  were considered significant.

**Figure 2.1 – Whole-cell patch clamp recording protocol in MEC – LII.**

**A)**



**B)**

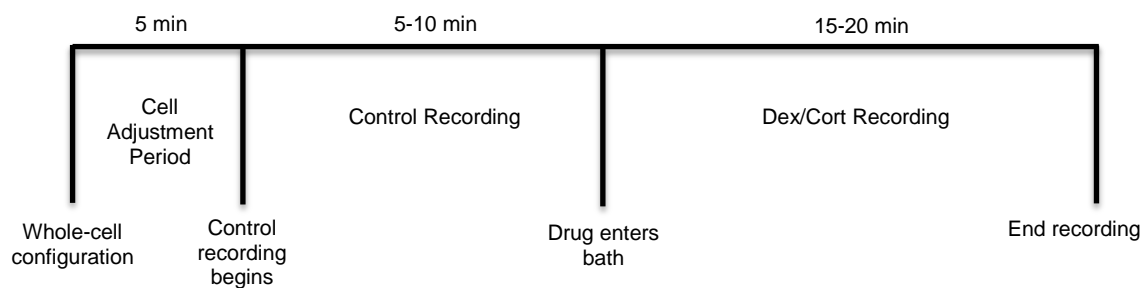


**Fig. 2.1: A)** Schematic of recording location for a parasagittal slice in layer II of the dorsal MEC. POR: post-rhinal cortex; PaS: parasubiculum; MEC: medial entorhinal cortex; LEC: lateral entorhinal cortex. Note the targeting of the principal cells at the most dorsal region of LII on the superficial edge bordering LI. (Adapted from Witter et al., 2000b). **B)** Timeline for whole-cell recordings of MEC-LII principal cells.

**Results:****Dexamethasone had no consistent effect on spontaneous excitatory synaptic activity in MEC – LII principal cells**

Spontaneous EPSCs (sEPSCs) were recorded at a holding potential of -65 mV (Fig 2.2 A). After ten minutes of Dex (1  $\mu$ M) perfusion, sEPSCs were recorded again (Fig. 2.2 B). Dex failed to significantly alter sEPSC frequency ( $p=0.18$ ), amplitude ( $p=0.53$ ), or decay time ( $p=0.15$ ) (Fig. 2.2 C-F), indicating that Dex does not significantly alter spontaneous excitatory signaling onto principal cells in MEC – LII (Table 1-3).

In order to ensure that Dex did not cause a terminal-specific effect on excitatory connections that was masked by spike-driven signaling, miniature EPSCs (mEPSCs) were recorded from MEC – LII principal cells (Fig. 2.3 A) in the presence of tetrodotoxin (TTX), a voltage-gated sodium channel blocker to block action potentials. After ten minutes of Dex (1  $\mu$ M) perfusion, mEPSCs were recorded again (Fig. 2.3 B). Dexamethasone failed to significantly alter mEPSC frequency ( $p=0.46$ ), amplitude ( $p=0.35$ ), or decay time ( $p=0.27$ ) (Fig. 2.3 C-F), indicating that Dex does not significantly alter terminal-specific glutamate release in MEC – LII principal cells (Table 1-3).

**Figure 2.2 – Dexamethasone application had no effect on spontaneous excitatory signaling in MEC – LII principal cells.**

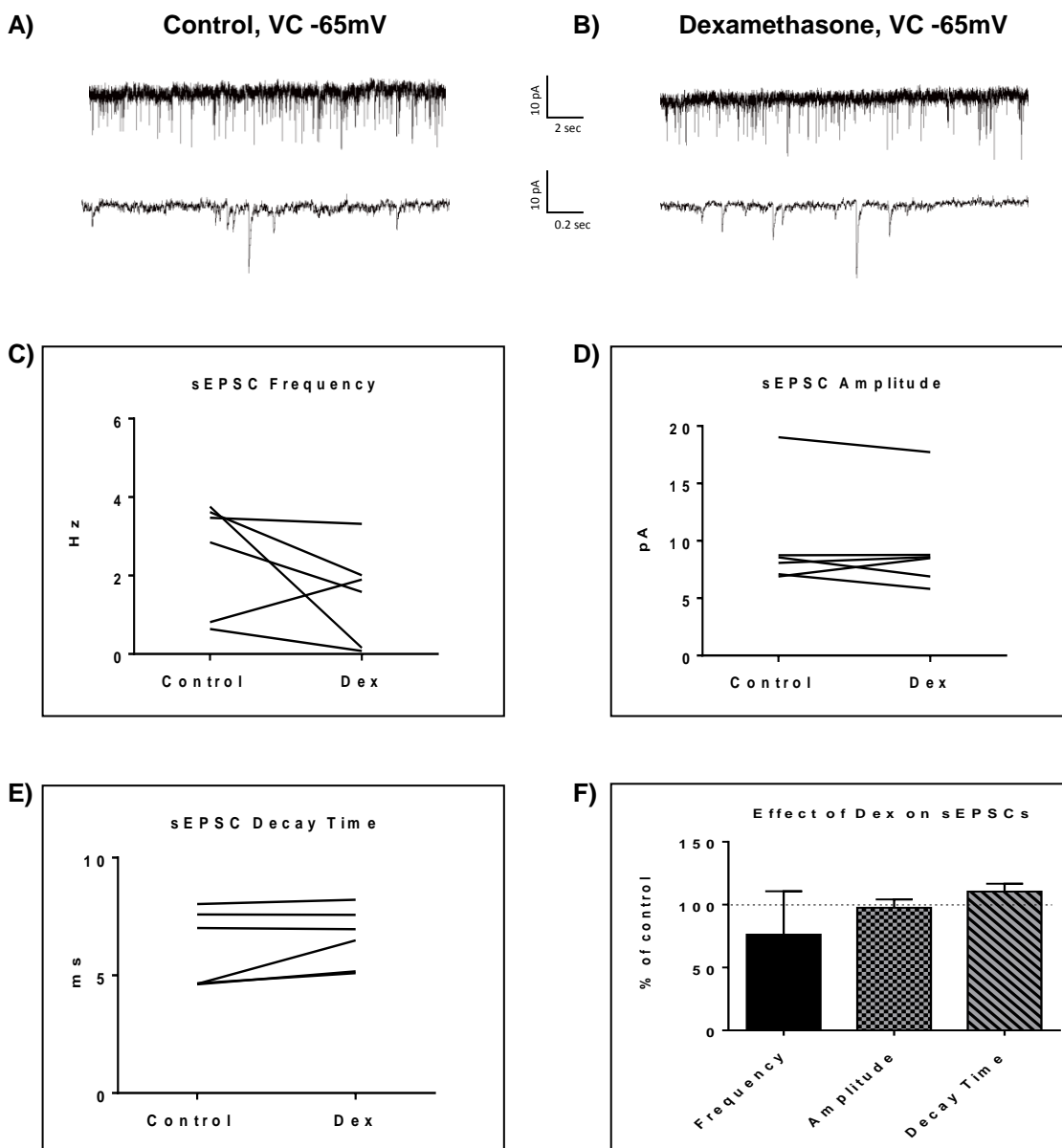


**Fig. 2.2: A,B Top)** 20 seconds of sEPSC voltage-clamp recordings representative of control (A) and Dex (B) conditions. **A,B Bottom)** 1 second interval from the voltage-clamp recording shown above. **C)** Dex had no effect on average sEPSC frequency. **D)** Dex had no effect on average sEPSC amplitude. **E)** Dex had no effect on average sEPSC decay time. **F)** Frequency, amplitude, and decay time in the Dex-treated condition plotted against the normalized average for each of the corresponding control groups. Dex had no effect on sEPSC frequency, decay time, or amplitude when normalized and compared to the corresponding control group average (n=6).

**Figure 2.3 – Dexamethasone had no effect on mEPSCs in MEC – LII principal cells.**

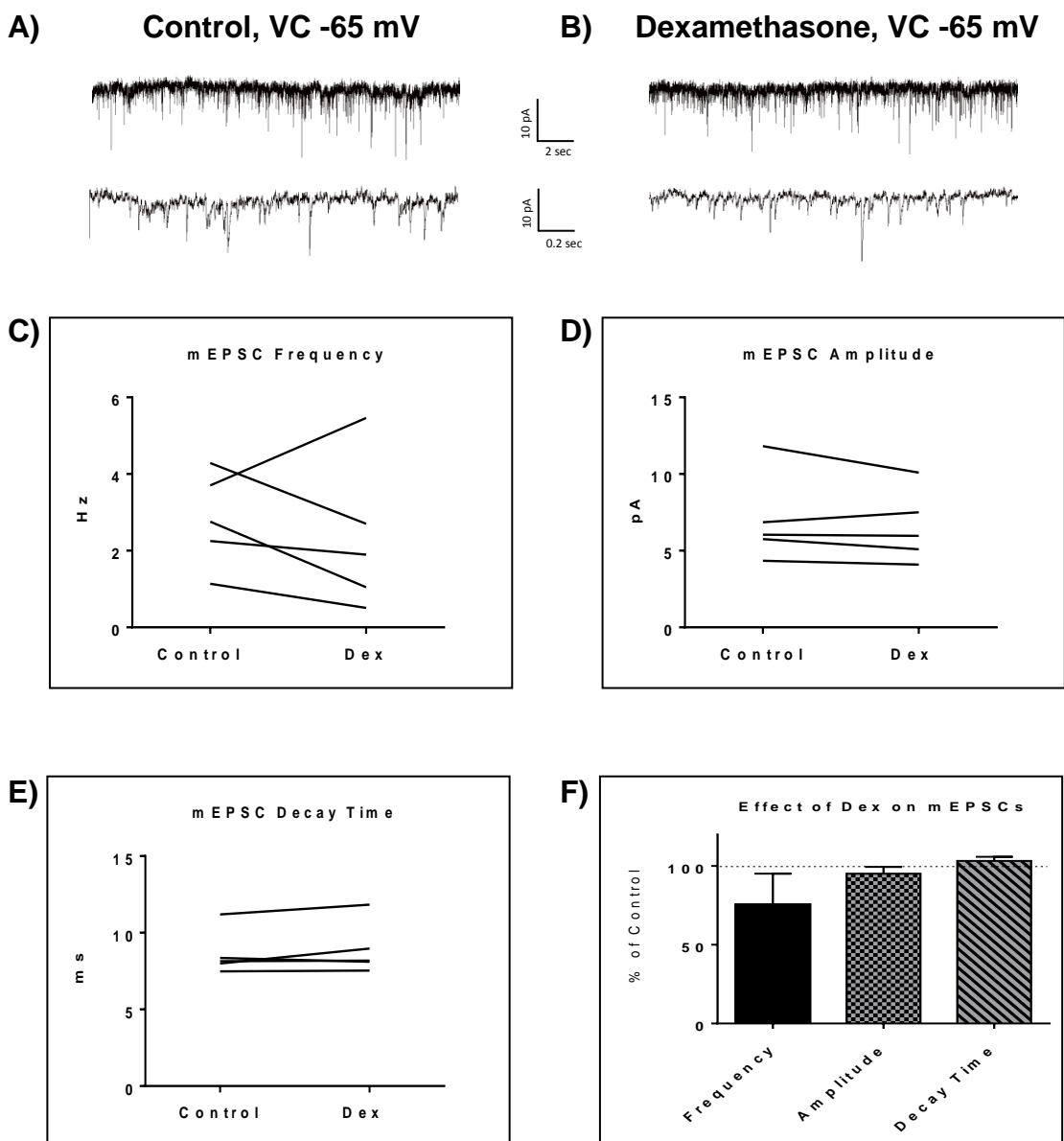


**Fig. 2.3: A,B Top)** 20 seconds of mEPSC voltage-clamp recordings representative of control (A) and Dex (B) conditions. **A,B Bottom)** 1 second interval from the voltage-clamp recording shown above. **C)** Dex had no effect on average mEPSC frequency. **D)** Dex had no effect on average mEPSC amplitude. **E)** Dex had no effect on average mEPSC decay time. **F)** Frequency, amplitude, and decay time in the Dex-treated condition plotted against the normalized average for each of the corresponding control groups. Dex had no effect on mEPSC frequency, decay time, or amplitude when normalized and compared to the corresponding control group average (n=5).

### **Dexamethasone significantly decreased spontaneous IPSC frequency, but not amplitude, in MEC – LII principal cells**

Spontaneous IPSCs (sIPSCs) were recorded at a holding potential of -65 mV (Fig 2.4 A). After ten minutes of Dex (1  $\mu$ M) perfusion, sIPSCs were recorded again (Fig. 2.4 B). Dex significantly decreased sIPSC frequency ( $p=0.04$ ), but did not significantly alter sIPSC amplitude ( $p=0.31$ ), or decay time ( $p=0.49$ ) (Fig. 2.4 C-F), indicating that Dex significantly decreased the frequency of spontaneous inhibitory signaling onto MEC – LII principal cells without significantly affecting amplitude or decay time of inhibitory synaptic events (Table 1-3).

In 4 of 15 (~27%) cells analyzed, dexamethasone application caused an initial increase in sIPSC frequency (during the first five minutes of perfusion) into the submersion chamber (Fig. 2.4 G). It appeared that initial exposure to dexamethasone caused bursting-like behavior in these cells; however, there were no significant differences in burst density (events per burst) or total number of bursts between control and dexamethasone conditions ( $t=0.5702$ ,  $df=14$ ,  $p=0.5776$ ) (Fig. 2.5 B).

Because the first several minutes of drug perfusion into the submersion chamber would expose the cells to lower concentrations of dexamethasone than later time points when the concentration reaches 1  $\mu$ M, we tested the effects of low concentrations (10 and 100nM) on sIPSC frequency, amplitude, and decay time. When recording modulation of synaptic signaling in brain slices of the amygdala and hippocampus, Dex and Cort half-maximal effective concentrations ( $EC_{50}$ ) have been reported as 50-350nM with 100nM and 1  $\mu$ M used as a

common dose (Di et al., 2016; Wiegart et al., 2006). We tested the effects of Dex on sIPSC frequency, amplitude, and decay time at concentrations of 10 nM, 100 nM, and 1  $\mu$ M. Dex failed to significantly alter sIPSC frequency at both 10 nM ( $p=0.44$ ) and 100 nM ( $p=0.79$ ), but does significantly decrease sIPSC frequency at 1  $\mu$ M ( $p=0.01$ ) (Fig. 2.6 A). Dex had no effect on sIPSC amplitude at 10 nM ( $p=0.69$ ), 100 nM ( $p=0.22$ ), or 1  $\mu$ M ( $p=0.57$ ) (Fig. 2.6 B). Dex also had no effect on sIPSC decay time at 10 nM ( $p=0.43$ ), 100 nM ( $p=0.11$ ), or 1  $\mu$ M ( $p=0.07$ ) (Fig. 2.6 C). Because Dex at 1  $\mu$ M was the only concentration to produce a significant change in frequency of spontaneous inhibitory signaling, all experiments were performed at this concentration (Table 1-3).

To determine the effect of Dex on miniature IPSCs (mIPSCs), recordings were performed on MEC – LII principal cells (Fig. 2.7 A) in the presence of tetrodotoxin (TTX), a voltage-gated sodium channel blocker. After ten minutes of Dex (1  $\mu$ M) perfusion, mIPSCs were recorded again (Fig. 2.7 B). Dex failed to significantly alter mIPSC frequency ( $p=0.59$ ), amplitude ( $p=0.65$ ), or decay time ( $p=0.20$ ) (Fig. 2.7 C-F), indicating that Dex does not significantly alter terminal-specific GABA signaling in MEC – LII principal cells (Table 1-3).

**Figure 2.4 – Dexamethasone significantly decreased frequency, but not amplitude, of spontaneous inhibitory signaling in MEC – LII principal cells.**

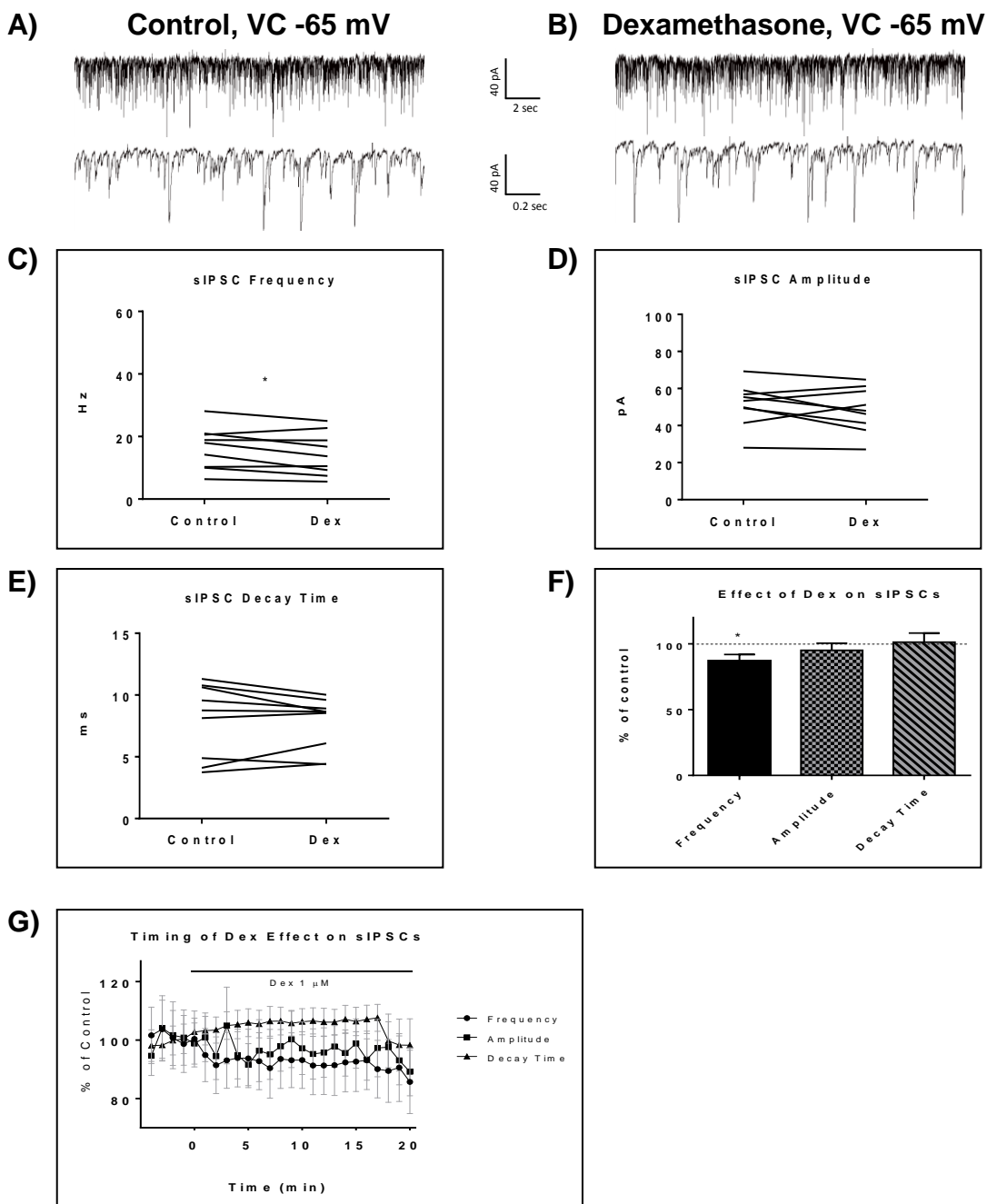


**Fig. 2.4: A,B Top)** 20 seconds of sIPSC voltage-clamp recordings representative of control (A) and Dex (B) conditions. **A,B Bottom)** 1 second of the voltage-clamp recordings shown above. **C)** Dex significantly decreased sIPSC frequency. **D)** Dex had no effect on sIPSC amplitude. **E)** Dex had no effect on average sIPSC decay time. **F)** Dex significantly decreased sIPSC frequency, but not decay time or amplitude, when normalized and compared to the corresponding control group average. **G)** Time course of the Dex effect in one-minute intervals. Dex enters at 0 min and quickly decreases frequency, but not amplitude or decay time (n=9).

**Figure 2.5 – Dexamethasone did not affect sIPSC burst behavior.**

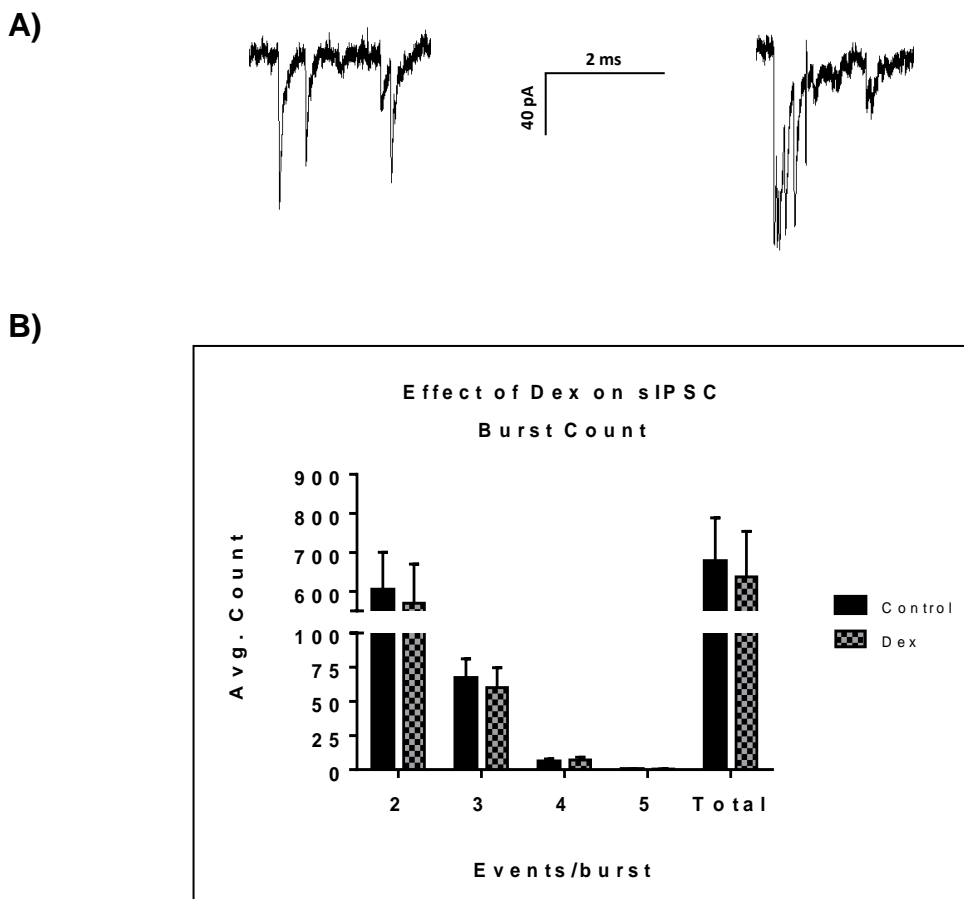


**Fig. 2.5: A)** Example voltage-clamp traces showing non-bursting sIPSCs (left) and a compound burst (right). **B)** X-axis: Bursting behavior was analyzed using MiniAnalysis. IPSC bursting was analyzed by counting the total number of bursts and separating them into groups based on number of events within a given burst. Bursting behavior calculation requires an inter-event interval of <10ms to be considered a burst. Y-axis: Number of bursts in Dex 1  $\mu$ M normalized to control number of bursts. A value of 100% indicates that number of control bursts is the same as in drug condition. 15 cells were analyzed for bursting behavior before and after Dex application. No significant differences in bursting behavior were found between control and Dex-treated cells.

**Figure 2.6 - Dose-dependent effects of dexamethasone on spontaneous IPSCs.**

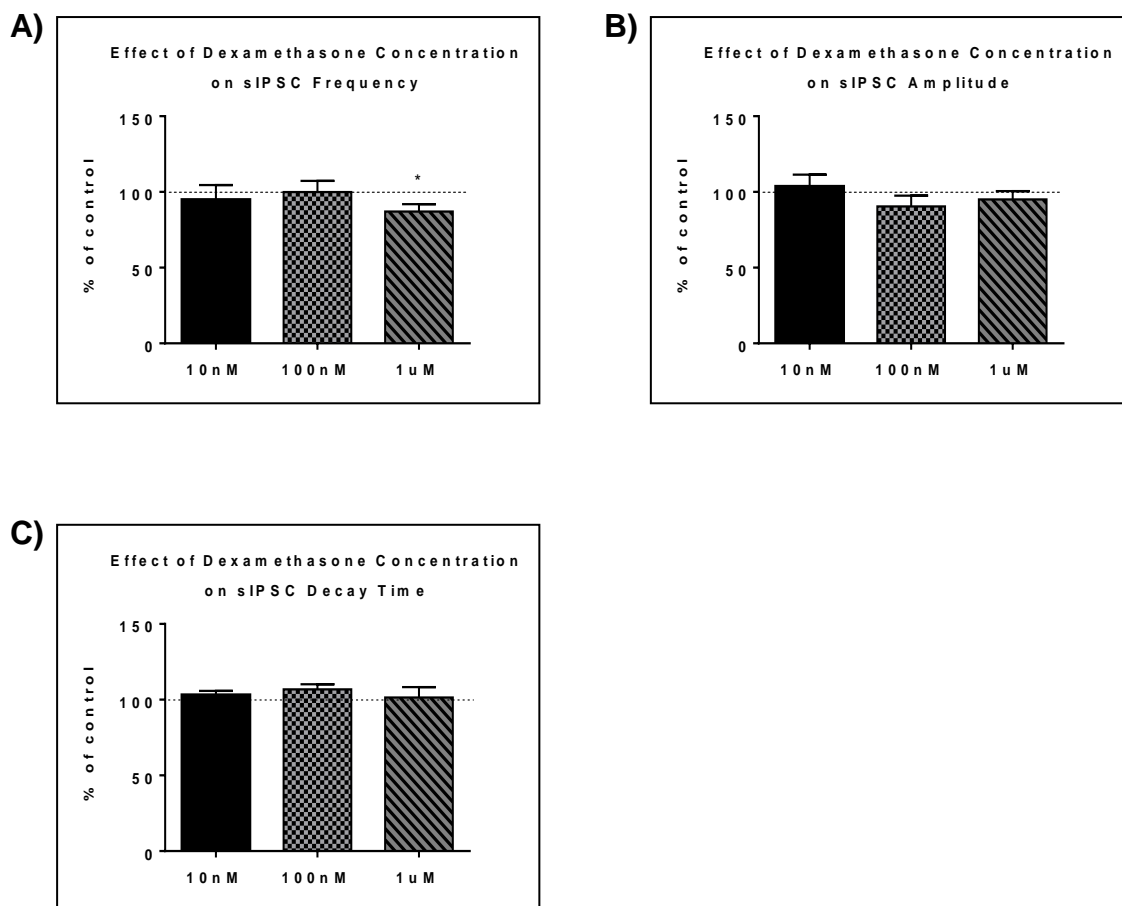


**Fig. 2.6: A)** Effect of Dex at varying concentrations on sIPSC frequency. Dex significantly decreased sIPSC frequency at 1 μM, but not 10 or 100 nM. **B)** Effect of Dex at varying concentrations on sIPSC amplitude. Dex had no effect on sIPSC amplitude at any of the three concentrations tested. **C)** Effect of Dex at varying concentration on sIPSC decay time. Dex had no effect on sIPSC decay time at any of the three concentrations tested.

**Figure 2.7 - Dexamethasone had no effect on terminal-specific inhibitory signaling in MEC – LII principal cells.**

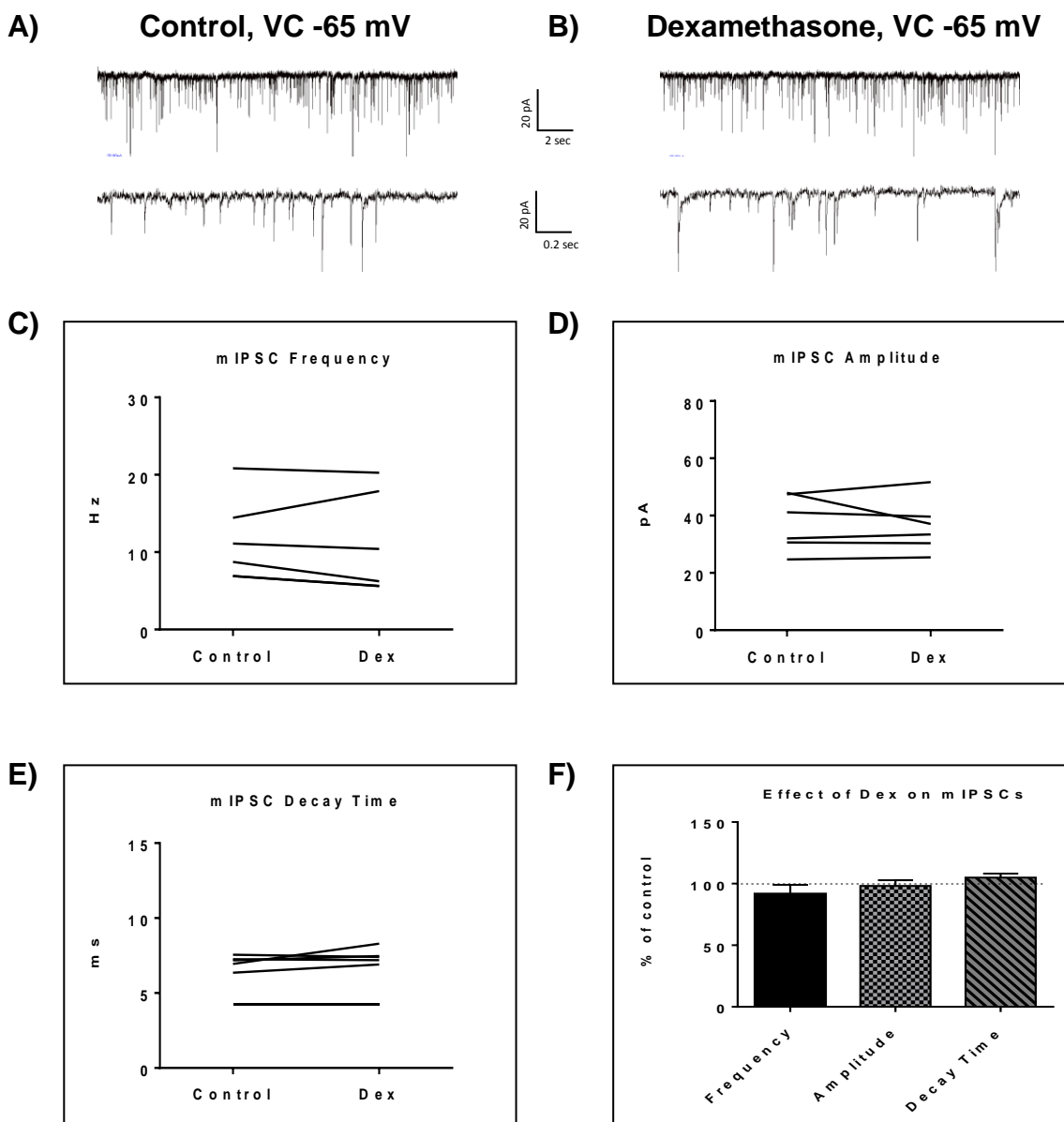


**Fig. 2.7: A,B Top)** 20 seconds of mIPSC voltage-clamp recordings representative of control (A) and Dex (B) conditions. **A,B Bottom)** 1 second of the voltage-clamp recordings shown above. **C)** Dex had no effect on mIPSC frequency. **D)** Dex had no effect on mIPSC amplitude. **E)** Dex had no effect on average mIPSC decay time. **F)** Dex had no effect on mIPSC frequency, decay time, or amplitude when normalized and compared to the corresponding control group average (n=6).

**Corticosterone significantly decreased spontaneous IPSC frequency, but not amplitude, in MEC – LII principal cells**

Because dexamethasone is a synthetic glucocorticoid and GR-specific agonist, it is necessary to replicate the Dex-induced decrease in sIPSC frequency using the naturally circulating glucocorticoid in male mice: corticosterone. sIPSCs were recorded at a holding potential of -65 mV (Fig 2.8 A). After ten minutes of Cort (1  $\mu$ M) perfusion, sIPSCs were recorded again (Fig. 2.8 B). Cort significantly decreased sIPSC frequency to ( $p=0.01$ ), but did not significantly alter sIPSC amplitude ( $p=0.09$ ) or decay time ( $p=0.17$ ) (Fig. 2.8 C-F), indicating that Cort significantly decreases the frequency of spontaneous inhibitory signaling onto MEC – LII principal cells without significantly affecting amplitude or decay time of inhibitory synaptic events. Cort application mimics the effect of dexamethasone application on inhibitory signaling in MEC – LII (Table 1-3).

**Figure 2.8 – Corticosterone significantly decreased frequency, but not amplitude, of spontaneous inhibitory signaling in MEC – LII principal cells.**

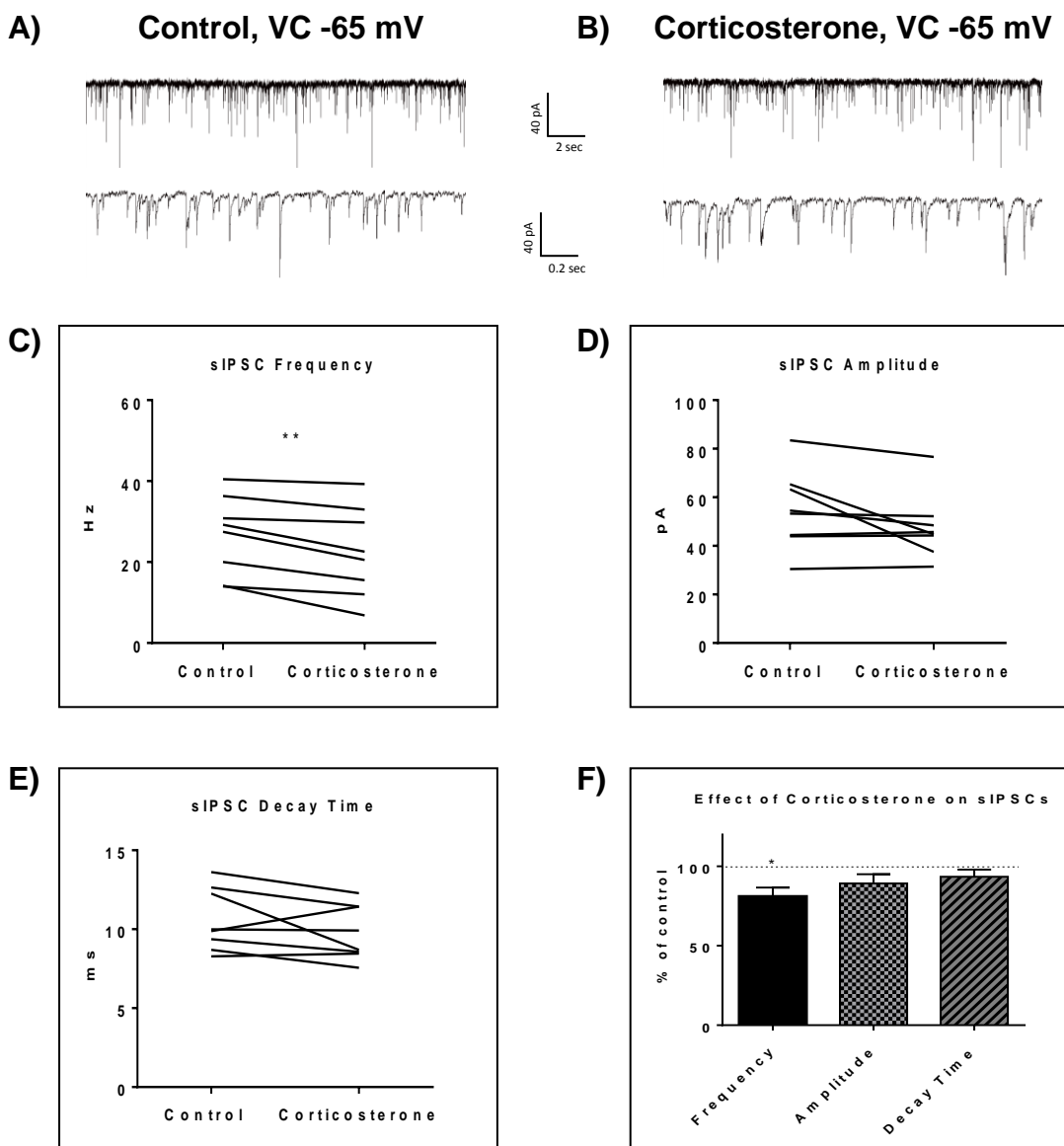


**Fig. 2.8: A,B Top)** 20 seconds of sIPSC voltage-clamp recordings representative of control (A) and Cort (B) conditions. **A,B Bottom)** 1 second of the voltage-clamp recordings shown above. **C)** Cort significantly decreased sIPSC frequency. **D)** Cort had no effect on sIPSC amplitude. **E)** Cort had no effect on sIPSC decay time. **F)** Cort had decreased sIPSC frequency, but not decay time or amplitude, when normalized and compared to the corresponding control group average (n=8).

**Table 1 – Effect of glucocorticoids on frequency of excitatory and inhibitory synaptic transmission**

Recording Type	Control (Hz ± SEM)	Dex -1 µM (Hz ± SEM)	t	df (n-1)	p	% of Control	t	df	p
sEPSCs	2.52 ± 1.13	1.51 ± 0.67	1.58	5	0.18	76.21 ± 34.45	0.69	5	0.52
mEPSCs	2.83 ± 1.26	2.32 ± 1.04	0.81	4	0.46	75.45 ± 33.74	1.25	4	0.28
sIPSCs	16.38 ± 2.26	14.4 ± 2.28	2.42	8	<b>0.04*</b>	87.01 ± 4.94	2.63	8	<b>0.03*</b>
sIPSCs Dex – 10nM	21.74 ± 4.92	19.21 ± 4.18	0.84	5	0.44	94.82 ± 9.79	0.53	5	0.62
sIPSCs Dex – 100nM	30.87 ± 4.74	31.60 ± 5.71	0.28	8	0.79	99.88 ± 7.39	0.02	8	0.99
mIPSCs	11.49 ± 2.21	11.01 ± 2.67	0.58	5	0.59	91.51 ± 7.50	1.13	5	0.31
sIPSCs Cort -1 µM	26.55 ± 3.46	22.44 ± 3.90	3.5	7	<b>0.01*</b>	81.05 ± 5.6	3.39	7	<b>0.01*</b>

**Table 2 – Effect of glucocorticoids on amplitude of excitatory and inhibitory synaptic transmission**

Recording Type	Control (pA ± SEM)	Dex - 1 µM (pA ± SEM)	t	df (n-1)	p	% of Control	t	df	p
sEPSCs	9.73 ± 4.35	9.38 ± 4.19	0.67	5	0.53	97.59 ± 6.60	0.36	5	0.73
mEPSCs	6.97 ± 3.12	6.55 ± 2.93	1.06	4	0.35	95.2 ± 42.57	1.13	4	0.32
sIPSCs	51.37 ± 3.87	48.45 ± 4.04	1.08	8	0.31	95.11 ± 5.41	0.91	8	0.39
sIPSCs Dex – 10nM	58.34 ± 9.44	60.66 ± 12.27	0.42	5	0.69	103.56 ± 7.85	0.45	5	0.67
sIPSCs Dex – 100nM	70.83 ± 9.19	62.45 ± 8.28	1.33	8	0.22	90.38 ± 7.17	1.34	8	0.22
mIPSCs	37.31 ± 3.93	36.28 ± 3.69	0.49	5	0.65	98.24 ± 4.53	0.39	5	0.71
sIPSCs Cort - 1 µM	54.85 ± 5.7	47.65 ± 4.72	1.96	7	0.09	89.21 ± 5.86	1.84	7	0.11

**Table 3 – Effect of glucocorticoids on decay time of excitatory and inhibitory synaptic transmission**

Recording Type	Control (ms ± SEM)	Dex - 1 μM (ms ± SEM)	t	df (n-1)	p	% of Control	t	df	p
sEPSCs	6.09 ± 2.49	6.58 ± 2.69	1.7	5	0.15	110.39 ± 6.27	1.66	5	0.16
mEPSCs	8.64 ± 3.86	8.93 ± 3.99	1.28	4	0.27	103.20 ± 46.15	1.21	4	0.29
sIPSCs	7.99 ± 1.0	7.70 ± .72	0.73	8	0.49	101.39 ± 6.91	0.2	8	0.85
sIPSCs Dex – 10nM	7.46 ± 0.62	7.62 ± 0.56	0.86	5	0.43	103.02 ± 2.83	1.07	5	0.34
sIPSCs Dex – 100nM	7.46 ± 0.60	7.95 ± 0.67	1.82	8	0.11	106.84 ± 3.33	2.05	8	0.07
mIPSCs	6.59 ± 0.50	6.92 ± 0.56	1.46	5	0.2	104.94 ± 3.30	1.5	5	0.19
sIPSCs Cort - 1 μM	10.59 ± 0.70	9.79 ± 0.61	1.53	7	0.17	93.40 ± 4.58	1.44	7	0.19

## Discussion

In this study, we demonstrated that dexamethasone does not affect excitatory transmission, but does alter inhibitory transmission. Dex at a relatively high concentration (1 $\mu$ M) does not have a reliable effect on excitatory signaling in MEC – LII principal cells. It is important to note the marked decrease in the sEPSC frequency average did not reach significance because 2 of the 6 cells showed an increase in frequency. Given the striking contrast in intrinsic properties and connectivity of the different principal cell types in MEC – LII, it is highly likely that Dex differentially affects excitatory signaling depending on cell type. This could explain the presence of seemingly opposite effects on frequency in 1/3 of the cells recorded; however, the number of cells recorded is low, and the addition of more recordings from principal cells could reveal any differential effects of Dex that would warrant a separation into response groupings. Identification of cell type paired with recordings of excitatory signaling could quickly determine if Dex differentially affects the four principal cell types in MEC – LII, and could prove useful for future experiments.

Given that signaling through inhibitory networks is necessary for proper functioning of grid cells and spatial memory processing, and that stress causes disruptions of spatial memory processing, it is not surprising that exposure to stress hormones, both Cort and Dex, is sufficient to consistently disrupt inhibitory signaling in MEC – LII principal cells. Furthermore, the Dex-induced decrease in frequency of inhibitory signaling is action potential-dependent, meaning that Dex is acting at the cell soma and not at the terminal to affect this signaling change. It

is important to note that the effect of Cort on miniature IPSC recordings was not tested; however, it is expected that the result would match the effect of Dex, and that the reduction of sIPSC frequency with Cort would require spiking. These results are consistent with the current understanding of the importance of the local MEC – LII inhibitory networks in terms of their high density and their role as an exclusive relay for signaling between stellate cells. These results also implicate signaling changes involving the MEC – LII inhibitory networks as a likely culprit underlying spatial memory deficits seen in male mice exposed to acute and chronic stressors. Behavioral manipulation in the form of acute or chronic stress may cause a disruption of the signaling within MEC – LII by modulating local inhibition to disrupt spatial memory processing. Ultimately, the glucocorticoid-induced decrease of sIPSC frequency in MEC – LII principal cells may prove sufficient to cause spatial memory processing deficits in an animal performing a spatial maze task, but this remains untested.

## **CHAPTER 3**

**ACTIVATION OF GLUCOCORTICOID  
RECEPTORS IN LAYER II OF THE  
MEDIAL ENTORHINAL CORTEX REVEALS  
ENHANCED NOREPINEPHRINE-  
MEDIATED INHIBITORY SIGNALING**

## **CHAPTER 3: ACTIVATION OF GLUCOCORTICOID RECEPTORS IN LAYER II OF THE MEDIAL ENTORHINAL CORTEX REVEALS ENHANCED NOREPINEPHRINE-MEDIATED INHIBITORY SIGNALING**

### **Introduction**

An organism's response to stress involves activation of two systems: the HPA axis and the sympathetic nervous system. Unlike HPA axis activation, stress-induced activation of the autonomic nervous system is almost immediate and works through neural innervation of organs, resulting in rapid alterations of physiological states (Ulrich-Lai and Herman, 2009). Activation of the sympathetic nervous system, also known as the fight or flight response, causes postganglionic neurons in the spinal cord to release catecholamines, epinephrine/adrenaline, which act on adrenergic receptors in the associated target organs (Malpas, 2010). The promptness of this fight or flight response allows an organism to quickly attend to the perceived stressor by simultaneously activating multiple organs, which results in a variety of responses including pupil dilation, increased blood glucose, increased heart rate, and elevated blood pressure (Tank and Lee Wong, 2015). Because epinephrine and norepinephrine do not readily cross the blood-brain barrier (Weil-Marlherbe and Bone, 1957; Gold, 2014), the systemic rise in catecholamine levels activates  $\beta$ -adrenergic receptors of the vagus nerve, which ultimately activates the nucleus of the solitary tract (NTS) and locus coeruleus (LC) to cause central norepinephrine

release (Roozendaal and McGaugh, 2011; Timmermans et al., 2013; Gold, 2014). Noradrenergic efferents from the LC and NTS regulate neuronal function in a variety of areas including those that are crucial for learning and memory: the hippocampus, prefrontal cortex, and amygdala (Gibbs and Summers, 2002; Roozendaal et al., 2009).

Because the LC is the major source of noradrenergic innervation for most brain areas and all of the hippocampal-dependent memory areas, altering release of NE from the LC can also alter spatial memory. Injection of  $\alpha_2$  agonists into the LC causes membrane hyperpolarization and inhibits NE release, resulting in disruption of discrimination memory in chicks (Gibbs 2010). Conversely, infusion of the  $\alpha_2$  antagonist, idazoxan, into the LC activates and increases release of NE onto its targets and enhances memory retrieval (Sara and Devauges, 1989). These studies highlight a striking ability of NE to modulate spatial memory processing networks through a variety of mechanisms that depend on region and local AR expression.

The entorhinal cortex expresses  $\alpha_1$  (Stanton et al., 1987),  $\alpha_2$  (Boyajian et al., 1987; Unnerstall et al., 1984, 1985; Mitrovic et al., 1992), and  $\beta$ -ARs (Booze et al., 1993). Inhibitory interneurons throughout the brain express both  $\alpha_1$  and  $\beta$ -ARs, but  $\beta_1$  and  $\beta_2$  expression levels vary widely depending on interneuron type (Papay et al., 2006; Cox et al., 2008). In general,  $\alpha$ -AR activation is inhibitory in terms of signaling by causing a decrease in glutamatergic transmission in the HC (Scanziani et al., 1993) and hyperpolarization of cells in the LC (Aghajanian and VanderMaelen, 1982), but behaviorally facilitates locomotion and arousal (Sirvio

and MacDonald, 1999). In 2-3 week old male rodents, NE activates  $\alpha$ 1-ARs and significantly increases sIPSC frequency and amplitude as well as mIPSC frequency, but not mIPSC amplitude in principal cells in MEC-LII and LIII (Lei et al., 2007). Agonists of  $\alpha$ 2-AR in the EC decrease glutamatergic transmission and hyperpolarize approximately 50% of MEC – LII principal cells (Pralong and Magistretti, 1994) by increasing a potassium conductance (Pralong and Magistretti, 1995). Interestingly,  $\alpha$ 2-induced hyperpolarization occurs in a higher proportion of MEC – LIII cells than MEC – LII, and this  $\alpha$ 2 activation does not alter cell excitability in MEC – LV and MEC – LVI (Xiao et al., 2009), highlighting the importance of recording from one discrete layer. Unlike  $\alpha$ -ARs,  $\beta$ -AR activation is generally excitatory, and in the EC,  $\beta$ -AR activation facilitates evoked glutamatergic transmission (Lacaille and Harley, 1985). Overall, NE application reduces action potential firing in more than 50% of MEC-LII and LIII principal cells (Lei et al., 2007). Taken together, the effects of NE on ARs in the MEC may demonstrate a crucial role of the connection between sympathetic nervous system activation and spatial memory processing deficits.

Given that stellate cells are both connected directly to hippocampal subregions (Varga et al., 2010) and possess intrinsic properties demonstrating the ability to encode spatial information (Alonso and Klink, 1993; Hafting et al., 2005), any disruption of spatial memory processing would likely need to affect stellate cell signaling. Because stellate cells are connected to each other through inhibitory interneurons and do not appear to form excitatory connections with other LII principal cells (Couey et al., 2013; Pastoll et al., 2013), alterations in

signaling between stellate cells and local inhibitory interneurons is the most likely mechanism for spatial processing disruption underlying the link between stress and spatial memory deficits. In the present study we test the effect of norepinephrine on inhibitory signaling in MEC – LII principal cells. Because the previous results mentioned above are taken from a mix of MEC-LII and LIII principal cells in rodents prior to full maturation of spatial properties in MEC-LII cells (spatially-tuned cells in MEC-LII are not fully mature until 4 weeks of age), as well as the known differences between LII and LIII including cell type, projection routes, intrinsic characteristics, and inhibitory networks, necessitate testing the effect of NE on solely MEC-LII principal cells in mature animals. Our results demonstrate that norepinephrine can significantly impact both spike-driven and terminal specific inhibitory signaling in MEC – LII principal cells through activation of both  $\alpha 1$  and  $\alpha 2$ -ARs.

In the previous chapter we demonstrated the effects of glucocorticoids, naturally released following HPA axis activation, on MEC-LII principal cells. Sympathetic nervous system-induced release of NE following stress increases NE concentration in the brain. The effects of NE, independent of glucocorticoids, on MEC-LII principal cells have been partially studied in immature rodents as part of a mix of recordings with MEC-LIII. In the previous chapter we demonstrated that glucocorticoids, applied independently, are sufficient to significantly alter inhibitory signaling onto MEC-LII principal cells. This chapter focuses on the effect of NE in mature male mice, solely recording from dorsal MEC-LII. We show that NE can significantly increase the frequency and amplitude of IPSCs in MEC-

LII principal cells; however, it is not known how glucocorticoids and norepinephrine affect MEC-LII principal cells when applied simultaneously, as would be naturally experienced by an organism following a perceived stressor.

Multiple lines of evidence from various systems demonstrate that co-administration of glucocorticoids and NE results in a synergistic effect. Chronic corticosterone elevation causes capillary constriction in rodent skeletal muscle, and that the constriction requires activation of  $\alpha$ 1-AR (Mandel et al., 2016). There is also evidence that corticosterone-induced memory improvement in rodents performing taste-aversion tasks, dorsolateral striatum-dependent habit tasks, and inhibitory avoidance tasks, require the activation of  $\beta$ -ARs (Goodman et al., 2015; Wichmann et al., 2012; McReynolds et al., 2010). Conversely, corticosterone-induced deficits in performance on the hippocampus-dependent novel object recognition task is blocked by  $\beta$ -AR antagonism (Dobarro et al., 2012). Surprisingly, corticosterone-induced improvement in recognition tasks in humans requires  $\alpha$ -AR activation to engage the pre-frontal areas, and without  $\alpha$ -AR activation only the amygdala and HC are activated (van Stegeren et al., 2010). In fact, corticosterone-induced increase in loss-aversion during financial decision making requires the activation of  $\alpha$ 2-AR (Margittai et al., 2017). Finally, corticosterone can excite or inhibit melatonin production in the pineal gland depending on the activation pattern of ARs, where corticosterone promotes wakefulness only if  $\alpha$ 1 and  $\beta$ -ARs are simultaneously active (Fernandes et al., 2017).

It is important to note that the above studies demonstrate changes to transcription that occur at 30 minutes post-drug exposure or later. The majority of genes affected by stress show transcriptional level changes at 30 minutes post-stress, and these changes are blocked by  $\beta$ 2-AR antagonists, and expression levels return to baseline after 90-120 minutes (Roszkowski et al., 2016). It is also known that NE-induced activation of ERK and CREB through  $\alpha$ 2-AR is enhanced by glucocorticoids (Yaniv et al., 2010), but it is also possible that some of the synergistic effects seen with co-administration of stress hormones may be due to glucocorticoid-induced upregulation of NE transporter (NET) expression through a non-conventional transcriptional mechanism (Zha et al., 2011).

In each of the experiments shown in this chapter, the synergistic effects of glucocorticoids and norepinephrine are seen before typical time points for transcriptional level changes via GR and AR, and we would not expect these effects to rely on transcription. There is evidence for rapid non-genomic effects of glucocorticoids on synaptic signaling in multiple brain regions. Corticosterone in the hippocampus can inhibit calcium currents through G-protein activation of protein kinase C (French-Mullen, 1995) and increase mEPSC frequency through the mineralocorticoid receptor (MR) in less than five minutes (Karst et al., 2005). In the hypothalamus, however, dexamethasone can suppress excitatory synaptic transmission and enhance inhibitory synaptic signaling through a GR-dependent mechanism (Nahar et al., 2015), thereby implicating both MR and GR as capable of producing rapid non-genomic effects on synaptic transmission. In this chapter, we show that co-administration of glucocorticoids and norepinephrine produces a

synergistic effect in MEC-LII principal cells that is unlikely to be due to genomic changes, whereby a population of cells previously insensitive to norepinephrine is primed to be norepinephrine-sensitive after 15 minutes of dexamethasone application.

### **Brain Slice Preparation**

The Tulane University Institutional Animal Care and Use Committee (IACUC) approved all procedures. C57Bl/6 male mice were obtained from Charles River and anesthetized with isoflurane (VetOne) inhalation and decapitated using a rodent guillotine. The mouse brains were immersed in 0-1°C NMDG-containing artificial cerebrospinal fluid (ACSF) composed of (in mM): 110 NMDG, 110 HCl, 3KCl, 10 MgCl<sub>2</sub>, 1.1 NaH<sub>2</sub>PO<sub>4</sub>, 0.5 CaCl<sub>2</sub>, 25 glucose, 3 pyruvic acid, 10 ascorbic acid, and 25 NaHCO<sub>3</sub>, with an osmolarity of 305-315 mOsm/L and a pH of 7.2-7.3. Sagittal slice preparations of 300 μm thickness were prepared and transferred to a storage chamber where they were maintained at room temperature in carboxygen-bubbled physiological artificial cerebrospinal fluid (ACSF) containing (in mM): 124 NaCl, 2.5 KCl, 25 NaHCO<sub>3</sub>, 1.2 NaH<sub>2</sub>PO<sub>4</sub>, 20 Glucose, 1 MgCl<sub>2</sub>, 2 CaCl<sub>2</sub>, with an osmolarity of 290-300 mOsm/L and a pH of 7.2-7.3.

## Electrophysiological Recordings

MEC slices were transferred to submersion recording chamber continuously perfused with 34-37°C ACSF. Whole-cell patch clamp recordings of principal cells were achieved in dorsal MEC – LII (Fig. 2.2) using a MultiClamp 700B amplifier (Molecular Devices) at a holding potential of -65 mV. Patch pipettes were formed on a horizontal puller (P97; Sutter Instruments) with a tip resistance of 2-6 M $\Omega$ .

For the majority of inhibitory post-synaptic current (IPSC) recordings, patch electrodes were filled with a high chloride intracellular solution containing (in mM): 120 CsCl, 30 HEPES, 2 MgCl<sub>2</sub>, 1 CaCl<sub>2</sub>, 11 EGTA, 4 ATP-Mg, with an osmolarity of 300-310 mOsm/L and a pH adjusted to 7.2-7.3 with CsOH. Excitatory glutamate receptor-mediated transmission was blocked by adding APV (50 $\mu$ M) and DNQX (20 $\mu$ M) to the bath. Tetrodotoxin (TTX, 1 $\mu$ M) was added to the bath when recording miniature IPSCs. Because CsCl is known to block potassium channels and does not allow for accurate recording of intrinsic cellular properties including membrane potential and input resistance, some IPSC recordings were performed with patch electrodes containing a high chloride intracellular solution without CsCl (in mM): 135 KCl, 10 HEPES, 2 Na-ATP, 0.2 Na-GTP, 2 MgCl<sub>2</sub>, and 0.1 EGTA, with an osmolarity of 300-310 mOsm/L and a pH adjusted to 7.2-7.4 with KOH.

Following achievement of whole-cell access, the cell was allowed to stabilize for five minutes prior to recording. Only cells with an access resistance

of less than 20 M $\Omega$  and less than 20% change in access resistance over the course of the recording were used. Recording conditions, when looking at the effect of NE and AR agonists, were performed with either norepinephrine (NE, 100  $\mu$ M), phenylephrine (100  $\mu$ M), UK14304 (1  $\mu$ M), or isoprenaline (1  $\mu$ M) perfused into the bath. IPSCs were recorded in voltage clamp at a holding potential of -65 mV for a minimum of five minutes in control condition prior to infusion of ACSF containing norepinephrine or any of the adrenergic receptor agonists. Voltage clamp recordings were obtained periodically over time following perfusion of the drug. Experimental conditions were achieved for a minimum of 10 minutes to ensure maximal drug effect.

During testing for differential effects of co-administration of glucocorticoids and NE, experimental recording conditions were performed with norepinephrine (NE, 100  $\mu$ M), dexamethasone (1 $\mu$ M), or both, perfused into the bath. IPSCs were recorded in voltage clamp at a holding potential of -65 mV for a minimum of five minutes in control condition prior to infusion of ACSF containing either norepinephrine or dexamethasone. Experimental conditions were achieved for a minimum of 10 minutes to ensure maximal drug effect prior to adding the second drug, resulting in both norepinephrine and dexamethasone being perfused into the bath together following ten minutes of the first experimental condition (Fig. 3.1).

Recordings of synaptic activity were analyzed using MiniAnalysis. Comparisons of one-minute averages representative of the control and maximum drug effect synaptic activity frequency, inter-event interval, amplitude, and decay

time between control and drug-treated cells were calculated using a repeated measures paired t-test. For comparisons of means for synaptic activity frequency and amplitude between control, experimental condition #1, and experimental condition #2 were calculated using a one-way analysis of variance (ANOVA) test followed by Tukey's multiple comparisons test. Comparisons between dexamethasone priming of the norepinephrine response versus dexamethasone priming of the phenylephrine response were calculated using a two-way ANOVA. All statistical tests were performed in GraphPad Prism. P-values <0.05 were considered significant.

**Figure 3.1 – Experimental design timeline.**

**A)**

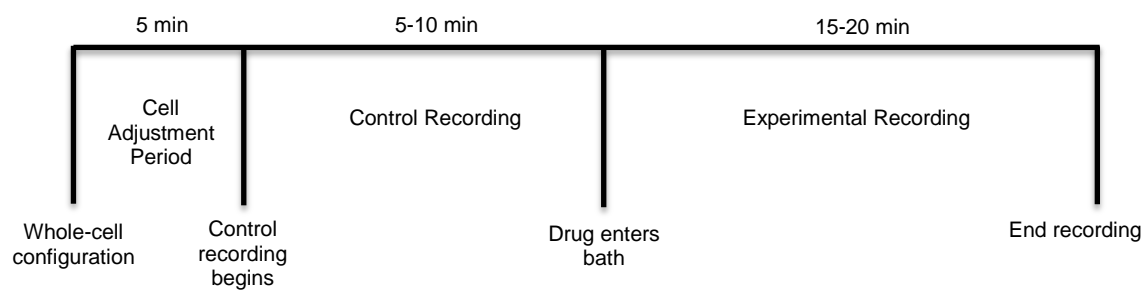


**Fig. 3.1: A)** Timeline of whole-cell recordings using NE or adrenergic receptor agonists.

**Results:****Norepinephrine increased frequency and amplitude of inhibitory signaling in a majority of MEC – LII principal cells.**

CsCl-based internal solutions are commonly used to increase chloride concentration for improved tracking of GABAergic transmission and IPSC measurements. For the majority of the IPSC studies conducted below, a CsCl-based internal solution was used; however, because CsCl blocks potassium channels and can significantly alter intrinsic cellular characteristics, the effect of NE on sIPSCs was first tested using a KCl-based high-chloride internal solution lacking CsCl. Using a KCl-based internal solution, control sIPSCs were recorded at -65mV in MEC-LII principal cells (Fig. 3.2 A). After ten minutes of NE (100  $\mu$ M) perfusion, sIPSCs were recorded at -65mV (Fig. 3.2 B). NE significantly increased sIPSC frequency ( $p=0.0005$ ) and amplitude ( $p=0.008$ ), but not decay time ( $p=0.06$ ) (Fig. 3.2 C-F). Importantly, 3 of the 13 (~23%) cells showed no change (less than 15% change from control) in sIPSC frequency following NE application (Fig. 3.2 G, Table 4-6).

Use of KCl-based high-chloride internal solution allowed for recording of intrinsic cellular characteristics in control and NE conditions. NE significantly increased the average input resistance from control condition ( $p=0.03$ ) (Fig. 3.3 A, F). Interestingly, NE-insensitive cells (<15% change in IPSC frequency following NE application) had a significantly larger average baseline input resistance when compared to NE-sensitive cells ( $p=0.04$ ) (Fig. 3.3 B, F). NE did not affect the average membrane potential ( $p=0.39$ ) in MEC-LII principal cells (Fig. 3.3 C, F);

however, the NE-insensitive group had a significantly depolarized average baseline membrane potential in comparison to the NE-sensitive group ( $p=0.04$ ) (Fig. 3.3 D, F). Average baseline sag amplitude in MEC-LII principal cells was larger in cells with an NE-induced increase in sIPSC frequency than NE-unaffected cells, but the difference is not significant ( $p=0.10$ ) (Fig.3.3 E, F).

After acquiring intrinsic cellular characteristics using a KCl-based internal solution, we switched to a CsCl-based internal solution for the remainder of the experiments. We first confirmed that the above effect of NE on MEC-LII principal cell sIPSCs was conserved when using the CsCl-based internal solution. Spontaneous IPSCs (sIPSCs) were recorded at a holding potential of  $-65$  mV in a CsCl-based high-chloride internal solution (Fig 3.4 A, C). After ten minutes of NE ( $100$   $\mu$ M) perfusion, sIPSCs were recorded (Fig. 3.4 B, C). NE significantly increased sIPSC frequency ( $p=0.0002$ ) and sIPSC amplitude ( $p=0.0006$ ), but not decay time ( $p=0.48$ ) (Fig. 3.4 D-G). NE began to increase average sIPSC frequency, amplitude, and decay time within the first minute of perfusion, and maximum effect on frequency and amplitude occurred within 5-9 minutes of NE application (Fig. 3.4 H). It is important to note that 3 of the 13 (~23%) cells were unaffected (less than 15% change from control) in terms of sIPSC frequency following NE application (Fig.3.4 I, Table 4-6).

To investigate if the NE-induced increase in sIPSC frequency, amplitude, and decay is exclusive to spike-driven signaling or also causes changes to terminal-specific inhibitory signaling, miniature IPSCs (mIPSCs) were recorded from MEC – LII principal cells in the presence of tetrodotoxin (TTX), a voltage-

gated sodium channel blocker (Fig. 3.5 A). After ten minutes of NE (100  $\mu$ M) perfusion, mIPSCs were recorded (Fig. 3.5 B). NE significantly increased mIPSC frequency ( $p=0.0001$ ) and decay time ( $p<0.0001$ ), but failed to significantly alter mIPSC amplitude ( $p=0.23$ ) (Fig. 3.5 C-F). Interestingly, 5 of the 19 cells (~26%) recorded were unaffected (less than 15% change from control) by NE application (Fig. 3.5 G, Table 4-6).

**Figure 3.2 – Norepinephrine significantly increased spontaneous IPSC frequency and amplitude, but not decay time, with a KCl-based intracellular solution.**

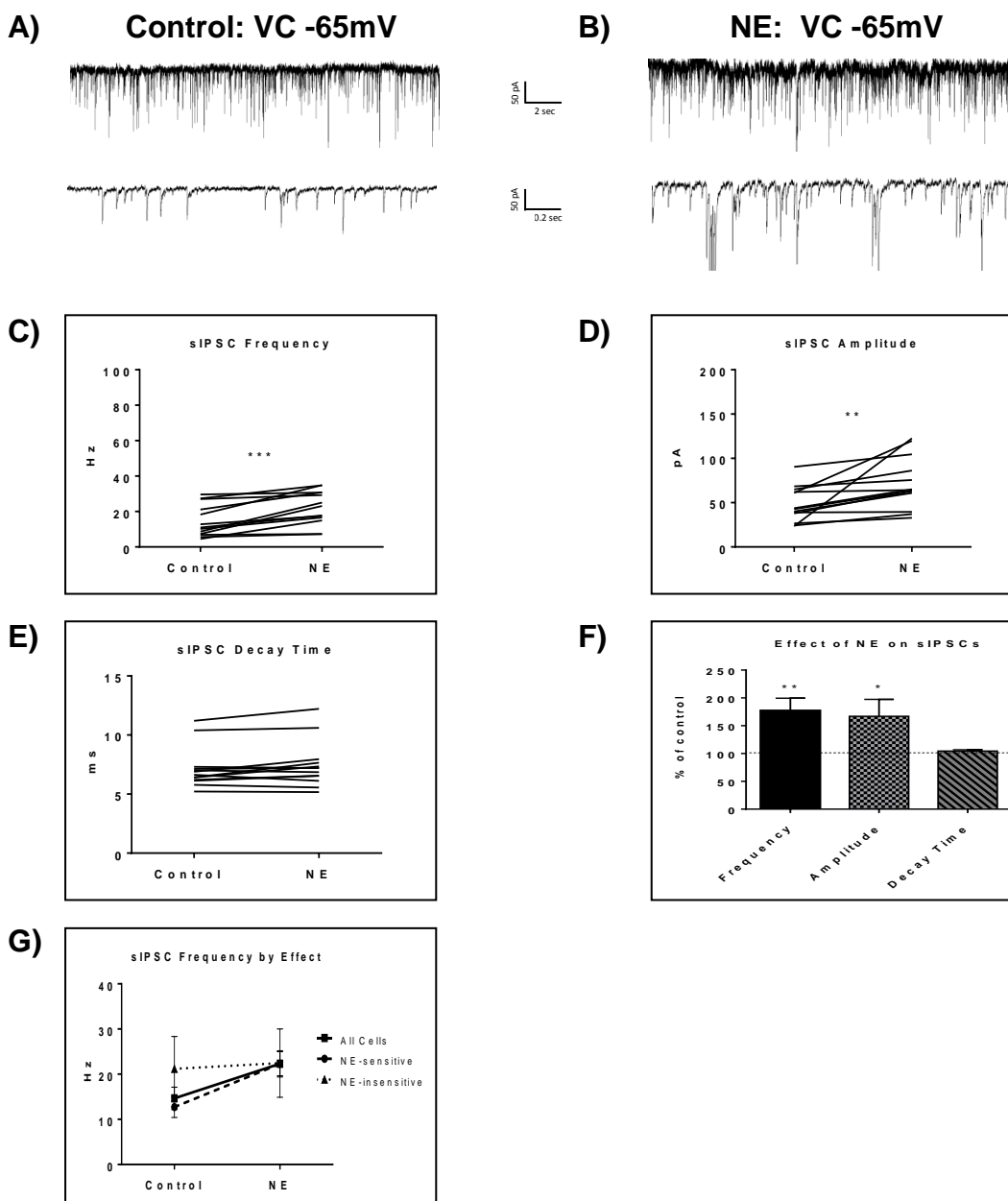


**Fig. 3.2: A, B Top )** 20 seconds of sIPSC voltage-clamp recordings representative of control (A) and NE (B) conditions. **A, B Bottom )** 2 seconds of the voltage-clamp recordings shown above. **C)** NE significantly increased average sIPSC frequency. **D)** NE significantly increased sIPSC amplitude. **E)** NE had no effect on sIPSC decay time. **F)** NE significantly increased sIPSC frequency and amplitude, but not decay time when normalized and compared to the corresponding control group average. **G)** Plot of average NE effect on sIPSC frequency (n=13) for the two different response groupings observed: NE-responsive (n=10) and NE-unresponsive (n=3).

**Figure 3.3 – Norepinephrine-sensitive cells had different intrinsic characteristics than norepinephrine-insensitive cells.**

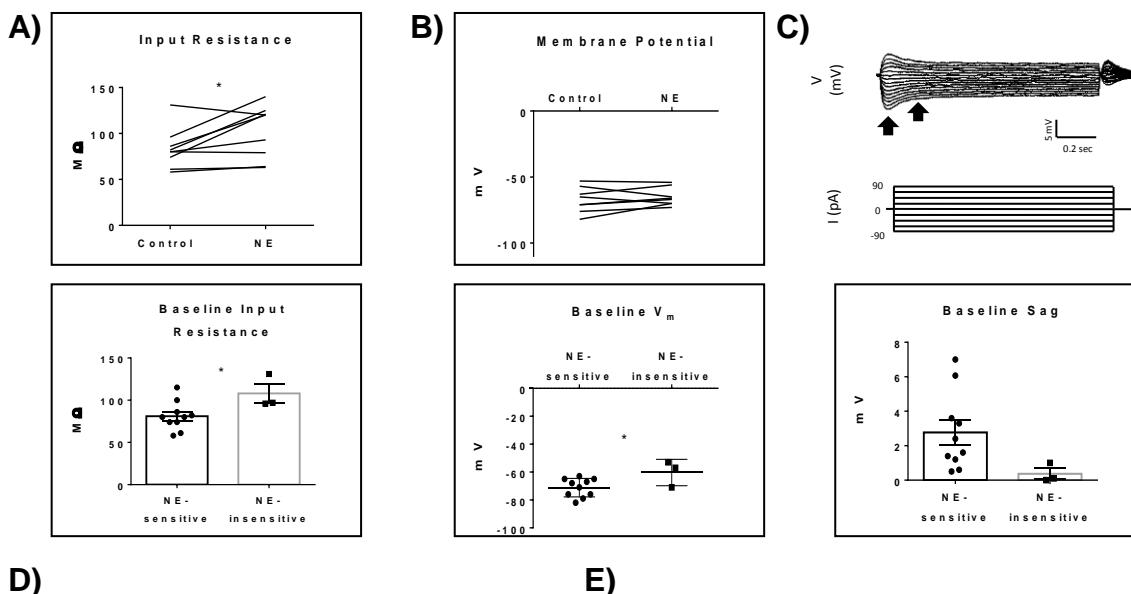


**Fig. 3.3: A)** Top: NE significantly increases average input resistance. Bottom: Comparison of baseline input resistance in cells that show >15% increase in sIPSC frequency (n=10) versus cells that show no change (n=3) in sIPSC frequency. **B)** Top: NE did not affect average membrane potential. Bottom: Comparison of baseline membrane potential in cells that show >15% increase in sIPSC frequency (n=10) versus cells that show no change (n=3). Note that the NE-insensitive group has a significantly depolarized average baseline membrane potential in comparison to the NE-sensitive group. **C)** Top: Example trace showing sag response (peak versus steady-state indicated by black arrows) due to  $I_h$  activation following hyperpolarizing steps in voltage clamp. Bottom: Comparison of baseline sag amplitude in cells that show >15% increase in sIPSC frequency (n=10) versus cells that show no change (n=3). Note that the NE-sensitive group has larger average baseline sag, though the difference is not significant potentially due to the low number of cells in the NE-insensitive group. **D)** Data table of intrinsic characteristics in MEC-LII principal cells in control conditions and after NE application. Data values shown are the average of each group  $\pm$  SEM. **E)** Cells were split into NE-sensitive groups (>15% change in frequency after NE application) and NE-insensitive groups to compare baseline intrinsic characteristics.

**Figure 3.4 – Norepinephrine significantly increased spontaneous IPSC frequency and amplitude, but not decay time, with a CsCl-based intracellular solution.**

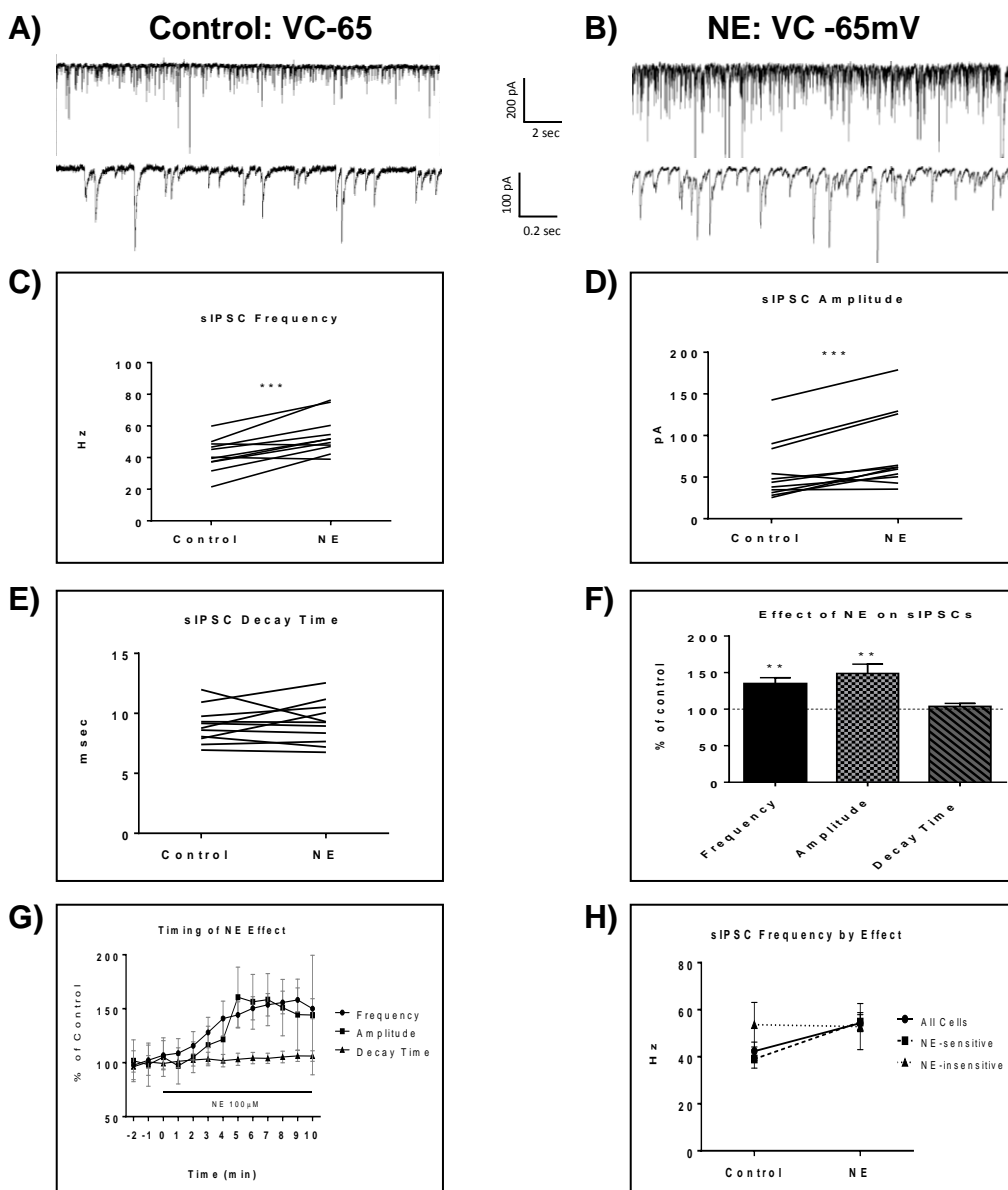


**Fig. 3.4: A, B Top** 20 seconds of sIPSC voltage-clamp recordings representative of control (A) and NE (B) conditions. **A,B Bottom** 2 seconds of the voltage-clamp recordings shown above. **C** NE significantly increased average sIPSC frequency. **D** NE significantly increased sIPSC amplitude. **E** NE had no effect on sIPSC decay time. **F** NE significantly increased sIPSC frequency and amplitude, but not decay time when normalized and compared to the corresponding control group average. **G** Time course of the NE effect in one-minute intervals. NE enters at 0 min and quickly increases frequency and amplitude, but not decay time. **H**) Plot of average NE effect on sIPSC frequency for the two different response groupings observed: NE-sensitive (n=10) and NE-insensitive (n=3).

**Figure 3.5 – Norepinephrine significantly increased miniature IPSC frequency and decay time, but not amplitude, in MEC – LII principal cells.**

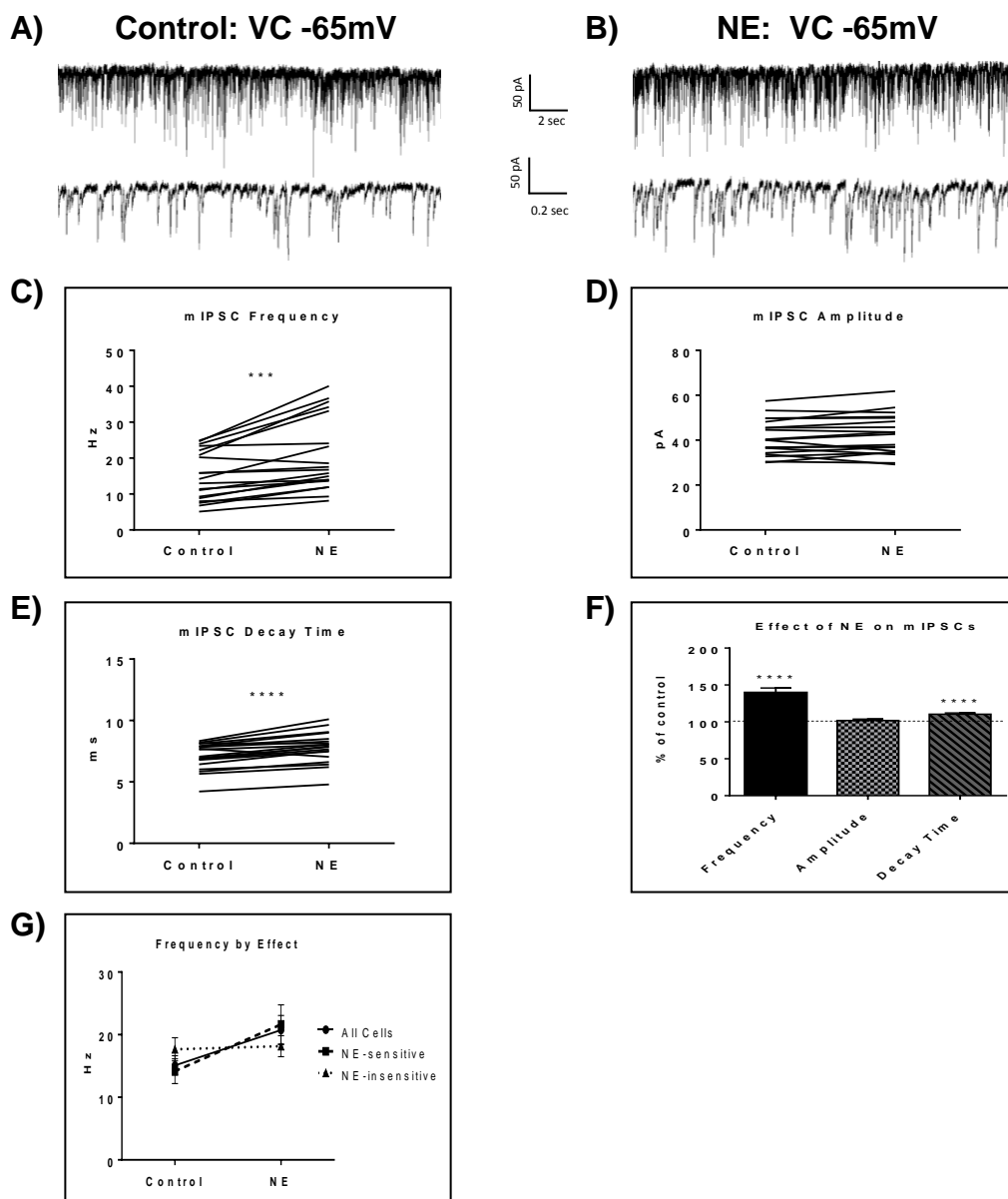


**Fig. 3.5: A, B Top)** 20 seconds of mIPSC voltage-clamp recordings representative of control (A) and NE (B) conditions. **A, B Bottom)** 2 seconds of the voltage-clamp recordings shown above. **C)** NE significantly increased average mIPSC frequency. **D)** Norepinephrine did not significantly alter mIPSC amplitude. **E)** NE significantly increased average mIPSC decay time. **F)** NE significantly increased mIPSC frequency and decay time, but not amplitude, when normalized and compared to the corresponding control group average. **G)** Plot of average NE effect on mIPSC frequency for the two different response groupings observed: NE-sensitive (n=14) and NE-insensitive (n=5).

**Phenylephrine, a  $\alpha$ 1-adrenoreceptor agonist, increased sIPSC frequency in a subset of neurons, but not miniature IPSC frequency, in a majority of MEC – LII principal cells.**

Spontaneous IPSCs (sIPSCs) were recorded at a holding potential of -65 mV in a CsCl-based high-chloride internal solution (Fig 3.6 A). After ten minutes of phenylephrine (PHE, 100  $\mu$ M) perfusion, sIPSCs were recorded (Fig. 3.6 B). Surprisingly, PHE failed to significantly increase sIPSC frequency ( $p=0.09$ ) and had no effect on sIPSC amplitude ( $p=0.64$ ) or decay time ( $p=0.11$ ) (Fig. 3.6 C-F). It is important to note that PHE caused marked frequency increases (>25%) in 5 of the 10 cells recorded, which measured as significantly higher than control conditions ( $p=0.03$ , Fig. 3.6 D). 5 of the 10 cells showed no change in sIPSC frequency following PHE application (Fig. 3.6 G, Table 4-6).

To investigate if the PHE-induced increase in sIPSC frequency in a proportion of the cells recorded was exclusive to spike-driven signaling or also caused changes to terminal-specific inhibitory signaling, miniature IPSCs (mIPSCs) were recorded from MEC – LII principal cells (Fig. 3.7 A) in the presence of tetrodotoxin (TTX), a voltage-gated sodium channel blocker. After ten minutes of PHE (100  $\mu$ M) perfusion, mIPSCs were recorded (Fig. 3.6 B). PHE had no effect on average mIPSC frequency ( $p=0.93$ ), amplitude ( $p=0.32$ ), or decay time ( $p=0.16$ ) (Fig. 3.7 C-F, Table 4-6).

**Figure 3.6 – Phenylephrine increased spontaneous IPSC frequency in a subset of neurons, and had no effect on amplitude or decay time.**

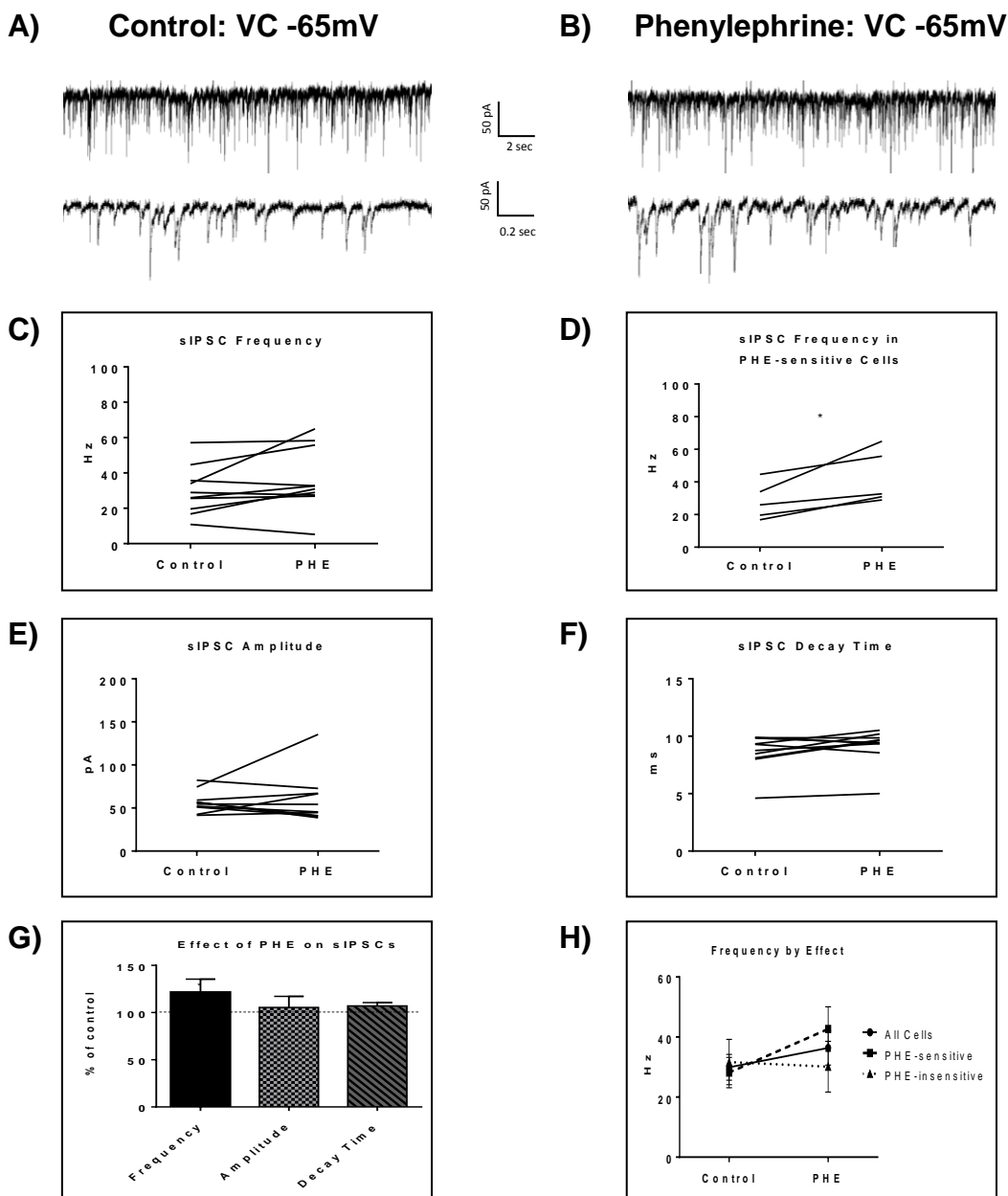


**Fig. 3.6: A, B Top )** 20 seconds of sIPSC voltage-clamp recordings representative of control (A) and PHE (B) conditions. **A,B Bottom)** 2 seconds of the voltage-clamp recordings shown above. **C)** PHE failed to significantly increase average sIPSC frequency. **D)** PHE significantly increased average sIPSC frequency in the 5 PHE-sensitive cells. **E)** PHE had no effect on average sIPSC amplitude. **F)** PHE had no effect on average sIPSC decay time. **F)** PHE failed to significantly increase sIPSC frequency despite large increases in 5 of 10 cells, and had no effect on amplitude or decay time when normalized and compared to the corresponding control group average. **G)** Plot of average PHE effect on sIPSC frequency for the two different response groupings observed: PHE-sensitive (n=5) and PHE-insensitive (n=5).

**Figure 3.7 – Phenylephrine had no effect on miniature IPSC frequency, amplitude, or decay time in MEC – LII principal cells.**

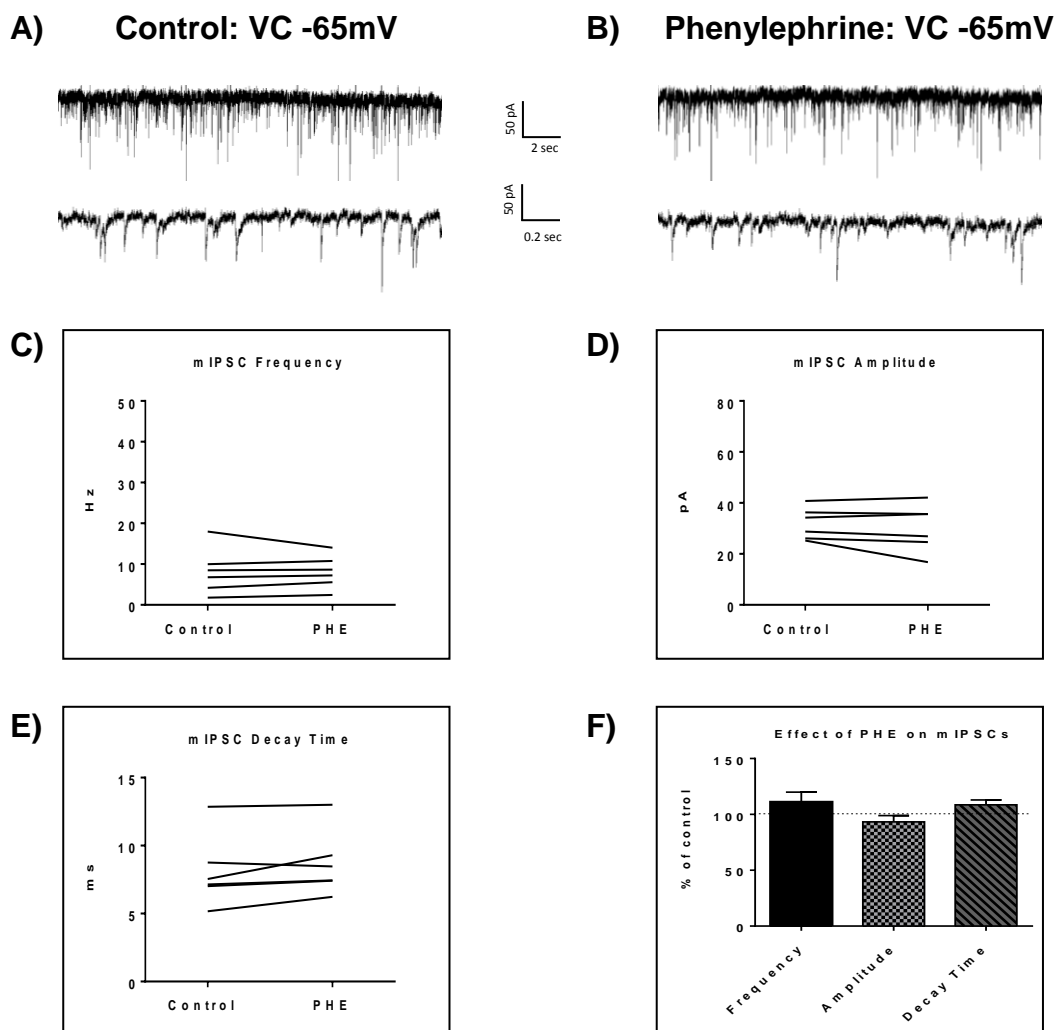


**Fig. 3.7: A, B Top )** 20 seconds of mIPSC voltage-clamp recordings representative of control (A) and PHE (B) conditions. **A,B Bottom)** 2 seconds of the voltage-clamp recordings shown above. **C)** PHE had no effect on average mIPSC frequency. **D)** PHE had no effect on average mIPSC amplitude. **E)** PHE had no effect on mIPSC decay time. **F)** PHE had no effect on frequency, amplitude, or decay time when normalized and compared to the corresponding control group average (n=6).

**UK14304, a  $\alpha$ 2-adrenoreceptor agonist significantly increased frequency of miniature IPSC signaling in a majority of MEC – LII principal cells**

Spontaneous IPSCs (sIPSCs) were recorded at a holding potential of -65 mV in a CsCl-based high-chloride internal solution (Fig 3.8 A). After ten minutes of UK14304 (1  $\mu$ M) perfusion, sIPSCs were recorded (Fig. 3.8 B). UK14304 had no effect on sIPSC frequency ( $p=0.13$ ), amplitude ( $p=0.47$ ) or decay time ( $p=0.37$ ) (Fig. 3.8 C-F, Table 4-6), indicating that UK14304 has no effect on spike-dependent spontaneous inhibitory signaling in MEC – LII principal cells.

To investigate the effect of UK14304 on terminal-specific inhibitory signaling, miniature IPSCs (mIPSCs) were recorded from MEC – LII principal cells (Fig. 3.9 A) in the presence of tetrodotoxin (TTX). After ten minutes of UK14304 (1  $\mu$ M) perfusion, mIPSCs were recorded (Fig. 3.9 B). UK14304 had no effect on average mIPSC frequency ( $p=0.75$ ) or amplitude ( $p=0.52$ ), but significantly increased average mIPSC decay time ( $p=0.004$ ) (Fig. 3.9 C-F, Table 4-6).

**Figure 3.8 – UK-14304 had no effect on sIPSC frequency, amplitude, or decay time in MEC – LII principal cells.**

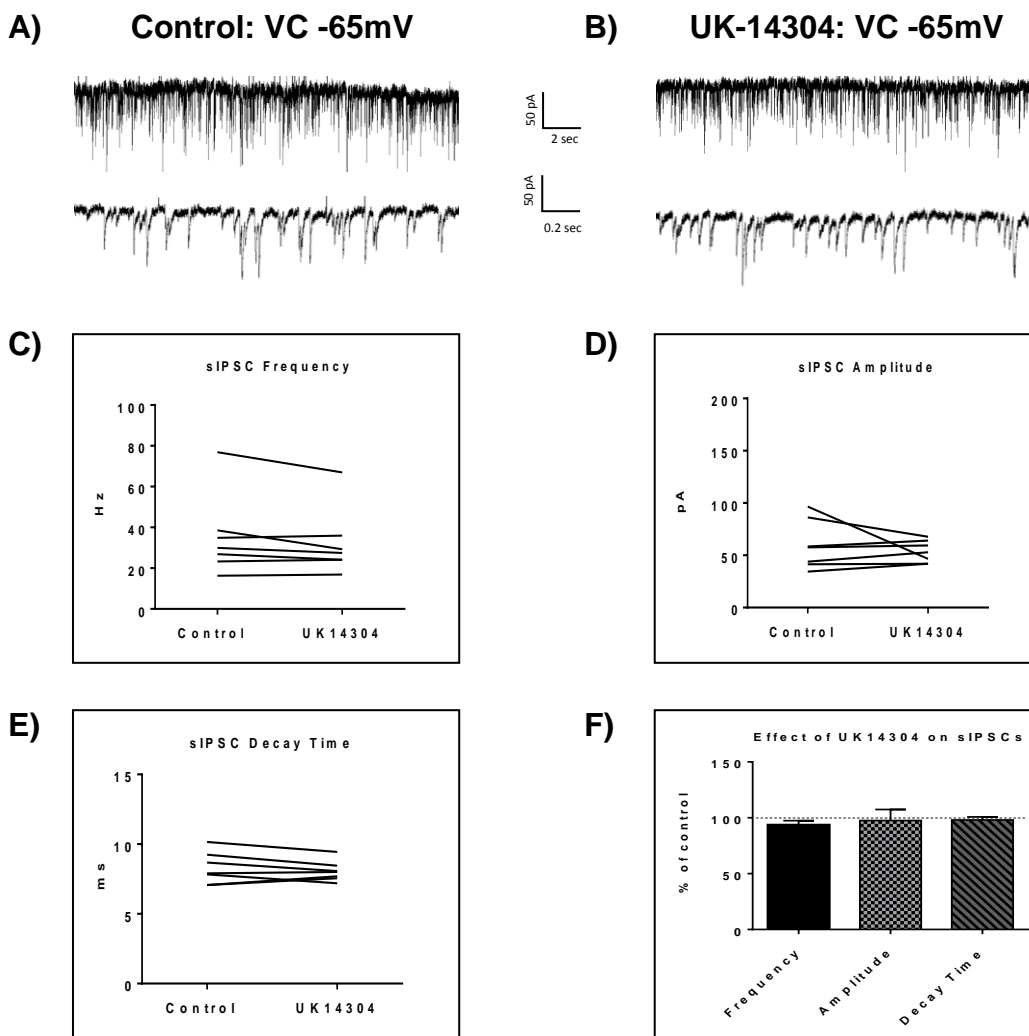


**Fig. 3.8: A, B Top )** 20 seconds of sIPSC voltage-clamp recordings representative of control (A) and UK14304 (B) conditions. **A,B Bottom)** 2 seconds of the voltage-clamp recordings shown above. **C)** UK14304 had no effect on average sIPSC frequency. **D)** UK14304 had no effect on average sIPSC amplitude. **E)** UK14304 had no effect average sIPSC decay time. **F)** UK14304 had no effect on sIPSC frequency, amplitude, or decay time when normalized and compared to the corresponding control group average (n=7).

**Figure 3.9 – UK14304 had no effect on IPSC frequency or amplitude, but significantly increased miniature IPSC decay time in MEC – LII principal cells.**

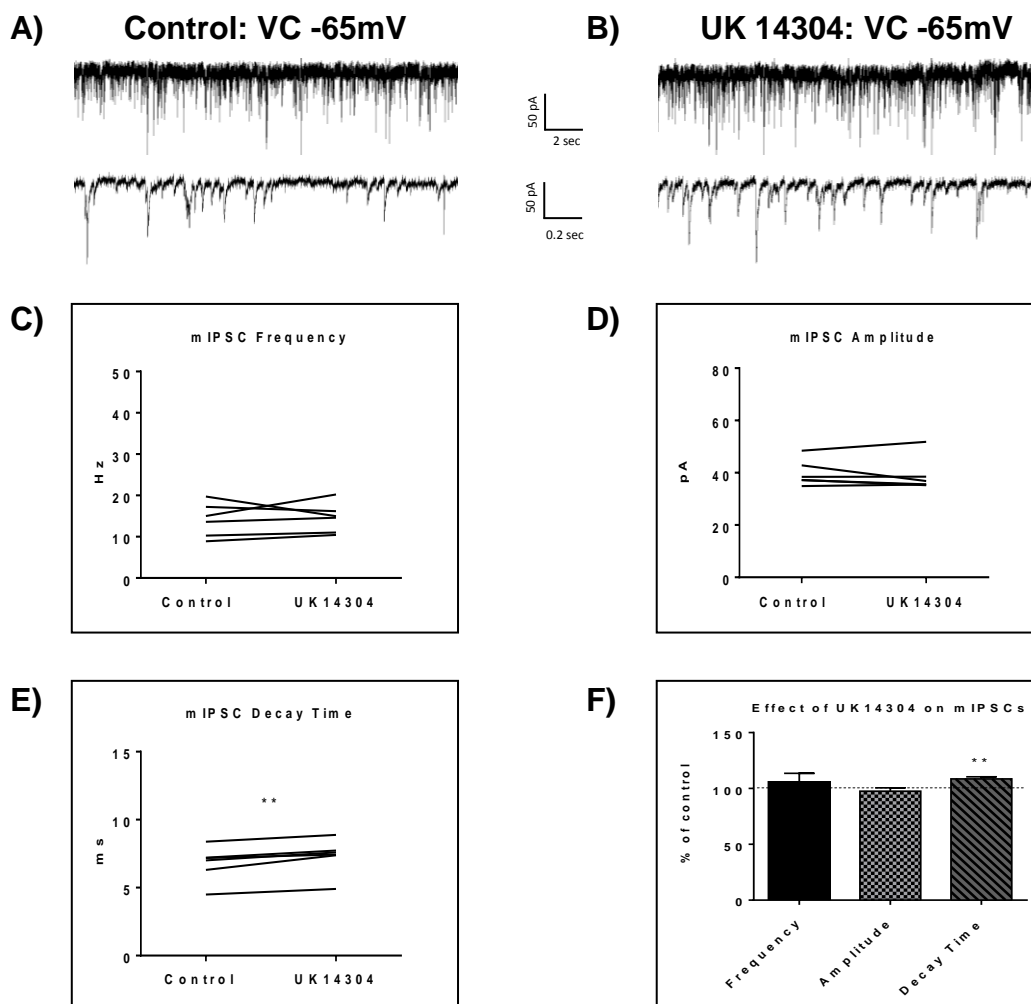


**Fig. 3.9: A, B Top )** 20 seconds of mIPSC voltage-clamp recordings representative of control (A) and UK14304 (B) conditions. **A,B Bottom )** 2 seconds of the voltage-clamp recordings shown above. **C)** UK14304 had no effect on average mIPSC frequency. **D)** UK14304 had no effect on average mIPSC amplitude. **E)** UK14304 significantly increased average mIPSC decay time. **F)** UK14304 significantly increased average mIPSC decay time, but not frequency or amplitude when normalized and compared to the corresponding control group average (n=6).

**Isoprenaline, a  $\beta$ -AR agonist, had no effect on spontaneous IPSCs in MEC-LII principal cells**

Spontaneous IPSCs (sIPSCs) were recorded at a holding potential of -65 mV in a CsCl-based high-chloride internal solution (Fig 3.10 A). After ten minutes of  $\beta$ -AR agonist, isoprenaline (1  $\mu$ M), perfusion, sIPSCs were recorded (Fig. 3.10 B). Isoprenaline had no effect on sIPSC frequency ( $p=0.67$ ), amplitude ( $p=0.98$ ), or decay time ( $p=0.25$ ) (Fig. 3.10 C-F, Table 4-6), indicating that isoprenaline has no effect on spike-dependent inhibitory signaling in MEC – LII principal cells.

**Figure 3.10 – Isoprenaline had no effect on sIPSC frequency, amplitude, or decay time in MEC-LII principal cells.**

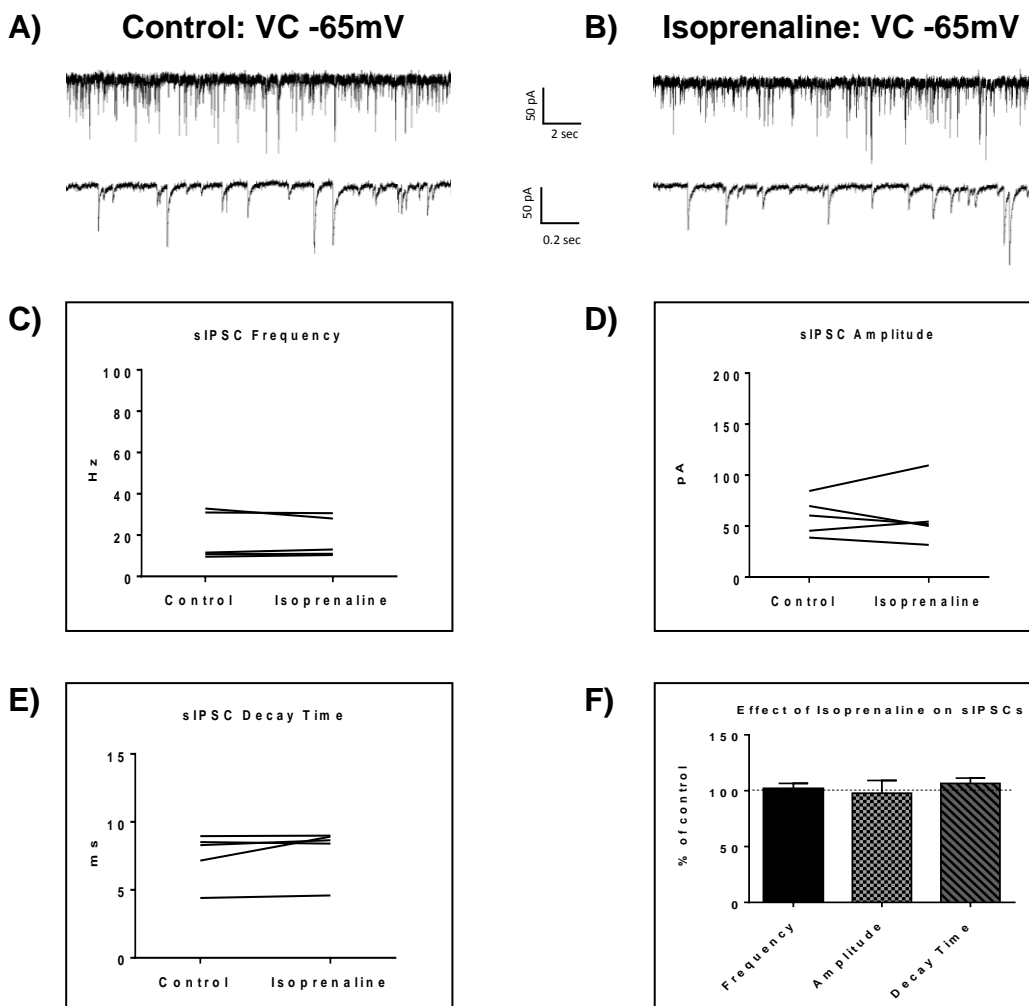


**Fig. 3.10: A, B Top )** 20 seconds of sIPSC voltage-clamp recordings representative of control (A) and isoprenaline (B) conditions. **A,B Bottom )** 2 seconds of the voltage-clamp recordings shown above. **C)** Isoprenaline had no effect on average sIPSC frequency. **D)** Isoprenaline had no effect on average sIPSC amplitude. **E)** Isoprenaline had no effect on average sIPSC decay time. **F)** Isoprenaline had no effect on sIPSC frequency, amplitude, or decay time when normalized and compared to the corresponding control group average (n=5).

**Table 4 – Effect of adrenergic receptor activation on IPSC frequency**

Recording Condition	Control Frequency (Hz)	NE/Agonist Frequency (Hz)	t	df	p	% of Control	t	df	p
sIPSCs NE (KCl int.)	14.65 ± 2.49	22.32 ± 2.65	4.77	12	<b>0.0005*</b>	177.19 ± 22.21	3.48	12	<b>0.005*</b>
sIPSCs NE	42.39 ± 3.89	54.32 ± 3.59	5.15	12	<b>0.0002*</b>	134.83 ± 8.31	4.19	12	<b>.001*</b>
mIPSCs NE	15.09 ± 1.56	20.73 ± 2.35	4.85	18	<b>.0001*</b>	139.65 ± 6.19	6.41	18	<b>&lt;0.0001*</b>
sIPSCs PHE	29.93 ± 4.33	36.39 ± 5.70	1.89	9	0.09	121.57 ± 13.84	1.56	9	0.15
mIPSCs PHE	8.19 ± 2.29	8.11 ± 1.65	0.1	5	0.93	111.02 ± 8.98	1.23	5	0.27
sIPSCs UK14304	35.25 ± 7.46	32.12 ± 6.20	1.78	6	0.13	93.54 ± 3.95	1.63	6	0.15
mIPSCs UK14304	14.12 ± 1.45	14.58 ± 1.27	0.34	5	0.75	106.05 ± 7.05	0.69	5	0.52
sIPSCs Isoprenaline	19.12 ± 4.14	18.62 ± 3.49	0.45	4	0.67	101.75 ± 3.83	0.36	4	0.74

**Table 5 – Effect of adrenergic receptor activation on IPSC amplitude**

Recording Condition	Control Amplitude (pA)	NE/Agonist Amplitude (pA)	t	df	p	% of Control	t	df	p
sIPSCs NE (KCl int.)	48.04 ± 5.54	71.90 ± 8.12	3.2	12	<b>0.008*</b>	167.04 ± 30.27	2.22	12	<b>0.047*</b>
sIPSCs NE	57.90 ± 9.34	80.61 ± 11.57	4.61	12	<b>0.0006*</b>	148.99 ± 12.66	3.87	12	<b>.002*</b>
mIPSCs NE	41.35 ± 1.82	42.20 ± 2.06	1.24	18	0.23	101.94 ± 1.77	1.1	18	0.29
sIPSCs PHE	57.09 ± 4.02	60.66 ± 9.19	0.48	9	0.64	105.49 ± 11.68	0.47	9	0.65
mIPSCs PHE	31.90 ± 2.52	30.28 ± 3.75	1.1	5	0.32	93.32 ± 5.65	1.18	5	0.29
sIPSCs UK14304	59.81 ± 8.84	53.55 ± 3.98	0.78	6	0.47	97.62 ± 9.87	0.24	6	0.82
mIPSCs UK14304	39.81 ± 1.75	38.91 ± 2.27	0.7	5	0.52	97.59 ± 2.56	0.81	5	0.45
sIPSCs Isoprenaline	59.74 ± 6.50	59.52 ± 10.39	0.03	4	0.98	97.77 ± 9.00	0.2	4	0.85

**Table 6 – Effect of adrenergic receptor activation on IPSC decay time**

Recording Condition	Control Decay Time (ms)	NE/Agonist Decay Time (ms)	t	df	p	% of Control	t	df	p
sIPSCs NE (KCl int.)	7.13 ± 0.48	7.46 ± 0.54	2.11	12	0.06	104.47 ± 2.27	1.97	12	0.07
sIPSCs NE	8.91 ± 0.50	9.18 ± 0.52	0.73	12	0.48	103.93 ± 3.92	1	12	0.34
mIPSCs NE	7.08 ± 0.25	7.80 ± 0.29	6.03	18	<b>&lt;0.0001*</b>	110.44 ± 1.57	6.67	18	<b>&lt;0.0001*</b>
sIPSCs PHE	8.62 ± 0.50	9.16 ± 0.49	1.79	9	0.11	107.04 ± 3.50	2.01	9	0.08
mIPSCs PHE	8.08 ± 1.07	8.64 ± 0.97	1.9	5	0.16	108.55 ± 4.40	1.95	5	0.11
sIPSCs UK14304	8.28 ± 0.43	8.06 ± 0.28	0.96	6	0.37	98.03 ± 2.81	0.7	6	0.51
mIPSCs UK14304	6.76 ± 0.46	7.32 ± 0.46	4.92	5	<b>0.004*</b>	108.52 ± 1.63	4.53	5	<b>0.006*</b>
sIPSCs Isoprenaline	7.46 ± 0.65	7.92 ± 0.66	1.33	4	0.25	106.57 ± 3.72	1.4	4	0.24

### **Pre-treatment with dexamethasone increased the proportion of cells with a norepinephrine-induced increase in sIPSC frequency**

To test for a differential effect of stress hormones applied together compared to the independent effects already shown, co-application of NE and Dex was used to test changes to sIPSCs in MEC-LII principal cells. In this design, control baselines were achieved prior to adding NE (100  $\mu$ M) alone, and then Dex (1  $\mu$ M) was added together with NE (Fig. 3.11 A). Frequency of sIPSCs in both the NE-alone and NE+Dex condition was significantly increased compared to the control condition (repeated measures 1-way ANOVA,  $p=0.002$ , Tukey post-hoc comparison: control versus NE = \*\*, control versus NE+dex = \*, NE versus NE+dex is not significantly different) (Fig. 3.11 B). NE significantly increased amplitude from control conditions (repeated measures 1-way ANOVA,  $p=0.007$ , Tukey post-hoc comparison: control versus NE = \*\*, control versus NE+dex = NS, NE versus NE+dex = NS) (Fig. 3.11 C), NE had no effect on decay time compared to the control condition (repeated measures 1-way ANOVA,  $p=0.37$ ) (Fig. 3.11 D). NE significantly increased sIPSC frequency in 10 of 13 cells recorded, and Dex did not affect sIPSC frequency in the 3 cells that were unresponsive to NE (Fig. 3.11 E), initially indicating that co-administration of Dex and NE had inhibitory signaling effects consistent with that seen when each drug was applied independently.

To confirm that the co-administration of Dex and NE is consistent with independent application of each drug, the order of drug application was reversed. After recording control baselines, Dex (1  $\mu$ M) was perfused for approximately 15

minutes prior to NE (100  $\mu$ M) +Dex entering the bath. Frequency of sIPSCs in all conditions were significantly different (repeated measures 1-way ANOVA,  $p < 0.0001$ , Tukey post-hoc comparison: control versus Dex = \*, control versus NE+Dex = \*\*\*\*, Dex versus NE+Dex = \*\*\*\*) (Fig. 3.12 A, Table 10). Amplitude of sIPSCs in the NE+Dex condition was significantly increased compared to both the control and Dex-alone condition (repeated measures 1-way ANOVA,  $p = 0.001$ , Tukey post-hoc comparison: control versus dex = NS, control versus NE+Dex = \*\*, Dex versus NE+Dex = \*\*) (Fig. 3.12 B, Table 11). Decay time of sIPSCs in the NE+Dex condition was significantly increased compared to both the control and Dex-alone condition (repeated measures 1-way ANOVA,  $p < 0.0001$ , Tukey post-hoc comparison: control versus dex = NS, control versus NE+Dex = \*\*\*, Dex versus NE+Dex = \*\*) (Fig. 3.12 C, Table 12). Surprisingly, NE increased sIPSC frequency from dexamethasone-alone conditions by greater than 15% in 15 of 15 cells recorded (Fig. 3.12 D). In control versus NE-alone, 3 of 13 cells did not have a change in sIPSC frequency  $> 15\%$ , whereas NE induced a greater than 15% increase in all 15 cells when first primed with Dex for approximately 15 minutes (Fig. 3.12 D). The increase in proportion of NE-affected cells from 10 of 13 to 15 of 15 is statistically significant (Chi-square expected versus observed,  $p < 0.05$ ) (Fig. 3.12 E, Table 13). The normalized effect of NE-alone was not significantly different than the NE+Dex condition for sIPSC frequency ( $p = 0.07$ ), amplitude ( $p = 0.90$ ), or decay time ( $p = 0.63$ ) (Fig. 3.12 F, G).

**Figure 3.11 – Effects of co-administration of dexamethasone and norepinephrine.**

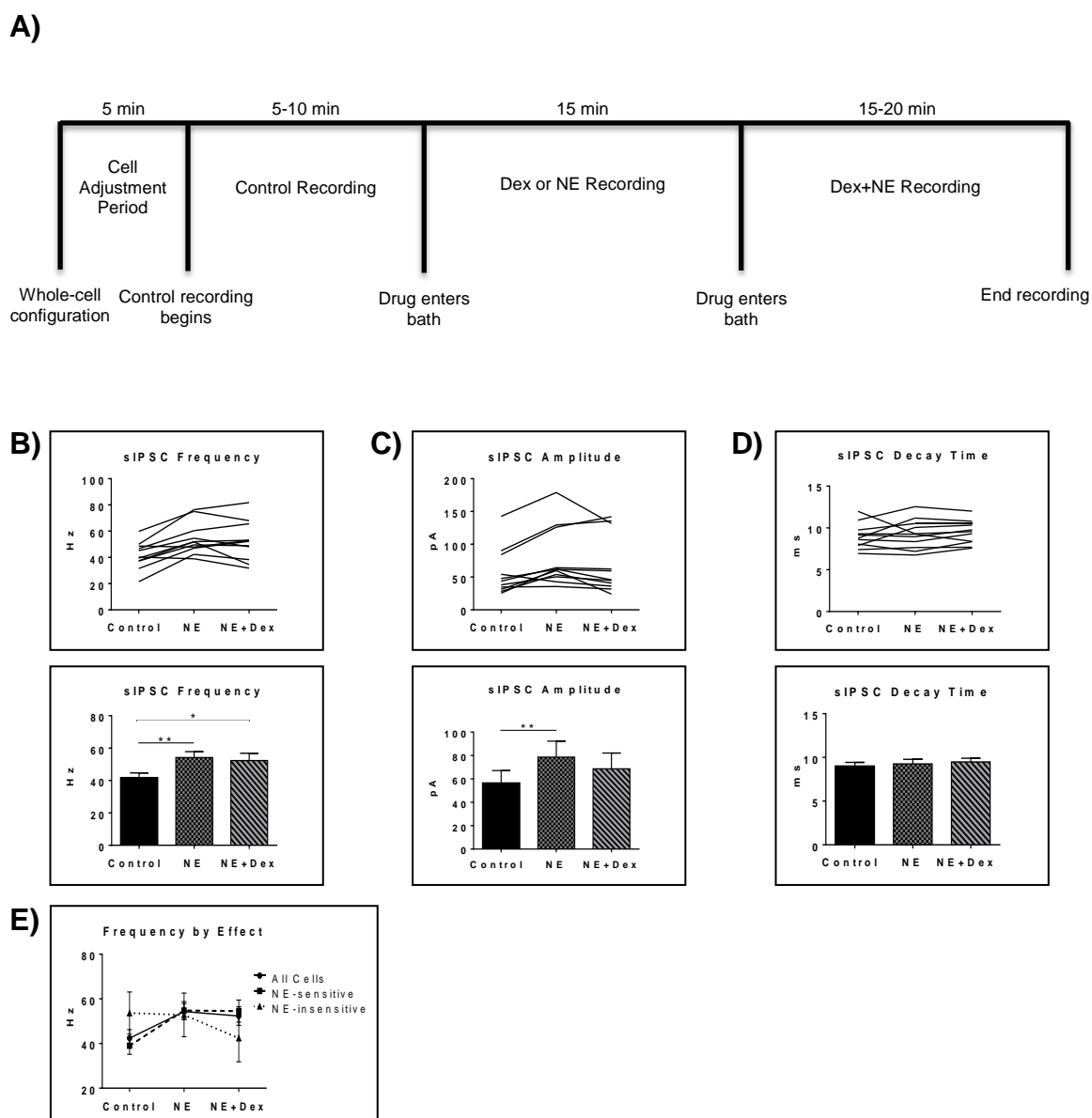


**Fig. 3.11: A)** Timeline of whole-cell recordings for co-administration studies using NE and Dex. **B-D Top)** Effect of NE and NE+Dex on sIPSC frequency by cell. **B-D Bottom)** Average of by-cell traces shown above. **B)** NE alone and NE+Dex significantly increased sIPSC frequency from control. **C)** NE alone significantly increased sIPSC amplitude when compared to control. **D)** Neither NE alone nor NE+Dex had an effect on sIPSC decay time. **E)** NE increased sIPSC frequency by more than 15% in 10 of 13 cells recorded. The averages in each drug condition were divided into three groups: all cells (n=13), NE-sensitive cells (n=10), and NE-insensitive cells (n=3).

**Figure 3.12 – Dexamethasone pre-treatment increased the proportion of MEC-LII principal cells affected by NE.**

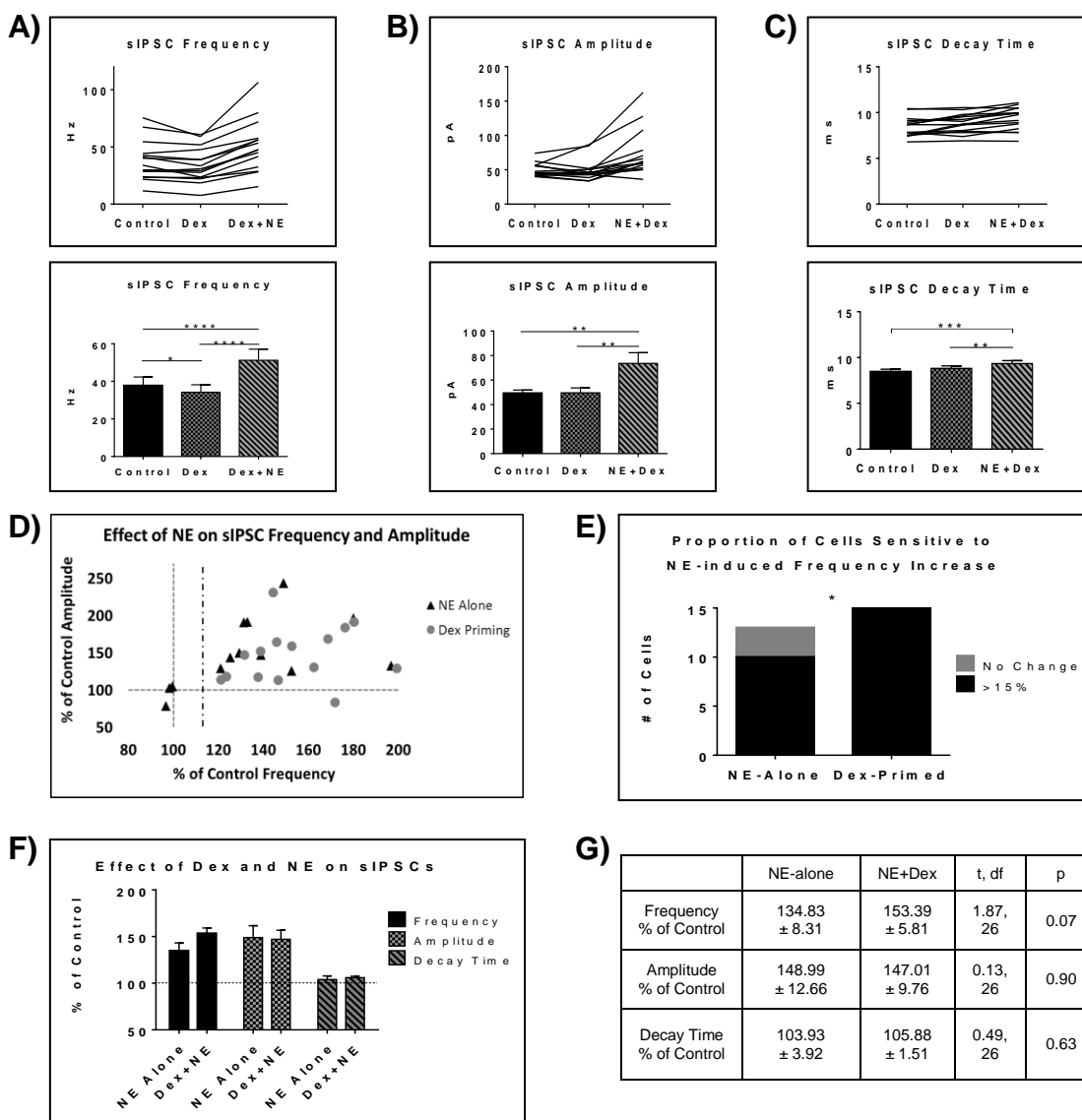


**Fig. 3.12: A-C Top)** By-cell effect of Dex and NE+Dex on sIPSC frequency, amplitude, and decay time. **A-C Bottom)** Average of by-cell traces shown above. **A)** Dex significantly decreased sIPSC frequency. Dex+NE significantly increased sIPSC frequency from Dex-alone and control. **B)** NE+Dex significantly increased sIPSC amplitude from Dex-alone and control. **C)** NE+Dex significantly increased sIPSC decay time from Dex-alone and control. **D)** Scatter plot of NE effect on % frequency and amplitude change in cells that were treated with NE-alone (triangles) versus cells that were pre-treated with Dex (circles) prior to NE application. The dotted line indicates the cut-off value for classifying a cell as NE-sensitive (>15% increase in sIPSC frequency). Note the three cells left of the cut-off line in the NE-alone condition and that all of the Dex-priming group are NE-sensitive. **E)** Chi-square analysis of proportion of NE-sensitive and insensitive cells in the NE-alone condition versus the Dex-primed condition. **F)** Comparison of NE effect on sIPSC frequency and amplitude when applied alone and when pre-treated with Dex. **G)** Table of unpaired two-tailed t-tests showing normalized values for NE-alone vs NE primed with Dex conditions for frequency, amplitude, and decay time.

### **Pre-treatment with dexamethasone increased the proportion of cells with a phenylephrine-induced increase in sIPSC frequency**

To determine if the effect of NE after Dex priming was  $\alpha$ 1-AR-mediated, we first tested the effect of adding the  $\alpha$ 1-AR agonist, phenylephrine (PHE, 100  $\mu$ M) independent of Dex (Fig. 3.13. A). Surprisingly, PHE failed to significantly increase sIPSC frequency ( $p=0.09$ ) and had no effect on sIPSC amplitude ( $p=0.64$ ) or decay time ( $p=0.11$ ) (Fig. 3.13 B-D). It is important to note that PHE caused marked frequency increases ( $>25\%$ ) in 5 of the 10 cells recorded (Fig. 3.13 E), which measured as significantly higher than control conditions ( $p=0.03$ , Fig. 3.13 B, Table 7). Five of the 10 cells showed no change in sIPSC frequency following PHE application (Fig. 3.13 G, Table 7-9). In cells sensitive to PHE-induced frequency changes ( $n=5$ ), PHE had no effect on amplitude ( $p=0.45$ ) or decay time ( $p=0.18$ ) (Fig. 3.13 C-D, Table 8-9).

To test if the Dex-induced increase in cell proportion sensitive to an NE-induced increase in sIPSC was  $\alpha$ 1-AR-mediated, the slice was perfused with Dex (1  $\mu$ M) for approximately 15 minutes prior to PHE (100  $\mu$ M) entering the bath. Frequencies of sIPSCs in all conditions were significantly different (repeated measures 1-way ANOVA,  $p<0.0001$ , Tukey post-hoc comparison: control versus Dex = \*\*, control versus PHE+Dex = \*\*\*\*, Dex versus PHE+Dex = \*\*\*\*) (Fig. 3.14 A, Table 10). Amplitude of sIPSCs in the PHE+Dex condition was significantly increased compared to the control condition (repeated measures 1-way ANOVA,  $p=0.01$ , Tukey post-hoc comparison: control versus Dex = not significant, control versus PHE+Dex = \*, Dex versus PHE+Dex = \*) (Fig. 3.14 B, Table 11). Decay

time of sIPSCs in the Dex+PHE condition were significantly higher than both the control and Dex-alone condition (repeated measures 1-way ANOVA,  $p < 0.0001$ , Tukey post-hoc comparison: control versus Dex = NS, control versus PHE+Dex = \*\*, Dex versus PHE+Dex = \*\*\*) (Fig. 3.14 C, Table 12). Surprisingly, PHE increased sIPSC frequency from Dex-alone conditions by greater than 15% in 15 of 15 cells recorded, (Fig. 3.14 D). In control versus PHE-alone, 5 of 10 cells did not have a change in sIPSC frequency of  $>15\%$ , whereas PHE induced a greater than 15% increase in all 15 cells if first primed with Dex for approximately 15 minutes. The increase in proportion of PHE-affected cells from 5 of 10 to 15 of 15 is statistically significant (Chi-square = 9.38,  $df = 1$ ,  $p < 0.01$ ) (Fig. 3.14 E, Table 14). Normalized sIPSC frequency changes in PHE primed with Dex vs Dex-alone were significantly larger than PHE-alone versus control ( $p = 0.04$ ) (Fig. 3.14 F, G). The normalized effect of PHE-alone was not significantly different than the PHE+Dex condition for sIPSC amplitude ( $p = 0.33$ ) or decay time ( $p = 0.13$ ) (Fig. 3.14 F, G).

**Figure 3.13 – Effects of co-administration of dexamethasone and phenylephrine.**

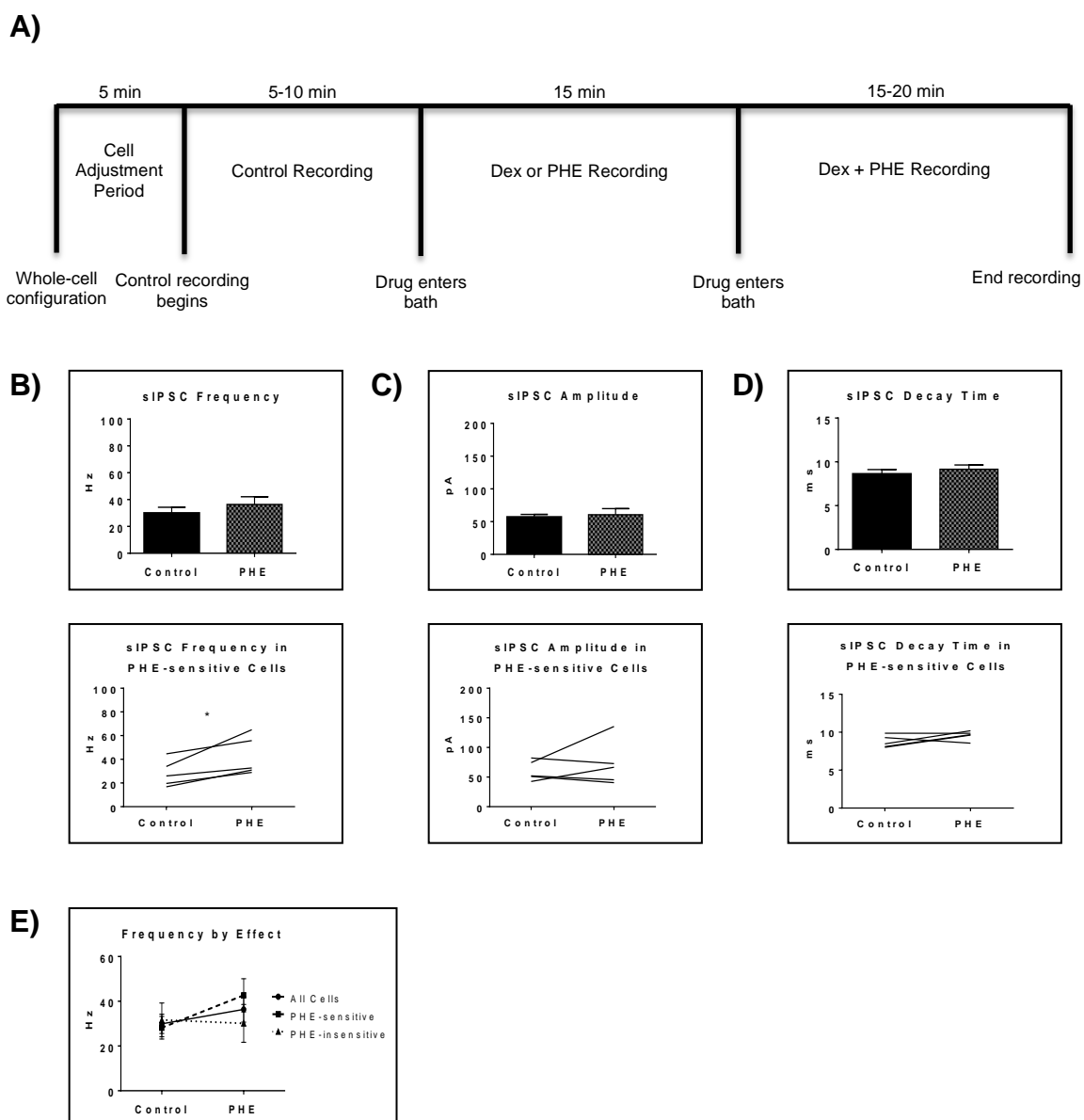


**Fig. 3.13: A)** Timeline of whole-cell recordings for co-administration studies using phenylephrine and dexamethasone. **B)** Top: Effect of PHE on average sIPSC frequency. Bottom: PHE significantly increased sIPSC frequency in PHE-sensitive cells ( $n=5$ ). **C)** Top: Effect of PHE on average sIPSC amplitude. Bottom: PHE did not affect sIPSC amplitude in PHE-sensitive cells ( $n=5$ ). **D)** Top: Effect of PHE on average sIPSC decay time. Bottom: PHE did not affect sIPSC decay time in PHE-sensitive cells ( $n=5$ ). **E)** PHE increased sIPSC frequency by more than 15% in 5 of 10 cells recorded. Plot shows average frequency for each response group: all cells ( $n=10$ ), PHE-sensitive cells ( $n=5$ ), and PHE-insensitive cells ( $n=5$ ).

**Table 7 – Effect of PHE on sIPSC frequency**

	Control (Hz $\pm$ SEM)	PHE (Hz $\pm$ SEM)	t, df	p
All Cells	29.93 $\pm$ 4.33	36.39 $\pm$ 5.70	1.89, 9	0.09
PHE-sensitive (n=5)	28.19 $\pm$ 5.07	42.67 $\pm$ 7.39	3.37, 4	<b>0.03*</b>
PHE-insensitive (n=5)	31.68 $\pm$ 7.55	30.11 $\pm$ 8.48	1.20, 4	0.3

**Table 8 – Effect of PHE on sIPSC amplitude**

	Control (pA $\pm$ SEM)	PHE (pA $\pm$ SEM)	t, df	p
All Cells	57.09 $\pm$ 4.02	60.66 $\pm$ 9.19	0.48, 9	0.64
PHE-sensitive (n=5)	60.50 $\pm$ 7.57	72.13 $\pm$ 16.94	0.84, 4	0.45
PHE-insensitive (n=5)	53.68 $\pm$ 3.11	49.20 $\pm$ 5.19	0.87, 4	0.43

**Table 9 – Effect of PHE on sIPSC decay time**

	Control (ms $\pm$ SEM)	PHE (ms $\pm$ SEM)	t, df	p
All Cells	8.62 $\pm$ 0.50	9.16 $\pm$ 0.49	1.79, 9	0.11
PHE-sensitive (n=5)	8.75 $\pm$ 0.36	9.58 $\pm$ 0.28	1.64, 4	0.18
PHE-insensitive (n=5)	8.48 $\pm$ 0.99	8.73 $\pm$ 0.96	0.75, 4	0.49

**Figure 3.14 – Dexamethasone pre-treatment increased the proportion of MEC-LII principal cells affected by phenylephrine.**

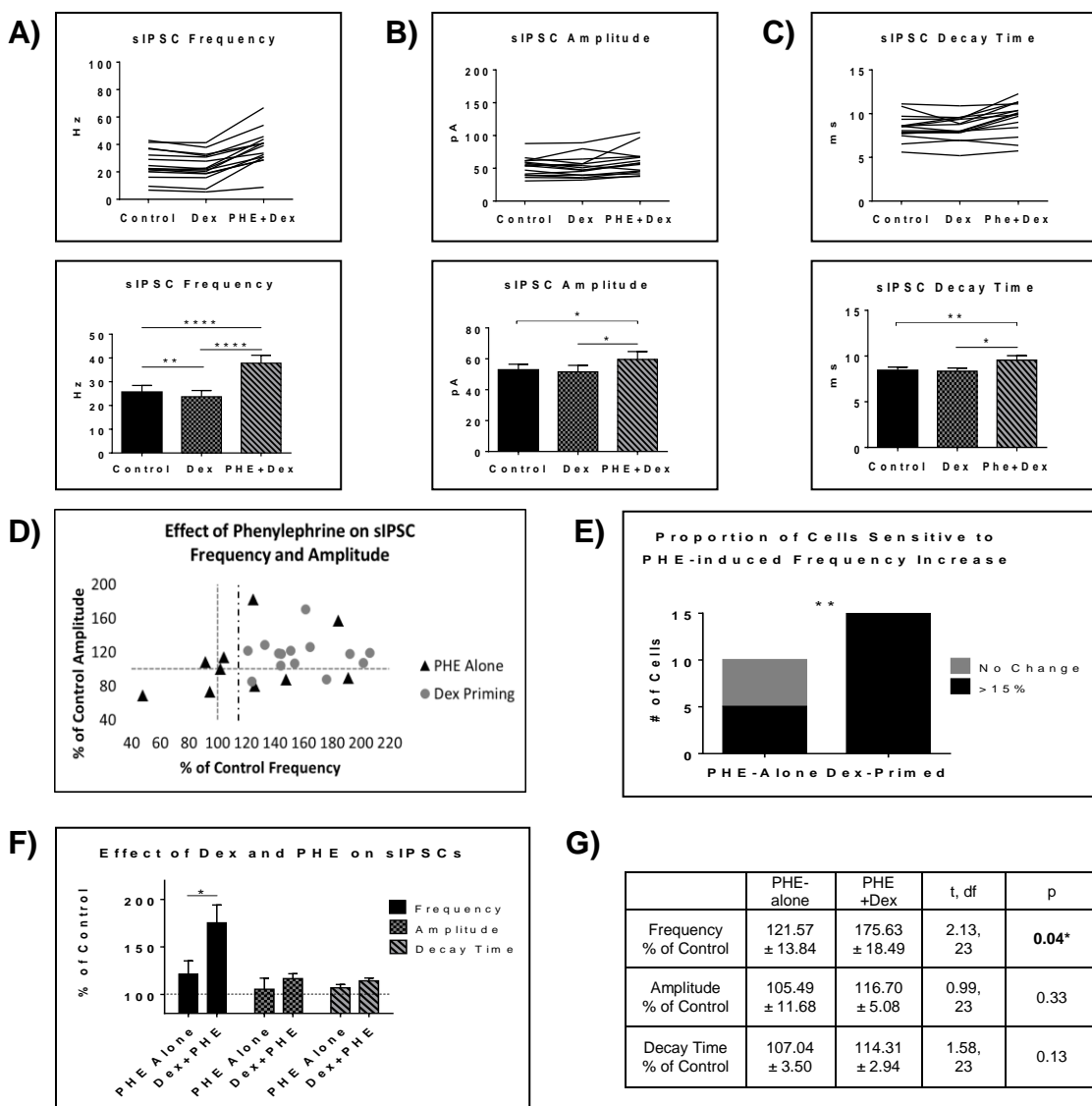


**Fig. 3.14: A-C Top)** Effect of Dex and PHE+Dex on sIPSC frequency, amplitude, and decay by cell. **A-C Bottom)** Average of by-cell traces shown above. **A)** Dex significantly decreased sIPSC frequency, and PHE+Dex significantly increased sIPSC frequency from Dex-alone and control. **B)** PHE+Dex significantly increased amplitude from Dex-alone and control. **C)** PHE+Dex significantly increased decay time from Dex-alone and control. **D)** Scatter plot of PHE effect on normalized frequency and amplitude changes in cells that were treated with PHE alone (triangles) versus cells that were pre-treated with Dex (circles) prior to PHE application. The dotted line indicates the cut-off value for classifying a cell as PHE-sensitive (>15% increase in sIPSC frequency). Note the five cells left of the cut-off line in the PHE-alone condition and that all of the Dex-priming group are PHE-sensitive. **E)** Chi-square analysis of proportion of PHE-sensitive and insensitive cells in the PHE-alone condition versus the Dex-priming condition. **F)** Comparison of PHE effect on sIPSC frequency and amplitude when applied alone and when cells were pre-treated with Dex. **G)** Table of unpaired two-tailed t-tests showing normalized values for PHE-alone vs PHE primed with Dex for frequency, amplitude, and decay time.

**Table 10 – Effect of adrenergic receptor activation on IPSC frequency with and without Dex pre-treatment**

	Control (Hz)	NE/PHE (Hz)	NE/PHE+Dex (Hz)	F	n	p	Con vs NE/PHE	Con vs NE/PHE+Dex	NE/PHE vs NE/PHE+Dex
NE+Dex	42.39 ± 3.89	54.32 ± 3.59	52.31 ± 4.16	11.77	11	0.002*	**	*	NS
PHE+Dex	29.93 ± 4.33	36.39 ± 5.70	n/a	t=1.89	df=9	0.09	NS	n/a	n/a

	Control (Hz)	Dex (Hz)	Dex+NE/PHE (Hz)	F	n	p	Con vs Dex	Con vs Dex+NE/PHE	Dex vs Dex+NE/PHE
Dex+NE	37.83 ± 4.49	34.24 ± 3.94	51.25 ± 5.87	42.61	15	<0.0001*	*	****	****
Dex+PHE	25.62 ± 2.82	23.69 ± 2.63	37.79 ± 3.37	51.73	15	<0.0001*	**	****	****

**Table 11 – Effect of adrenergic receptor activation on IPSC amplitude with and without Dex pre-treatment**

	Control (pA)	NE/Agonist (pA)	NE/Agonist +Dex (pA)	F	n	p	Con vs NE/PHE	Con vs NE/PHE+Dex	NE/PHE vs NE/PHE+Dex
NE+Dex	57.90 ± 9.34	80.61 ± 11.57	68.58 ± 13.56	7.11	11	0.007*	**	NS	NS
PHE+Dex	57.09 ± 4.02	60.66 ± 9.19	n/a	t=0.48	df=9	0.64	NS	n/a	n/a

	Control (pA)	Dex (pA)	Dex+NE/Agonist (pA)	F	n	p	Con vs Dex	Con vs Dex+NE/PHE	Dex vs Dex+NE/PHE
Dex+NE	49.38 ± 2.52	49.60 ± 4.04	73.63 ± 8.72	13.44	15	0.001*	NS	**	**
Dex+PHE	52.75 ± 3.74	51.55 ± 4.19	59.62 ± 5.10	6.14	15	0.01*	NS	*	*

**Table 12 – Effect of adrenergic receptor activation on IPSC decay time with and without Dex pre-treatment**

	Control (ms)	NE/Agonist (ms)	NE/Agonist +Dex (ms)	F	n	p	Con vs NE/PHE	Con vs NE/PHE+Dex	NE/PHE vs NE/PHE+Dex
NE+ Dex	8.91 ± 0.50	9.18 ± 0.52	9.48 ± 0.42	0.96	11	0.96	n/a	n/a	n/a
PHE + Dex	8.62 ± 0.50	9.16 ± 0.49	n/a	t=1.79	df=9	0.11	NS	n/a	n/a

	Control (ms)	Dex (ms)	Dex+NE/ Agonist (ms)	F	n	p	Con vs Dex	Con vs Dex+NE/PHE	Dex vs Dex+NE/PHE
Dex+ NE	8.46 ± 0.28	8.82 ± 0.27	9.35 ± 0.32	16.27	15	<0.0001*	NS	***	**
Dex+ PHE	8.42 ± 0.37	8.34 ± 0.36	9.55 ± 0.48	17.42	15	<0.0001*	NS	**	***

**Table 13 – Chi-square comparison of NE-alone versus Dex-primed NE**

Chi-Square	Increased Frequency	No Change in Frequency
NE-Alone	10	3
Dex-Primed	15	0

$\chi^2$	3.88
df	1
P-Value	0.05 to 0.02
Significance	*

**Table 14 – Chi-square comparison of PHE-alone versus Dex-primed PHE**

Chi-Square	Increased Frequency	No Change in Frequency
PHE-Alone	5	5
Dex-Primed	15	0

$\chi^2$	9.38
df	1
P-Value	0.01 to 0.001
Significance	**

## Discussion

The effect of norepinephrine on sIPSC frequency is in striking contrast to the effect of dexamethasone shown in chapter 2. Where Dex caused a small, though consistent, sIPSC frequency decrease, NE caused a dramatic increase in sIPSC frequency in MEC-LII principal cells. In general, NE quickly caused a robust increase in both sIPSC frequency and amplitude, and a gradual increase in decay time over time. NE also significantly increased frequency of terminal-specific inhibitory signaling, but even more surprising is that the miniature ISPC frequency increase seen after NE also only occurs in 70-80% of principal cells in MEC-LII. It is unclear if the subset of cells with unaltered inhibitory input following NE (20-30%) is a distinct type of principal cell. It is certainly possible that choice of principal cell recorded from was unbiased, leading to an even distribution of recordings from each of the four principal cell types found in MEC-LII. If one of the four cell types is insensitive to NE-induced changes to inhibitory signaling, it could account for the 20-30% subset of insensitive cells seen in these experiments.

In terms of intrinsic properties, previous studies have shown that NE hyperpolarizes 50% of cells in the MEC and is blocked by  $\alpha 2$ -AR antagonism, though this hyperpolarization occurs in higher proportion in LIII than LII (Xiao et al., 2009). Our findings show that NE caused hyperpolarization of  $V_m$  in only 3 of 8 cells, which is consistent with previous findings. Furthermore, average baseline  $V_m$  in NE-sensitive cells was significantly hyperpolarized compared to NE-insensitive cells, suggesting cell type differences consistent with the idea that

different cell types in MEC-LII have different resting membrane potentials. Also, average baseline input resistance of NE-insensitive cells was significantly greater compared to cells that show NE-induced changes in inhibitory signaling. Furthermore, average sag was close to zero in all three cells that failed to show an NE-induced increase in sIPSC frequency, though the average was not significantly different from the NE-sensitive group. This difference in intrinsic properties could be an indication that the NE-insensitive cells are a different cell type. True stellate cells are consistently measured as having the lowest input resistance and largest sag amplitude, true pyramidal cells have the highest input resistance and smallest sag amplitude, and the intermediate stellate and pyramidal cells measure on a gradient between the true stellate and pyramidal cell groups (Fuchs et al., 2016; Alonso and Klink, 1993). The number of NE-insensitive cells (n=3) seen in the experiment measuring intrinsic characteristics is very low, and increasing the overall number recorded may reveal a significant difference in baseline sag between NE-sensitive and NE-insensitive cells. In this case, the true pyramidal cell class is the most likely subset of cells that fail to show NE-induced changes to inhibitory inputs.

Because NE primarily affects frequency of both spontaneous and terminal-specific signaling seen in the MEC-LII principal cells, the effect can likely be localized to the pre-synaptic GABAergic cells located locally and sending inputs to the principal cells. There is no evidence of differential expression of adrenergic receptors between the inhibitory or principal cell classes, but AR expression levels could be dramatically different between the different cell types. Given the

complex network of inhibitory inputs and the selective nature of the distinct interneuron classes in terms of targeting different principal cell classes, varying expression of ARs in the different interneuron classes could account for the NE-sensitive and NE-insensitive groups seen in these experiments. It is important to consider that the subset of insensitive cells seen in these experiments, whether or not they can be classified as one of the four current principal cell type divisions, may not be due to cell-specific differences in adrenergic receptor level expression.

Previous studies have demonstrated the lack of an NE-induced increase in sIPSC frequency and amplitude in the presence of a  $\alpha$ 1-AR antagonist (Lei et al., 2007). Surprisingly, we show that the  $\alpha$ 1-AR agonist, phenylephrine, fails to significantly increase sIPSC frequency; however, 5 of 10 cells recorded showed an increase in sIPSC frequency similar to that seen with norepinephrine application (Fig. 3.14 A). NE also caused a marked increase in mIPSC frequency that was not fully accounted for by the increases seen independently with  $\alpha$ 1 or  $\alpha$ 2-AR activation (Fig. 3.14 B). In fact, the  $\alpha$ 2-AR agonist, UK14304, failed to significantly impact spontaneous inhibitory signaling in MEC-LII principal cells, but significantly increased decay time of terminal-specific mIPSCs without affecting frequency or amplitude. Isoprenaline, a  $\beta$ -AR agonist, had no effect on frequency, amplitude, or decay time of sIPSCs, and mIPSCs were not tested. The marked amplitude increase in sIPSC amplitude seen with norepinephrine application could not be completely accounted for by any one of the AR agonists, and it is therefore assumed that the large amplitude increases are due to the

combined activation of multiple AR types (Fig. 3.14 A), though simultaneous activation of  $\alpha 1$  and  $\alpha 2$ -ARs was not tested.

In the experiments shown above, 50% (33 of 66) of all cells did not respond (<15% increase) to NE,  $\alpha 1$ -AR agonist, or  $\alpha 2$ -AR agonist application in terms of changes to spontaneous or miniature IPSC frequency compared to control conditions. Testing with the  $\beta$ -AR agonist revealed a higher percentage of cells with sIPSC frequencies unaffected by NE application (4 of 5 total cells). It is also important to note that adding Dex to the bath following application of NE or  $\alpha 1$ -AR agonist resulted in a decrease in average sIPSC frequency in each condition, consistent with the effects of Dex applied alone. Surprisingly, when Dex was added to the bath after the control condition and allowed to perfuse for nearly fifteen minutes prior to adding either NE or the  $\alpha 1$ -AR agonist, every cell responded with a greater than 15% increase in sIPSC frequency after a ten minute application of NE (15 of 15 cells) or  $\alpha 1$ -AR agonist (15 of 15 cells). This finding suggests two previously unidentified effects in MEC-LII principal cells. First, there are a proportion of cells in MEC-LII that are unresponsive to NE in terms of changes to frequency of IPSC signaling. Second, incubation of MEC-LII principal cells in dexamethasone eliminates this set of non-responders so that all principal cells in MEC-LII show an NE-induced increase in sIPSC frequency. Based on the data shown above, we suggest that dexamethasone is priming a subset of cells to become responsive to NE application that were previously unaffected, and that this priming effect occurs rapidly and is likely to be working through GR in a transcription-independent fashion.

**Figure 3.14 – Effect of AR activation on IPSCs in MEC-LII principal cells.**

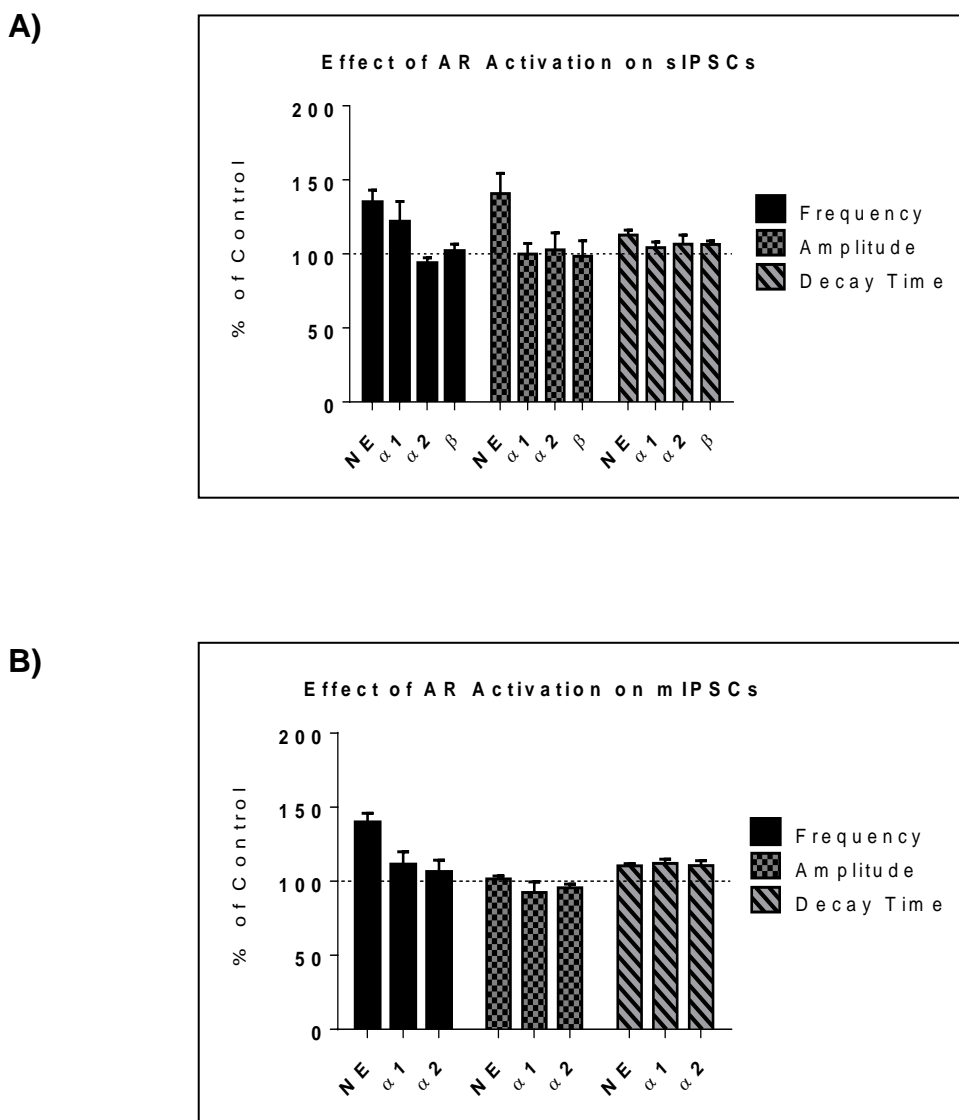


**Fig. 3.14:** X-axis: AR agonist. Y-axis: Percentage of measured IPSC characteristic (frequency, amplitude, or decay) in drug normalized to the corresponding control value. **A)** Effects on spontaneous IPSCs only. **B)** Effects on miniature IPSCs only.

## **CHAPTER 4**

## **CONCLUSIONS**

## CHAPTER 4: CONCLUSIONS

These findings demonstrate the ability of stress hormones to markedly alter inhibitory signaling within MEC-LII circuits. Glucocorticoids, both corticosterone and dexamethasone, consistently and rapidly decrease frequency of spontaneous inhibitory signaling in MEC-LII principal cells. Naturally, MR has a high affinity for glucocorticoids and is bound and activated at much lower concentrations than GR, which has a much lower affinity for glucocorticoids, and the GR is not activated until concentrations are greatly increased above basal levels (Timmermans et al., 2013; de Kloet et al., 1998). Because the same effect on sIPSC frequency is seen in the presence of both Cort and Dex, and the fact that Dex is a glucocorticoid receptor (GR)-specific agonist, glucocorticoids likely exert this frequency modulation by acting through GR rather than the mineralocorticoid receptor (MR). Because glucocorticoids did not alter miniature IPSCs in MEC-LII principal cells and failed to alter IPSC amplitude, we conclude that GR activation resulting in decreased sIPSC frequency cannot be due to pre-synaptic GR-induced modulation of terminal-specific GABA release or post-synaptic GABA<sub>A</sub> receptor modulation. It is more likely that activation of membrane GR occurs at the pre-synaptic cell to decrease frequency of spike-evoked GABA release. However, we cannot rule-out the idea that post-synaptic GR activation leads to retrograde release of endocannabinoids or nitric oxide

(Kano et al., 2009). Depolarization-induced suppression of inhibition (DSI) is a commonly known mechanism in which endocannabinoid release from the post-synaptic cell acts on pre-synaptic endocannabinoid receptors to decrease GABA release. Glucocorticoids are also known to trigger release of NO through activation of GR, which acts on pre-synaptic GABAergic cells to increase spiking (Nahar et al., 2015). To localize the mechanism of rapid glucocorticoid action it would be necessary to see if the glucocorticoid-induced frequency effect persists in the presence of G-protein and retrograde signaling blockers.

Within minutes of perception of a stressful situation, blood glucocorticoid levels rise to concentrations sufficient for GR binding, thereby enacting another pathway to enable the organism to better attend to the burden. This sort of spillover effect leading to the activation of GR indicates a biological mechanism for dealing with stressful stimuli, and is likely the reason for the effects seen on signaling in the above experiments. We show that glucocorticoids, at levels normally seen in the circulating blood of an organism recently exposed to a stressor, activate GR to dampen inhibitory signaling within MEC-LII. Rapid effects of membrane GR are seen in multiple species and are considered an evolutionarily conserved mechanism (Dallman, 2005), indicating that this response is adaptive and maybe an effective means of dealing with stressful stimuli. Independent of other stress hormones, it might then be reasonable to hypothesize that decreased frequency of inhibitory signaling in stressful situations is an organism's means of increasing excitability and timing of functional output of MEC-LII cells to enhance signaling along the known memory

pathways from the MEC to the hippocampus. One factor to consider for this increase in signal-to-noise ratio hypothesis is that decreased inhibition does not necessarily make a cell more excitable, and the cellular output would need to be tested. Furthermore, given the known importance of oscillatory activity in MEC-LII, a change in signal-to-noise ratio could dramatically alter theta-nested gamma known to be crucial for spatial memory processing. The results of this study do not provide a complete explanation for GR's role in stress-induced modulation of spatial processing, but they clearly define how GR, independent of other stress hormones, can modulate inhibitory signaling within spatial memory processing pathways.

Glucocorticoid levels are not the only hormones to rapidly rise during stress. The stress response includes activation of the sympathetic nervous system to increase NE release. In fact, NE release following stress achieves a systemic response more quickly than glucocorticoids. Not surprisingly, activation of adrenergic receptors (ARs) also rapidly modulated inhibitory signaling within MEC-LII circuits. Unlike glucocorticoids, NE dramatically increased both the frequency and amplitude of inhibitory inputs onto MEC-LII principal cells at levels 2-3-fold higher than the decrease seen after glucocorticoid application (~35% increase in NE versus ~13% decrease in Dex and ~19% decrease in Cort). Application of a  $\alpha$ 1-AR agonist was able to mimic the large increase in sIPSC frequency seen with NE in only half of the cells tested, and failed to mimic the NE-induced increase in sIPSC amplitude. We hypothesize that simultaneous activation of the different  $\alpha$  and  $\beta$ -ARs is the only way to mimic the NE-induced

amplitude increase, but this was not tested. Interestingly, we also show that NE increased frequency of miniature IPSCs indicating that spontaneous GABA release at the synaptic terminal increases even in the absence of cell spiking. The terminal-specific increase in mIPSC frequency was not mimicked by either the  $\alpha 1$  or  $\alpha 2$ -AR agonist alone. We therefore hypothesize that both  $\alpha 1$  and  $\alpha 2$ -ARs together must contribute to the NE-induced increase in terminal-specific GABA release. We hypothesize that the NE-induced increase in IPSC frequency is a pre-synaptic effect through activation of ARs located at the pre-synaptic cell terminal to increase GABA release. No matter the mechanism, NE causes a strikingly large increase in inhibitory signaling in MEC-LII. The reason for this level of increased inhibitory tone is unclear, though it does not necessarily follow that increased inhibition in MEC-LII decreases functional output. In fact, sufficiently large hyperpolarizing pulses in MEC-LII stellate cells cause rebound spiking through activation of HCN channels ( $I_h$ ) (Alonso and Klink, 1993), meaning inhibition can be readily converted to an increase in cellular output, though this remains to be tested.

Because stressful stimuli cause nearly simultaneous release of NE and glucocorticoids, an organism would not naturally experience the effects of these hormones independently. Three factors make it necessary to understand the interplay between the different responses to the two stress hormones when applied separately: first, the magnitude of the NE inhibitory response is greater than the opposing glucocorticoid effect, second, the NE and glucocorticoid responses counter each other in terms of direction of frequency modulation, and

third, glucocorticoids seem to exert consistent sIPSC frequency modulation across all cells while AR activation fails to modulate frequency of either spontaneous or miniature IPSCs in 50% of MEC-LII principal cells (66 cells were tested with NE or AR agonists, and 33 showed less than 15% increase from control in either spontaneous or mini IPSC frequency). We show that co-administration of the two stress hormones, dexamethasone and NE, causes differential responses depending on the order of application. Adding NE first and allowing NE to exert its full effects prior to adding Dex led to results that were consistent with each of the drug's effects seen when administered individually, including the subset of cells (~23%) that were unresponsive to NE. However, when Dex was perfused for 15 minutes prior to receiving NE, every cell responded to the NE with a larger than 15% increase in sIPSC frequency. This finding is novel in two ways. First, it suggests that there is a subset of cells in MEC-LII that are unresponsive to NE without prior activation of GR. Previous tests on a mix of cells from MEC-LII and LIII in rats less than three weeks of age when MEC circuitry is not yet fully developed, showed that 100% of cells were affected by NE (Lei et al., 2007). This is the first test of NE's effects when recording exclusively from cells in dorsal MEC-LII in animals old enough to have fully matured grid cells. Second, incubation of MEC-LII principal cells in Dex eliminates this set of non-responders so that all principal cells in MEC-LII show an NE-induced increase in sIPSC frequency. Thus, activation of GR by Dex is priming a subset of cells to become responsive to NE application that were previously unaffected.

To further our understanding of how Dex primes ARs, we show that a subset of cells in MEC-LII (50%) are also insensitive to the  $\alpha$ 1-AR agonist, PHE, and that incubation with Dex prior to adding PHE results in all cells (15 of 15) showing an  $\alpha$ 1-AR-induced increase in sIPSC frequency. The effect of priming the PHE-treated cells with Dex closely matched the priming effect with NE-treated cells in terms of frequency (2-way ANOVA interaction,  $p=0.18$ ), amplitude (2-way ANOVA interaction,  $p=0.51$ ), and decay time (2-way ANOVA interaction,  $p=0.38$ ) (Fig. 4.1 A, B, Table 15-17). Priming MEC-LII principal cells with Dex prior to adding  $\alpha$ 2 and  $\beta$ -AR agonists was not performed here because the effect of the  $\alpha$ 1-AR agonist fully accounted for the frequency increase seen with NE application.  $\alpha$ 2 and  $\beta$ -AR agonists applied alone failed to elicit frequency changes in nearly every cell tested (16 of 18 cells had less than 15% increase in IPSC frequency), so it is possible that Dex could prime these cells to become sensitive to their respective agonists.

The priming effect observed with co-administration of NE and dexamethasone occurs too rapidly to be accounted for by transcriptional changes, which are generally seen more than 30 minutes after GR activation (Roszkowski et al., 2016). The priming effect seen here might be explained by an indirect interaction downstream of G-protein activation. In rats, both membrane GRs and ARs can rapidly alter signaling through transcription-independent mechanisms involving G-protein activation. The exact mechanism of rapid signaling changes following membrane GR activation remains unclear, so we cannot suggest an indirect connection between the downstream targets of GR and AR that could

lead to the synergistic effect seen during co-application of Dex and NE seen in these studies. In order to determine if the mechanism of the priming effect is G-protein-dependent, we would need to add a G-protein blocker to the recording pipette to see if the priming effect persists; however, this remains to be done.

The lack of NE effect seen in >20% of cells recorded emphasizes the need for identification of cell type in MEC-LII. The existence of NE-insensitive cells may suggest differential expression of ARs based on MEC-LII interneuron class or principal cell type, and immunohistochemistry may be able to determine if there are differences in AR expression between stellate and pyramidal cells. It would also be important to know if a subset of MEC-LII principal cells have differential sub-cellular locations of  $\alpha$ 1-ARs. Given that the different cell types have differences in type of inhibitory input as well as downstream projection targets, this lack of sensitivity for NE in one specific MEC-LII principal cell type could reveal important mechanisms by which memory-associated regions process spatial information.

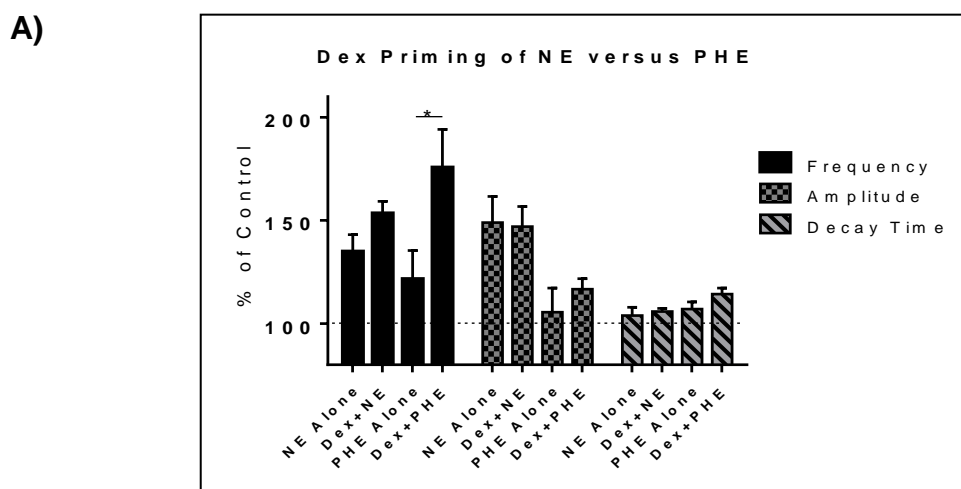
Though we are yet to investigate the mechanism of this priming effect, there is evidence that GR can interact with ARs. In the hypothalamus, GR activation by Dex internalizes  $\alpha$ 1-ARs to make the cells unresponsive to an NE-induced increase in sIPSC frequency (Tasker, SFN abstract, 2015). Mechanistically, this suggests that Dex application can interact with ARs to influence their sub-cellular positioning. Our results would require activation of GR to cause AR membrane insertion in cells with mostly internalized  $\alpha$ 1-ARs. Evidence suggests that sub-cellular positioning can determine effectiveness and

affinity of AR agonists. In Cos-7 cell cultures,  $\alpha 1_A$ -ARs are primarily located internally while  $\alpha 1_B$ -ARs are primarily located in the cell membrane (Tsujiimoto et al., 1998). Furthermore,  $\alpha 1$ -AR affinity for an agonist depends on whether or not the receptor is inserted in the membrane (Sugawara et al., 2002). If GR activation causes insertion of ARs into the membrane in the subset of cells that were previously unresponsive to NE, it could account for the priming effect observed. We hypothesize that this subset of NE/PHE-insensitive cells are true pyramidal cells. Interestingly, true pyramidal cells have the highest input resistance and smallest sag responses of the principal cells in MEC-LII (Fuchs et al., 2016; Alonso and Klink, 1993). Our results demonstrate that approximately one quarter of MEC-LII principal cells are insensitive to NE/PHE-induced frequency increases, that these insensitive cells have a significantly higher baseline input resistance compared to NE/PHE-sensitive cells, and that the insensitive cells have small (<1-2mv) or no sag response. Furthermore, 5HT<sub>3A</sub> interneurons exclusively inhibit true pyramidal cells in MEC-LII, and PV<sup>+</sup> fast-spiking interneurons synapse onto all MEC-LII principal cells except true pyramidal cells (Fuchs et al., 2016). Thus, sensitization of true pyramidal cells could be explained by GR-induced  $\alpha 1$ -AR membrane insertion in pre-synaptic 5HT<sub>3A</sub> interneurons that do not express membrane-bound  $\alpha 1$ -ARs without GR-activation (Fig. 4.2).

No matter the mechanism, because the stress response is evolutionarily conserved, it is likely that the subset of NE-insensitive cells serves as an advantage to the organism in normal circumstances, though it remains unclear if

these cells are sensitized to respond to NE only in stressful situations, and what effect this has on the organism's behavior. Interestingly, low magnesium-induced epileptic activity in the entorhinal cortex can be blocked by  $\alpha$ 1-AR activation following NE application (Stanton et al., 1987), suggesting an interaction between stress hormone pathways and that the observed increase in inhibition is important to suppress hyperactivity leading to epilepsy within known spatial processing circuits. Ultimately, a better understanding of the connection between stress and spatial memory processing has implications for both our understanding and ability to treat populations affected by epilepsy, post-traumatic stress disorder, Alzheimer's disease, and learning and memory disorders. Determining the contribution of MEC-LII signaling modulation to stress-induced spatial memory deficits is the first step in creating a targeted approach for treatment in those afflicted.

**Figure 4.1 – Comparison of effects of NE and PHE on sIPSC frequency, amplitude, and decay with and without Dex pre-treatment.**



**B)**

	NE-alone vs Con	PHE-alone vs Con	NE-Dex vs Dex-alone	PHE-Dex vs Dex-alone
Frequency % of Control	134.83 ± 8.31	121.57 ± 13.84	153.39 ± 5.81	175.63 ± 18.49
Amplitude % of Control	148.99 ± 12.66	105.49 ± 11.68	147.01 ± 9.76	116.70 ± 5.08
Decay Time % of Control	103.93 ± 3.92	107.04 ± 3.50	105.88 ± 1.51	114.31 ± 2.94

**Fig. 4.1: A)** X-axis: Treatment condition comparing the effects of NE and PHE when primed or not with Dex for sIPSC frequency, amplitude, and decay time. Y-axis: sIPSC characteristic normalized to its corresponding control. **B)** Table comparing the normalized effects of NE and PHE with and without Dex priming for sIPSC frequency, amplitude, and decay time.

**Table 15 – 2-way ANOVA table for normalized sIPSC frequency effect of NE and PHE with or without Dex**

	SS	DF	MS	F (DFn, DFd)	P value
Interaction	4062	1	4062	F (1, 49) = 1.862	0.18
Dex or not	16998	1	16998	F (1, 49) = 7.791	<b>0.008</b>
NE or PHE	260	1	260	F (1, 49) = 0.1192	0.73

**Table 16 – 2-way ANOVA table for normalized sIPSC amplitude effect of NE and PHE with or without Dex**

	SS	DF	MS	F (DFn, DFd)	P value
Interaction	560.5	1	560.5	F (1, 49) = 0.4378	0.51
Dex or not	274.5	1	274.5	F (1, 49) = 0.2144	0.65
NE or PHE	17559	1	17559	F (1, 49) = 13.71	<b>0.0005</b>

**Table 17 – 2-way ANOVA table for normalized sIPSC decay time effect of NE and PHE with or without Dex**

	SS	DF	MS	F (DFn, DFd)	P value
Interaction	91.17	1	91.17	F (1, 49) = 0.7705	0.38
Dex or not	274.2	1	274.2	F (1, 49) = 2.318	0.13
NE or PHE	429	1	429	F (1, 49) = 3.625	0.06

**Figure 4.2 – Functional hypothesis for Dex-induced sensitization of NE/PHE-insensitive cells.**

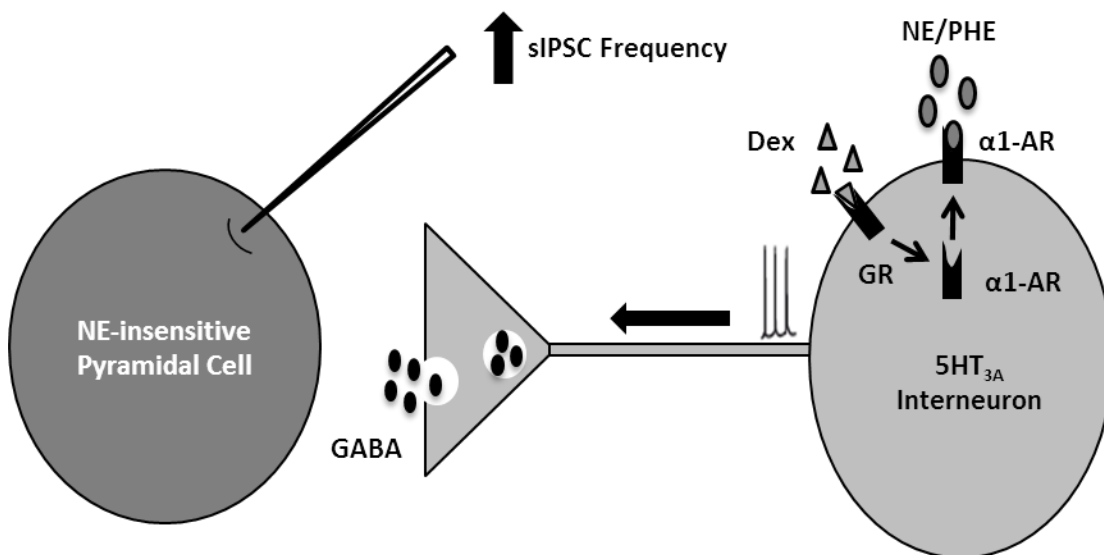


**Fig. 4.2:** Proposed model demonstrating how true pyramidal cells in MEC-LII could be insensitive to adrenergic receptor activation prior to Dex treatment. GR: glucocorticoid receptor; NE: norepinephrine; PHE: phenylephrine; AR: adrenergic receptor. This model proposes that  $\alpha 1$ -ARs are internalized in 5HT<sub>3A</sub> interneurons and therefore insensitive to NE/PHE application. Dex activation of GR leads to insertion of cytosolic  $\alpha 1$ -ARs into the membrane. Membrane-bound  $\alpha 1$ -ARs are activated by NE/PHE to increase GABA release from the pre-synaptic terminal and increase sIPSC frequency recorded from the post-synaptic pyramidal cell. This model also suggests that the NE-sensitive principal cells in MEC-LII can be explained by  $\alpha 1$ -AR activation in pre-synaptic fast-spiking interneurons that naturally express membrane-bound  $\alpha 1$ -ARs, but do not synapse onto pyramidal cells (not shown).

## LIST OF REFERENCES

- Aghajanian, G. K., & VanderMaelen, C. P. (1982). Alpha 2-adrenoceptor-mediated hyperpolarization of locus coeruleus neurons: Intracellular studies in vivo. *Science*, 215(4538), 1394-1396.
- Aimone, James Deng, Wei Gage, Fred. (2011). Resolving new memories: A critical look at the dentate gyrus, adult neurogenesis, and pattern separation. *Neuron*, 70(4), 589-596.
- Alonso, A., de Curtis, M., & Llinás, R. (1990). Postsynaptic hebbian and non-hebbian long-term potentiation of synaptic efficacy in the entorhinal cortex in slices and in the isolated adult guinea pig brain. *Proceedings of the National Academy of Sciences of the United States of America*, 87(23), 9280-9284.
- Alonso, A. K., R. (1993). Differential electroresponsiveness of stellate and pyramidal-like cells of medial entorhinal cortex layer II. *Journal of Neurophysiology*, 70(1), 128-143.
- Amaral, D., Scharfman, H., & Lavenex, P. (2007). The dentate gyrus: Fundamental neuroanatomical organization (dentate gyrus for dummies). *Prog Brain Res*, 163, 3-22.
- Barnes, C. A., McNaughton, B. L., Mizumori, S. J., Leonard, B. W., & Lin, L. H. (1990). Comparison of spatial and temporal characteristics of neuronal activity in sequential stages of hippocampal processing. *Prog Brain Res*, 83, 287-300.
- Beed, Prateep Bendels, Michael H K Wiegand, Hauke Leibold, Christian Johenning, Friedrich Schmitz, Dietmar. (2010). Analysis of excitatory microcircuitry in the medial entorhinal cortex reveals cell-type-specific differences. *Neuron*, 68(6), 1059-1066.
- Beed, Prateep Gundlfinger, Anja Schneiderbauer, Sophie Song, Jie Böhm, Claudia Burgalossi, Andrea Brecht, Michael Vida, Imre Schmitz, Dietmar. (2013). Inhibitory gradient along the dorsoventral axis in the medial entorhinal cortex. *Neuron*, 79(6), 1197-1207.

- Bellgowan, Patrick S F Buffalo, Elizabeth Bodurka, Jerzy Martin, Alex. (2009). Lateralized spatial and object memory encoding in entorhinal and perirhinal cortices. *Learning & Memory*, 16(7), 433-438.
- Bergles, D. E., Doze, V. A., Madison, D. V., & Smith, S. J. (1996). Excitatory actions of norepinephrine on multiple classes of hippocampal CA1 interneurons. *The Journal of Neuroscience*, 16(2), 572-585.
- BLACKSTAD, T. W. (1956). Commissural connections of the hippocampal region in the rat, with special reference to their mode of termination. *Journal of Comparative Neurology*, 105(3), 417-537.
- Bonnevie, Tora Dunn, Benjamin Fyhn, Marianne Hafting, Torkel Derdikman, Dori Kubie, John Roudi, Yasser Moser, Edvard Moser, May-Britt. (2013). Grid cells require excitatory drive from the hippocampus. *Nature Neuroscience*, 16(3), 309-317.
- Booze, R. M., Crisostomo, E. A., & Davis, J. N. (1993). Beta-adrenergic receptors in the hippocampal and retrohippocampal regions of rats and guinea pigs: Autoradiographic and immunohistochemical studies. *Synapse*, 13(3), 206-214.
- Bowman, R E Ferguson, D Luine, V N. (2002). Effects of chronic restraint stress and estradiol on open field activity, spatial memory, and monoaminergic neurotransmitters in ovariectomized rats. *Neuroscience*, 113(2), 401-410.
- Boyajian, C. L., Loughlin, S. E., & Leslie, F. M. (1987). Anatomical evidence for alpha-2 adrenoceptor heterogeneity: Differential autoradiographic distributions of [3H]rauwolscine and [3H]idazoxan in rat brain. *The Journal of Pharmacology and Experimental Therapeutics*, 241(3), 1079-1091.
- Braak, H., & Braak, E. (1991). Neuropathological staging of alzheimer-related changes. *Acta Neuropathologica*, 82(4), 239-259.
- Bragin, A Jandó, G Nádasdy, Z Hetke, J Wise, K Buzsáki, G. (1995). Gamma (40-100 hz) oscillation in the hippocampus of the behaving rat. *The Journal of Neuroscience*, 15(1), 47-60.
- Brandon, M., Bogaard, A., Libby, C., Connerney, M., Gupta, K., & Hasselmo, M. (2011). Reduction of theta rhythm dissociates grid cell spatial periodicity from directional tuning. *Science*, 332(6029), 595-9.
- Buetfering, C., Allen, K., & Monyer, H. (2014). Parvalbumin interneurons provide grid cell-driven recurrent inhibition in the medial entorhinal cortex. *Nature Neuroscience*, 17(5), 710-8.

- Burak, Y. F., Ila. (2009). Accurate path integration in continuous attractor network models of grid cells. *PLoS Computational Biology*, 5(2), e1000291-e1000291.
- Burgalossi, A. B., Michael. (2014). Cellular, columnar and modular organization of spatial representations in medial entorhinal cortex. *Current Opinion in Neurobiology*, 24C, 47-54.
- Burgess, Neil Barry, Caswell O'Keefe, John. (2007). An oscillatory interference model of grid cell firing. *Hippocampus*, 17(9), 801-812.
- Burgess, N., Maguire, E., & O'Keefe, J. (2002). The human hippocampus and spatial and episodic memory. *Neuron*, 35(4), 625-641.
- Buzsáki, G. D., Andreas. (2004). Neuronal oscillations in cortical networks. *Science*, 304(5679), 1926-1929.
- Buzsáki, G. M., Edvard. (2013). Memory, navigation and theta rhythm in the hippocampal-entorhinal system. *Nature Neuroscience*, 16(2), 130-138.
- Buzsáki, G., & Wang, X. (2012). Mechanisms of gamma oscillations. *Annual Review of Neuroscience*, 35, 203-25.
- Canto, C., Wouterlood, F., & Witter, M. (2008). What does the anatomical organization of the entorhinal cortex tell us? *Neural Plasticity*, 2008, 381243-381243.
- Cassaday, H. J., & Rawlins, J. N. (1997). The hippocampus, objects, and their contexts. *Behavioral Neuroscience*, 111(6), 1228-1244.
- Castañeda, P., Muñoz, M., García Rojo, G., Ulloa, J., Bravo, J., Márquez, R., et al. (2015). Association of N-cadherin levels and downstream effectors of rho GTPases with dendritic spine loss induced by chronic stress in rat hippocampal neurons. *Journal of Neuroscience Research*, 93(10), 1476-1491.
- Cerqueira, J., Pêgo, J., Taipa, R., Bessa, J., Almeida, O. F. X., & Sousa, N. (2005). Morphological correlates of corticosteroid-induced changes in prefrontal cortex-dependent behaviors. *The Journal of Neuroscience*, 25(34), 7792-7800.
- Chrobak, J. J., Stackman, R. W., & Walsh, T. J. (1989). Intraseptal administration of muscimol produces dose-dependent memory impairments in the rat. *Behavioral and Neural Biology*, 52(3), 357-369.
- Chrobak, J. J., & Buzsáki, G. (1998). Gamma oscillations in the entorhinal cortex of the freely behaving rat. *The Journal of Neuroscience*, 18(1), 388-398.

- Chrousos, G. (2009). Stress and disorders of the stress system. *Nature Reviews.Endocrinology*, 5(7), 374-381.
- Colgin, Laura Denninger, Tobias Fyhn, Marianne Hafting, Torkel Bonnevie, Tora Jensen, Ole Moser, May-Britt Moser, Edvard. (2009). Frequency of gamma oscillations routes flow of information in the hippocampus. *Nature*, 462(7271), 353-357.
- Conrad, C D Galea, L A Kuroda, Y McEwen, B S. (1996). Chronic stress impairs rat spatial memory on the Y maze, and this effect is blocked by tianeptine pretreatment. *Behavioral Neuroscience*, 110(6), 1321-1334.
- Conrad, C. D., LeDoux, J. E., Magariños, A. M., & McEwen, B. S. (1999). Repeated restraint stress facilitates fear conditioning independently of causing hippocampal CA3 dendritic atrophy. *Behavioral Neuroscience*, 113(5), 902-913.
- Conrad, Cheryl Jackson, Jamie Wieczorek, Lindsay Baran, Sarah Harman, James Wright, Ryan Korol, Donna. (2004). Acute stress impairs spatial memory in male but not female rats: Influence of estrous cycle. *Pharmacology, Biochemistry and Behavior*, 78(3), 569-579.
- Couey, Jonathan Witoelar, Aree Zhang, Sheng-Jia Zheng, Kang Ye, Jing Dunn, Benjamin Czajkowski, Rafal Moser, May-Britt Moser, Edvard Roudi, Yasser Witter, Menno. (2013). Recurrent inhibitory circuitry as a mechanism for grid formation. *Nature Neuroscience*, 16(3), 318-324.
- Cox, D., Racca, C., & LeBeau, F. E. N. (2008). Beta-adrenergic receptors are differentially expressed in distinct interneuron subtypes in the rat hippocampus. *Journal of Comparative Neurology*, 509(6), 551-565.
- Crane, J., & Milner, B. (2005). What went where? impaired object-location learning in patients with right hippocampal lesions. *Hippocampus*, 15(2), 216-231.
- Cullinan, W. E., Herman, J. P., & Watson, S. J. (1993). Ventral subicular interaction with the hypothalamic paraventricular nucleus: Evidence for a relay in the bed nucleus of the stria terminalis. *Journal of Comparative Neurology*, 332(1), 1-20.
- Cunningham, M., Davies, C., Buhl, E., Kopell, N., & Whittington, M. (2003). Gamma oscillations induced by kainate receptor activation in the entorhinal cortex in vitro. *The Journal of Neuroscience*, 23(30), 9761-9769.
- Dallman, M. (2005). Fast glucocorticoid actions on brain: Back to the future. *Frontiers in Neuroendocrinology*, 26(3-4), 103-108.

- de Kloet, E. R., Joëls, M., & Holsboer, F. (2005). Stress and the brain: From adaptation to disease. *Nature Reviews.Neuroscience*, 6(6), 463-475.
- De Kloet, E. R., Sutanto, W., Rots, N., van Haarst, A., van den Berg, D., Oitzl, M., et al. (1991). Plasticity and function of brain corticosteroid receptors during aging. *Acta Endocrinologica*, 125 Suppl 1, 65-72.
- De Kloet, E. R., Vreugdenhil, E., Oitzl, M. S., & Joëls, M. (1998). Brain corticosteroid receptor balance in health and disease. *Endocrine Reviews*, 19(3), 269-301.
- De Kloet, E. R., Vreugdenhil, E., Oitzl, M. S., & Joëls, M. (1998). Brain corticosteroid receptor balance in health and disease. *Endocrine Reviews*, 19(3), 269-301.
- De Vos, H., Bricca, G., De Keyser, J., De Backer, J. P., Bousquet, P., & Vauquelin, G. (1994). Imidazoline receptors, non-adrenergic idazoxan binding sites and alpha 2-adrenoceptors in the human central nervous system. *Neuroscience*, 59(3), 589-598.
- Derdikman, Dori Whitlock, Jonathan Tsao, Albert Fyhn, Marianne Hafting, Torkel Moser, May-Britt Moser, Edvard. (2009). Fragmentation of grid cell maps in a multicompartement environment. *Nature Neuroscience*, 12(10), 1325-1332.
- Devauges, V., & Sara, S. J. (1991). Memory retrieval enhancement by locus coeruleus stimulation: Evidence for mediation by beta-receptors. *Behavioural Brain Research*, 43(1), 93-97.
- Di, S., Malcher Lopes, R., Halmos, K., & Tasker, J. (2003). Nongenomic glucocorticoid inhibition via endocannabinoid release in the hypothalamus: A fast feedback mechanism. *The Journal of Neuroscience*, 23(12), 4850-4857.
- Diamond, D M Fleshner, M Ingersoll, N Rose, G M. (1996). Psychological stress impairs spatial working memory: Relevance to electrophysiological studies of hippocampal function. *Behavioral Neuroscience*, 110(4), 661-672.
- Diamond, D. M., Bennett, M. C., Fleshner, M., & Rose, G. M. (1992). Inverted-U relationship between the level of peripheral corticosterone and the magnitude of hippocampal primed burst potentiation. *Hippocampus*, 2(4), 421-430.
- Diamond, D., Campbell, A., Park, C., Woodson, J., Conrad, C., Bachstetter, A., et al. (2006). Influence of predator stress on the consolidation versus retrieval of long-term spatial memory and hippocampal spinogenesis. *Hippocampus*, 16(7), 571-576.

- Dickson, C T Magistretti, J Shalinsky, M H Fransén, E Hasselmo, M E Alonso, A. (2000). Properties and role of I(h) in the pacing of subthreshold oscillations in entorhinal cortex layer II neurons. *Journal of Neurophysiology*, 83(5), 2562-2579.
- Dickson, C., Biella, G., & de Curtis, M. (2003). Slow periodic events and their transition to gamma oscillations in the entorhinal cortex of the isolated guinea pig brain. *Journal of Neurophysiology*, 90(1), 39-46.
- Dobarro, M., Orejana, L., Aguirre, N., & Ramírez, M. (2013). Propranolol reduces cognitive deficits, amyloid  $\beta$  levels, tau phosphorylation and insulin resistance in response to chronic corticosterone administration. *The International Journal of Neuropsychopharmacology*, 16(6), 1351-1360.
- Doeller, Christian Barry, Caswell Burgess, Neil. (2010). Evidence for grid cells in a human memory network. *Nature*, 463(7281), 657-661.
- Dolorfo, C. L., & Amaral, D. G. (1998). Entorhinal cortex of the rat: Topographic organization of the cells of origin of the perforant path projection to the dentate gyrus. *Journal of Comparative Neurology*, 398(1), 25-48.
- Domnisoru, Cristina Kinkhabwala, Amina Tank, David. (2013). Membrane potential dynamics of grid cells. *Nature*, 495(7440), 199-204.
- Doze, V. A., Cohen, G. A., & Madison, D. V. (1991). Synaptic localization of adrenergic disinhibition in the rat hippocampus. *Neuron*, 6(6), 889-900.
- Droste, S., de Groote, L., Atkinson, H., Lightman, S., Reul, Johannes M H M, & Linthorst, A. C. E. (2008). Corticosterone levels in the brain show a distinct ultradian rhythm but a delayed response to forced swim stress. *Endocrinology*, 149(7), 3244-3253.
- Eichenbaum, H Yonelinas, A P Ranganath, C. (2007). The medial temporal lobe and recognition memory. *Annual Review of Neuroscience*, 30, 123-152.
- Eichenbaum, H., Stewart, C., & Morris, R. G. (1990). Hippocampal representation in place learning. *The Journal of Neuroscience*, 10(11), 3531-3542.
- Engelmann, M., Landgraf, R., & Wotjak, C. (2004). The hypothalamic-neurohypophysial system regulates the hypothalamic-pituitary-adrenal axis under stress: An old concept revisited. *Frontiers in Neuroendocrinology*, 25(3-4), 132-149.

- Esclassan, Frederic Coutureau, Etienne Di Scala, Georges Marchand, Alain. (2009). A cholinergic-dependent role for the entorhinal cortex in trace fear conditioning. *The Journal of Neuroscience*, 29(25), 8087-8093.
- Evanson, N., Tasker, J., Hill, M., Hillard, C., & Herman, J. (2010). Fast feedback inhibition of the HPA axis by glucocorticoids is mediated by endocannabinoid signaling. *Endocrinology*, 151(10), 4811-4819.
- Fanselow, M., & Dong, H. (2010). Are the dorsal and ventral hippocampus functionally distinct structures? *Neuron*, 65(1), 7-19.
- Fernandes, P., Tamura, E., D'Argenio Garcia, L., Muxel, S., da Silveira Cruz-Machado, S., Marçola, M., et al. (2017). Dual effect of catecholamines and corticosterone crosstalk on pineal gland melatonin synthesis. *Neuroendocrinology*, 104(2), 126-134.
- French Mullen, J. M. (1995). Cortisol inhibition of calcium currents in guinea pig hippocampal CA1 neurons via G-protein-coupled activation of protein kinase C. *The Journal of Neuroscience*, 15(1), 903-911.
- Freund, T., & Katona, I. (2007). Perisomatic inhibition. *Neuron*, 56(1), 33-42.
- Fries, P. (2009). Neuronal gamma-band synchronization as a fundamental process in cortical computation. *Annual Review of Neuroscience*, 32, 209-224.
- Fuchs, E., Neitz, A., Pinna, R., Melzer, S., Caputi, A., & Monyer, H. (2016). Local and distant input controlling excitation in layer II of the medial entorhinal cortex. *Neuron*, 89(1), 194-208.
- Funder, J. (2017). Apparent mineralocorticoid excess. *The Journal of Steroid Biochemistry and Molecular Biology*, 165(A), 151-153.
- Fyhn, Marianne Molden, Sturla Witter, Menno Moser, Edvard Moser, May-Britt. (2004). Spatial representation in the entorhinal cortex. *Science*, 305(5688), 1258-1264.
- Gaffan, D. (1994). Scene-specific memory for objects: A model of episodic memory impairment in monkeys with fornix transection. *Journal of Cognitive Neuroscience*, 6(4), 305-320.
- Ge, S., Yang, C., Hsu, K., Ming, G., & Song, H. (2007). A critical period for enhanced synaptic plasticity in newly generated neurons of the adult brain. *Neuron*, 54(4), 559-566.

- Gelinas, J., Banko, J., Hou, L., Sonenberg, N., Weeber, E., Klann, E., et al. (2007). ERK and mTOR signaling couple beta-adrenergic receptors to translation initiation machinery to gate induction of protein synthesis-dependent long-term potentiation. *Journal of Biological Chemistry*, 282(37), 27527-27535.
- Gelinas, J., & Nguyen, P. (2005). Beta-adrenergic receptor activation facilitates induction of a protein synthesis-dependent late phase of long-term potentiation. *The Journal of Neuroscience*, 25(13), 3294-3303.
- Gibbs, M. E., Hutchinson, D. S., & Summers, R. J. (2010). Noradrenaline release in the locus coeruleus modulates memory formation and consolidation; roles for  $\alpha$ - and  $\beta$ -adrenergic receptors. *Neuroscience*, 170(4), 1209-1222.
- Gibbs, M., & Summers, R. (2002). Role of adrenoceptor subtypes in memory consolidation. *Progress in Neurobiology*, 67(5), 345-391.
- Giocomo, Lisa Zilli, Eric Fransén, Erik Hasselmo, Michael. (2007). Temporal frequency of subthreshold oscillations scales with entorhinal grid cell field spacing. *Science*, 315(5819), 1719-1722.
- Givens, B., & Olton, D. S. (1994). Local modulation of basal forebrain: Effects on working and reference memory. *The Journal of Neuroscience*, 14(6), 3578-3587.
- Gold, P. (2014). Regulation of memory - from the adrenal medulla to liver to astrocytes to neurons. *Brain Research Bulletin*, 105, 25-35.
- Gómez Sánchez, E. P. (1997). Central hypertensive effects of aldosterone. *Frontiers in Neuroendocrinology*, 18(4), 440-462.
- Goodman, J., Leong, K., & Packard, M. G. (2015). Glucocorticoid enhancement of dorsolateral striatum-dependent habit memory requires concurrent noradrenergic activity. *Neuroscience*, 311, 1-8.
- Gothard, K. M., Skaggs, W. E., Moore, K. M., & McNaughton, B. L. (1996). Binding of hippocampal CA1 neural activity to multiple reference frames in a landmark-based navigation task. *The Journal of Neuroscience*, 16(2), 823-835.
- Guo, N., & Li, B. (2007). Cellular and subcellular distributions of beta1- and beta2-adrenoceptors in the CA1 and CA3 regions of the rat hippocampus. *Neuroscience*, 146(1), 298-305.

- Hafting, Torkel Fyhn, Marianne Bonnevie, Tora Moser, May-Britt Moser, Edvard. (2008). Hippocampus-independent phase precession in entorhinal grid cells. *Nature*, 453(7199), 1248-1252.
- Hafting, Torkel Fyhn, Marianne Molden, Sturla Moser, May-Britt Moser, Edvard. (2005). Microstructure of a spatial map in the entorhinal cortex. *Nature*, 436(7052), 801-806.
- Hájos, N., Pálhalmi, J., Mann, E., Németh, B., Paulsen, O., & Freund, T. (2004). Spike timing of distinct types of GABAergic interneuron during hippocampal gamma oscillations in vitro. *The Journal of Neuroscience*, 24(41), 9127-9137.
- Hájos, N., & Paulsen, O. (2009). Network mechanisms of gamma oscillations in the CA3 region of the hippocampus. *Neural Networks*, 22(8), 1113-1119.
- Haller, J., Mikics, E., & Makara, G. (2008). The effects of non-genomic glucocorticoid mechanisms on bodily functions and the central neural system. A critical evaluation of findings. *Frontiers in Neuroendocrinology*, 29(2), 273-291.
- Hanukoglu, I., Feuchtwanger, R., & Hanukoglu, A. (1990). Mechanism of corticotropin and cAMP induction of mitochondrial cytochrome P450 system enzymes in adrenal cortex cells. *Journal of Biological Chemistry*, 265(33), 20602-20608.
- Hargreaves, Eric Rao, Geeta Lee, Inah Knierim, James. (2005). Major dissociation between medial and lateral entorhinal input to dorsal hippocampus. *Science*, 308(5729), 1792-1794.
- Hasenstaub, A., Shu, Y., Haider, B., Kraushaar, U., Duque, A., & McCormick, D. (2005). Inhibitory postsynaptic potentials carry synchronized frequency information in active cortical networks. *Neuron*, 47(3), 423-435.
- Hasselmo, Michael Giocomo, Lisa Zilli, Eric. (2007). Grid cell firing may arise from interference of theta frequency membrane potential oscillations in single neurons. *Hippocampus*, 17(12), 1252-1271.
- Herman, J. P., Dolgas, C. M., & Carlson, S. L. (1998). Ventral subiculum regulates hypothalamo-pituitary-adrenocortical and behavioural responses to cognitive stressors. *Neuroscience*, 86(2), 449-459.
- Herman, J., Figueiredo, H., Mueller, N., Ulrich-Lai, Y., Ostrander, M., Choi, D., et al. (2003). Central mechanisms of stress integration: Hierarchical circuitry controlling hypothalamo-pituitary-adrenocortical responsiveness. *Frontiers in Neuroendocrinology*, 24(3), 151-180.

- Herman, J., McKlveen, J., Ghosal, S., Kopp, B., Wulsin, A., Makinson, R., et al. (2016). Regulation of the hypothalamic-pituitary-adrenocortical stress response. *Compr Physiol*, 6(2), 603-621.
- Hillman, K., Doze, V., & Porter, J. (2007). Alpha1A-adrenergic receptors are functionally expressed by a subpopulation of cornu ammonis 1 interneurons in rat hippocampus. *The Journal of Pharmacology and Experimental Therapeutics*, 321(3), 1062-1068.
- Hillman, K., Knudson, C., Carr, P., Doze, V., & Porter, J. (2005). Adrenergic receptor characterization of CA1 hippocampal neurons using real time single cell RT-PCR. *Molecular Brain Research*, 139(2), 267-276.
- Holderbach, R., Clark, K., Moreau, J., Bischofberger, J., & Normann, C. (2007). Enhanced long-term synaptic depression in an animal model of depression. *Biological Psychiatry*, 62(1), 92-100.
- Huang, P., Li, C., Fu, T., Zhao, D., Yi, Z., Lu, Q., et al. (2015). Flupirtine attenuates chronic restraint stress-induced cognitive deficits and hippocampal apoptosis in male mice. *Behavioural Brain Research*, 288, 1-10.
- Iachini, Ina Iavarone, Alessandro Senese, Vincenzo Ruotolo, Francesco Ruggiero, Gennaro. (2009). Visuospatial memory in healthy elderly, AD and MCI: A review. *Current Aging Science*, 2(1), 43-59.
- Iachini, T., Ruggiero, G., & Ruotolo, F. (2009). The effect of age on egocentric and allocentric spatial frames of reference. *Cognitive Processing*, 10 Suppl 2, S222-S224.
- Jacobs, J., Weidemann, C., Miller, J., Solway, A., Burke, J., Wei, X., et al. (2013). Direct recordings of grid-like neuronal activity in human spatial navigation. *Nature Neuroscience*, 16(9), 1188-1190.
- Jarrard, L. E. (1993). On the role of the hippocampus in learning and memory in the rat. *Behavioral and Neural Biology*, 60(1), 9-26.
- Jeffery, K. J., Donnett, J. G., & O'Keefe, J. (1995). Medial septal control of theta-correlated unit firing in the entorhinal cortex of awake rats. *Neuroreport*, 6(16), 2166-2170.
- Ji, J., Zhang, X., & Li, B. (2003). Deficient spatial memory induced by blockade of beta-adrenoceptors in the hippocampal CA1 region. *Behavioral Neuroscience*, 117(6), 1378-1384.
- Joëls, M., Fernandez, G., & Roozendaal, B. (2011). Stress and emotional memory: A matter of timing. *Trends in Cognitive Sciences*, 15(6), 280-288.

- Joëls, M., Pu, Z., Wiegert, O., Oitzl, M., & Krugers, H. (2006). Learning under stress: How does it work? *Trends in Cognitive Sciences*, *10*(4), 152-158.
- Jones, R. S., & Bühl, E. H. (1993). Basket-like interneurons in layer II of the entorhinal cortex exhibit a powerful NMDA-mediated synaptic excitation. *Neuroscience Letters*, *149*(1), 35-39.
- Jones, R. S., & Lambert, J. D. (1990). The role of excitatory amino acid receptors in the propagation of epileptiform discharges from the entorhinal cortex to the dentate gyrus in vitro. *Experimental Brain Research*, *80*(2), 310-322.
- Jones, R. S., & Heinemann, U. (1988). Synaptic and intrinsic responses of medial entorhinal cortical cells in normal and magnesium-free medium in vitro. *Journal of Neurophysiology*, *59*(5), 1476-1496.
- Kalsbeek, A., van der Spek, R., Lei, J., Endert, E., Buijs, R. M., & Fliers, E. (2012). Circadian rhythms in the hypothalamo-pituitary-adrenal (HPA) axis. *Molecular and Cellular Endocrinology*, *349*(1), 20-29.
- Kano, Masanobu Ohno Shosaku, Takako Hashimotodani, Yuki Uchigashima, Motokazu Watanabe, Masahiko. (2009). Endocannabinoid-mediated control of synaptic transmission. *Physiological Reviews*, *89*(1), 309-380.
- Karst, H., Berger, S., Turiault, M., Tronche, F., Schütz, G., & Joëls, M. (2005). Mineralocorticoid receptors are indispensable for nongenomic modulation of hippocampal glutamate transmission by corticosterone. *Proceedings of the National Academy of Sciences of the United States of America*, *102*(52), 19204-7.
- Kassem, M., Lagopoulos, J., Stait Gardner, T., Price, W., Chohan, T., Arnold, J., et al. (2013). Stress-induced grey matter loss determined by MRI is primarily due to loss of dendrites and their synapses. *Molecular Neurobiology*, *47*(2), 645-661.
- Kerr, Kristin Agster, Kara Furtak, Sharon Burwell, Rebecca. (2007). Functional neuroanatomy of the parahippocampal region: The lateral and medial entorhinal areas. *Hippocampus*, *17*(9), 697-708.
- Kerr, D. S. (1994). Modulation of hippocampal long-term potentiation and long-term depression by corticosteroid receptor activation. *Psychobiology*, *22*(2), 123-133.
- Kesner, R. P., Gilbert, P. E., & Wallenstein, G. V. (2000). Testing neural network models of memory with behavioral experiments. *Current Opinion in Neurobiology*, *10*(2), 260-265.

- Kesner, R. P., & Rolls, E. T. (2001). Role of long-term synaptic modification in short-term memory. *Hippocampus*, 11(3), 240-250.
- Killian, Nathaniel Jutras, Michael Buffalo, Elizabeth. (2012). A map of visual space in the primate entorhinal cortex. *Nature*, 491(7426), 761-764.
- Kitamura, T., Pignatelli, M., Suh, J., Kohara, K., Yoshiki, A., Abe, K., et al. (2014). Island cells control temporal association memory. *Science*, 343(6173), 896-901.
- Kitamura, T., Sun, C., Martin, J., Kitch, L., Schnitzer, M., & Tonegawa, S. (2015). Entorhinal cortical ocean cells encode specific contexts and drive context-specific fear memory. *Neuron*, 87(6), 1317-1331.
- Knierim, J. J., Kudrimoti, H. S., & McNaughton, B. L. (1998). Interactions between idiothetic cues and external landmarks in the control of place cells and head direction cells. *Journal of Neurophysiology*, 80(1), 425-446.
- Koenig, Julie Linder, Ashley Leutgeb, Jill Leutgeb, Stefan. (2011). The spatial periodicity of grid cells is not sustained during reduced theta oscillations. *Science*, 332(6029), 592-595.
- Köhler, C. (1985). Intrinsic projections of the retrohippocampal region in the rat brain. I. the subicular complex. *Journal of Comparative Neurology*, 236(4), 504-522.
- Koolhaas, J. M., Bartolomucci, A., Buwalda, B., de Boer, S. F., Flügge, G., Korte, S. M., et al. (2011). Stress revisited: A critical evaluation of the stress concept. *Neuroscience & Biobehavioral Reviews*, 35(5), 1291-1301.
- KRIEG, W. J. S. (1946). Connections of the cerebral cortex; the albino rat; structure of the cortical areas. *Journal of Comparative Neurology*, 84, 277-323.
- KRIEG, W. J. S. (1946). Connections of the cerebral cortex; the albino rat; topography of the cortical areas. *Journal of Comparative Neurology*, 84, 221-275.
- Kropff, E., Carmichael, J., Moser, M., & Moser, E. (2015). Speed cells in the medial entorhinal cortex. *Nature*, 523(7561), 419-424.
- Krozowski, Z. S., & Funder, J. W. (1983). Renal mineralocorticoid receptors and hippocampal corticosterone-binding species have identical intrinsic steroid specificity. *Proceedings of the National Academy of Sciences of the United States of America*, 80(19), 6056-6060.

- Krupic, Julija Burgess, Neil O'Keefe, John. (2012). Neural representations of location composed of spatially periodic bands. *Science*, 337(6096), 853-857.
- Lacaille, J. C., & Harley, C. W. (1985). The action of norepinephrine in the dentate gyrus: Beta-mediated facilitation of evoked potentials in vitro. *Brain Research*, 358(1-2), 210-220.
- Langston, R., Ainge, J., Couey, J., Canto, C., Bjerknes, T., Witter, M., et al. (2010). Development of the spatial representation system in the rat. *Science*, 328(5985), 1576-1580.
- Lee, S., Hjerling Leffler, J., Zagha, E., Fishell, G., & Rudy, B. (2010). The largest group of superficial neocortical GABAergic interneurons expresses ionotropic serotonin receptors. *The Journal of Neuroscience*, 30(50), 16796-16808.
- Lei, S., Deng, P., Porter, J., & Shin, H. (2007). Adrenergic facilitation of GABAergic transmission in rat entorhinal cortex. *Journal of Neurophysiology*, 98(5), 2868-2877.
- Levcík, D., Stuchlík, A., & Klement, D. (2013). Effect of block of  $\alpha$ -1-adrenoceptors on overall motor activity but not on spatial cognition in the object-position recognition task. *Physiological Research*, 62(5), 561-567.
- Li, Y., Mu, Y., & Gage, F. (2009). Development of neural circuits in the adult hippocampus. *Curr Top Dev Biol*, 87, 149-174.
- Luine, V., Villegas, M., Martinez, C., & McEwen, B. S. (1994). Repeated stress causes reversible impairments of spatial memory performance. *Brain Research*, 639(1), 167-170.
- Lupien, S. J., & McEwen, B. S. (1997). The acute effects of corticosteroids on cognition: Integration of animal and human model studies. *Brain Research Reviews*, 24(1), 1-27.
- Ma, L. Y., Itharat, P., Fluharty, S. J., & Sakai, R. R. (1997). Intracerebroventricular administration of mineralocorticoid receptor antisense oligonucleotides attenuates salt appetite in the rat. *Stress*, 2(1), 37-50.
- Ma, T., Tzavaras, N., Tsokas, P., Landau, E., & Blitzer, R. (2011). Synaptic stimulation of mTOR is mediated by wnt signaling and regulation of glycogen synthetase kinase-3. *The Journal of Neuroscience*, 31(48), 17537-17546.
- Madison, D. V., & Nicoll, R. A. (1982). Noradrenaline blocks accommodation of pyramidal cell discharge in the hippocampus. *Nature*, 299(5884), 636-638.

- Magariños, A. M., & McEwen, B. S. (1995). Stress-induced atrophy of apical dendrites of hippocampal CA3c neurons: Involvement of glucocorticoid secretion and excitatory amino acid receptors. *Neuroscience*, *69*(1), 89-98.
- Magariños, A. M., Orchinik, M., & McEwen, B. S. (1998). Morphological changes in the hippocampal CA3 region induced by non-invasive glucocorticoid administration: A paradox. *Brain Research*, *809*(2), 314-318.
- Malpas, S. (2010). Sympathetic nervous system overactivity and its role in the development of cardiovascular disease. *Physiological Reviews*, *90*(2), 513-557.
- Malykhin, N. V., & Coupland, N. J. (2015). Hippocampal neuroplasticity in major depressive disorder. *Neuroscience*, *309*, 200-213.
- Mandel, E., Dunford, E., Trifonova, A., Abdifarkosh, G., Teich, T., Riddell, M., et al. (2016). Prazosin can prevent glucocorticoid mediated capillary rarefaction. *PLoS One*, *11*(11), e0166899-e0166899.
- Margittai, Z., Nave, G., Van Wingerden, M., Schnitzler, A., Schwabe, L., & Kalenscher, T. (2017). Combined effects of glucocorticoid and noradrenergic activity on loss aversion. *Neuropsychopharmacology*,
- Martin, M., Horn, K., Kusman, K., & Wallace, D. (2007). Medial septum lesions disrupt exploratory trip organization: Evidence for septohippocampal involvement in dead reckoning. *Physiology & Behavior*, *90*(2-3), 412-424.
- Martin, S. J., Grimwood, P. D., & Morris, R. G. (2000). Synaptic plasticity and memory: An evaluation of the hypothesis. *Annual Review of Neuroscience*, *23*, 649-711.
- McClelland, J. L., & Goddard, N. H. (1996). Considerations arising from a complementary learning systems perspective on hippocampus and neocortex. *Hippocampus*, *6*(6), 654-665.
- McEwen, B. S., De Kloet, E. R., & Rostene, W. (1986). Adrenal steroid receptors and actions in the nervous system. *Physiological Reviews*, *66*(4), 1121-1188.
- McEwen, B. S., Lambdin, L. T., Rainbow, T. C., & De Nicola, A. F. (1986). Aldosterone effects on salt appetite in adrenalectomized rats. *Neuroendocrinology*, *43*(1), 38-43.
- McEwen, B. (2007). Physiology and neurobiology of stress and adaptation: Central role of the brain. *Physiological Reviews*, *87*(3), 873-904.

- McEwen, B. (2016). Stress-induced remodeling of hippocampal CA3 pyramidal neurons. *Brain Research*, 1645, 50-54.
- McHugh, T., Jones, M., Quinn, J., Balthasar, N., Coppari, R., Elmquist, J., et al. (2007). Dentate gyrus NMDA receptors mediate rapid pattern separation in the hippocampal network. *Science*, 317(5834), 94-99.
- McNaughton, B. L., Barnes, C. A., Gerrard, J. L., Gothard, K., Jung, M. W., Knierim, J. J., et al. (1996). Deciphering the hippocampal polyglot: The hippocampus as a path integration system. *Journal of Experimental Biology*, 199(1), 173-185.
- McNaughton, Bruce Battaglia, Francesco Jensen, Ole Moser, Edvard Moser, May-Britt. (2006). Path integration and the neural basis of the 'cognitive map'. *Nature Reviews Neuroscience*, 7(8), 663-678.
- McReynolds, J., Donowho, K., Abdi, A., McGaugh, J., Roozendaal, B., & McIntyre, C. (2010). Memory-enhancing corticosterone treatment increases amygdala norepinephrine and arc protein expression in hippocampal synaptic fractions. *Neurobiology of Learning and Memory*, 93(3), 312-321.
- Meibach, R. C., & Siegel, A. (1977). Efferent connections of the septal area in the rat: An analysis utilizing retrograde and anterograde transport methods. *Brain Research*, 119(1), 1-20.
- Miettinen, M., Koivisto, E., Riekkinen, P., & Miettinen, R. (1996). Coexistence of parvalbumin and GABA in nonpyramidal neurons of the rat entorhinal cortex. *Brain Research*, 706(1), 113-22.
- Miller, D., & O'Callaghan, J. (2002). Neuroendocrine aspects of the response to stress. *Metabolism, Clinical and Experimental*, 51(6 Suppl 1), 5-10.
- Mitchell, S. J., Rawlins, J. N., Steward, O., & Olton, D. S. (1982). Medial septal area lesions disrupt theta rhythm and cholinergic staining in medial entorhinal cortex and produce impaired radial arm maze behavior in rats. *The Journal of Neuroscience*, 2(3), 292-302.
- Mitrovic, N., Le Saux, F., Giovanni, H., Giovanni, Y., Besson, M. J., & Maurin, Y. (1992). Distribution of [3H]clonidine binding sites in the brain of the convulsive mutant quaking mouse: A radioautographic analysis. *Brain Research*, 578(1-2), 26-32.
- Mizumori, S. J., Perez, G. M., Alvarado, M. C., Barnes, C. A., & McNaughton, B. L. (1990). Reversible inactivation of the medial septum differentially affects two forms of learning in rats. *Brain Research*, 528(1), 12-20.

- Mizumori, S. J., & Williams, J. D. (1993). Directionally selective mnemonic properties of neurons in the lateral dorsal nucleus of the thalamus of rats. *The Journal of Neuroscience*, *13*(9), 4015-4028.
- Mizuseki, K., Sirota, A., Pastalkova, E., & Buzsáki, G. (2009). Theta oscillations provide temporal windows for local circuit computation in the entorhinal-hippocampal loop. *Neuron*, *64*(2), 267-280.
- Morales, M., & Bloom, F. E. (1997). The 5-HT<sub>3</sub> receptor is present in different subpopulations of GABAergic neurons in the rat telencephalon. *The Journal of Neuroscience*, *17*(9), 3157-3167.
- Mormann, F., Fell, J., Axmacher, N., Weber, B., Lehnertz, K., Elger, C., et al. (2005). Phase/amplitude reset and theta-gamma interaction in the human medial temporal lobe during a continuous word recognition memory task. *Hippocampus*, *15*(7), 890-900.
- Moser, E. I., Krobot, K. A., Moser, M. B., & Morris, R. G. (1998). Impaired spatial learning after saturation of long-term potentiation. *Science*, *281*(5385), 2038-2042.
- Moser, Edvard Kropff, Emilio Moser, May-Britt. (2008). Place cells, grid cells, and the brain's spatial representation system. *Annual Review of Neuroscience*, *31*, 69-89.
- Moser, M. B., Moser, E. I., Forrest, E., Andersen, P., & Morris, R. G. (1995). Spatial learning with a minislab in the dorsal hippocampus. *Proceedings of the National Academy of Sciences of the United States of America*, *92*(21), 9697-9701.
- Mueller, A. L., Hoffer, B. J., & Dunwiddie, T. V. (1981). Noradrenergic responses in rat hippocampus: Evidence for mediation by alpha and beta receptors in the in vitro slice. *Brain Research*, *214*(1), 113-126.
- Murchison, C., Zhang, X., Zhang, W., Ouyang, M., Lee, A., & Thomas, S. (2004). A distinct role for norepinephrine in memory retrieval. *Cell*, *117*(1), 131-143.
- Murray, E. A., Baxter, M. G., & Gaffan, D. (1998). Monkeys with rhinal cortex damage or neurotoxic hippocampal lesions are impaired on spatial scene learning and object reversals. *Behavioral Neuroscience*, *112*(6), 1291-1303.
- Mynlieff, M., & Dunwiddie, T. V. (1988). Noradrenergic depression of synaptic responses in hippocampus of rat: Evidence for mediation by alpha 1-receptors. *Neuropharmacology*, *27*(4), 391-398.

- Nahar, J., Haam, J., Chen, C., Jiang, Z., Glatzer, N., Muglia, L., et al. (2015). Rapid nongenomic glucocorticoid actions in male mouse hypothalamic neuroendocrine cells are dependent on the nuclear glucocorticoid receptor. *Endocrinology*, *156*(8), 2831-2842.
- Nakashiba, Toshiaki Young, Jennie McHugh, Thomas Buhl, Derek Tonegawa, Susumu. (2008). Transgenic inhibition of synaptic transmission reveals role of CA3 output in hippocampal learning. *Science*, *319*(5867), 1260-1264.
- Nakashiba, T., Cushman, J., Pelkey, K., Renaudineau, S., Buhl, D., McHugh, T., et al. (2012). Young dentate granule cells mediate pattern separation, whereas old granule cells facilitate pattern completion. *Cell*, *149*(1), 188-201.
- Nakazawa, K., McHugh, T., Wilson, M., & Tonegawa, S. (2004). NMDA receptors, place cells and hippocampal spatial memory. *Nature Reviews Neuroscience*, *5*(5), 361-372.
- Nakazawa, K., Quirk, M., Chitwood, R., Watanabe, M., Yeckel, M., Sun, L., et al. (2002). Requirement for hippocampal CA3 NMDA receptors in associative memory recall. *Science*, *297*(5579), 211-218.
- Newman, Ehren Climer, Jason Hasselmo, Michael. (2014). Grid cell spatial tuning reduced following systemic muscarinic receptor blockade. *Hippocampus*,
- Nicholas, A. P., Pieribone, V. A., & Hökfelt, T. (1993). Cellular localization of messenger RNA for beta-1 and beta-2 adrenergic receptors in rat brain: An in situ hybridization study. *Neuroscience*, *56*(4), 1023-1039.
- Nolan, Matthew Dudman, Joshua Dodson, Paul Santoro, Bina. (2007). HCN1 channels control resting and active integrative properties of stellate cells from layer II of the entorhinal cortex. *The Journal of Neuroscience*, *27*(46), 12440-12451.
- O'Dell, T., Connor, S., Gelinias, J., & Nguyen, P. (2010). Viagra for your synapses: Enhancement of hippocampal long-term potentiation by activation of beta-adrenergic receptors. *Cellular Signalling*, *22*(5), 728-736.
- O'Dell, T., Connor, S., Guglietta, R., & Nguyen, P. (2015).  $\beta$ -Adrenergic receptor signaling and modulation of long-term potentiation in the mammalian hippocampus. *Learning & Memory*, *22*(9), 461-471.
- Oitzl, M. S., de Kloet, E. R., Joëls, M., Schmid, W., & Cole, T. J. (1997). Spatial learning deficits in mice with a targeted glucocorticoid receptor gene disruption. *European Journal of Neuroscience*, *9*(11), 2284-2296.

- O'Keefe, J., & Nadel, L. (Eds.). (1978). *The hippocampus as a cognitive map*. New York: Oxford University Press.
- O'Keefe, J., & Recce, M. L. (1993). Phase relationship between hippocampal place units and the EEG theta rhythm. *Hippocampus*, 3(3), 317-330.
- O'Keefe, J. (1976). Place units in the hippocampus of the freely moving rat. *Experimental Neurology*, 51(1), 78-109.
- O'Keefe, J., & Dostrovsky, J. (1971). The hippocampus as a spatial map. preliminary evidence from unit activity in the freely-moving rat. *Brain Research*, 34(1), 171-175.
- O'Keefe, J., & Burgess, N. (1996). Geometric determinants of the place fields of hippocampal neurons. *Nature*, 381(6581), 425-428.
- O'Keefe, J., & Burgess, N. (2005). Dual phase and rate coding in hippocampal place cells: Theoretical significance and relationship to entorhinal grid cells. *Hippocampus*, 15(7), 853-866.
- Olijslagers, J. E., de Kloet, E. R., Elgersma, Y., van Woerden, G. M., Joëls, M., & Karst, H. (2008). Rapid changes in hippocampal CA1 pyramidal cell function via pre- as well as postsynaptic membrane mineralocorticoid receptors. *European Journal of Neuroscience*, 27(10), 2542-50.
- O'Reilly, R. C., & McClelland, J. L. (1994). Hippocampal conjunctive encoding, storage, and recall: Avoiding a trade-off. *Hippocampus*, 4(6), 661-682.
- Otto, C., Reichardt, H. M., & Schütz, G. (1997). Absence of glucocorticoid receptor-beta in mice. *Journal of Biological Chemistry*, 272(42), 26665-26668.
- Papay, R., Gaivin, R., Jha, A., McCune, D., McGrath, J., Rodrigo, M., et al. (2006). Localization of the mouse alpha1A-adrenergic receptor (AR) in the brain: Alpha1AAR is expressed in neurons, GABAergic interneurons, and NG2 oligodendrocyte progenitors. *Journal of Comparative Neurology*, 497(2), 209-222.
- Paré, D., deCurtis, M., & Llinás, R. (1992). Role of the hippocampal-entorhinal loop in temporal lobe epilepsy: Extra- and intracellular study in the isolated guinea pig brain in vitro. *The Journal of Neuroscience*, 12(5), 1867-1881.
- Park, C R Campbell, A M Diamond, D M. (2001). Chronic psychosocial stress impairs learning and memory and increases sensitivity to yohimbine in adult rats. *Biological Psychiatry*, 50(12), 994-1004.

- Parkinson, J. K., Murray, E. A., & Mishkin, M. (1988). A selective mnemonic role for the hippocampus in monkeys: Memory for the location of objects. *The Journal of Neuroscience*, *8*(11), 4159-4167.
- Parron, C. S., Etienne. (2004). Evidence for entorhinal and parietal cortices involvement in path integration in the rat. *Experimental Brain Research*, *159*(3), 349-359.
- Pastoll, Hugh Ramsden, Helen Nolan, Matthew. (2012). Intrinsic electrophysiological properties of entorhinal cortex stellate cells and their contribution to grid cell firing fields. *Frontiers in Neural Circuits*, *6*, 17-17.
- Pastoll, Hugh Solanka, Lukas van Rossum, Mark C W Nolan, Matthew. (2013). Feedback inhibition enables  $\theta$ -nested  $\gamma$  oscillations and grid firing fields. *Neuron*, *77*(1), 141-154.
- Pavlidis, C., Kimura, A., Magariños, A. M., & McEwen, B. S. (1995). Hippocampal homosynaptic long-term depression/depotentiation induced by adrenal steroids. *Neuroscience*, *68*(2), 379-385.
- Pavlidis, C., Ogawa, S., Kimura, A., & McEwen, B. S. (1996). Role of adrenal steroid mineralocorticoid and glucocorticoid receptors in long-term potentiation in the CA1 field of hippocampal slices. *Brain Research*, *738*(2), 229-235.
- Pavlopoulos, Elias Jones, Sidonie Kosmidis, Stylianos Close, Maggie Kim, Carla Kovalerchik, Olga Small, Scott Kandel, Eric. (2013). Molecular mechanism for age-related memory loss: The histone-binding protein RbAp48. *Science Translational Medicine*, *5*(200), 200ra115-200ra115.
- Pawlak, R., Rao, B. S. S., Melchor, J., Chattarji, S., McEwen, B., & Strickland, S. (2005). Tissue plasminogen activator and plasminogen mediate stress-induced decline of neuronal and cognitive functions in the mouse hippocampus. *Proceedings of the National Academy of Sciences of the United States of America*, *102*(50), 18201-18206.
- Pham, K., Nacher, J., Hof, P., & McEwen, B. (2003). Repeated restraint stress suppresses neurogenesis and induces biphasic PSA-NCAM expression in the adult rat dentate gyrus. *European Journal of Neuroscience*, *17*(4), 879-886.
- Pralong, E., & Magistretti, P. J. (1994). Noradrenaline reduces synaptic responses in normal and tottering mouse entorhinal cortex via alpha 2 receptors. *Neuroscience Letters*, *179*(1-2), 145-148.

- Pralong, E., & Magistretti, P. J. (1995). Noradrenaline increases K-conductance and reduces glutamatergic transmission in the mouse entorhinal cortex by activation of alpha 2-adrenoreceptors. *European Journal of Neuroscience*, 7(12), 2370-2378.
- Przybylski, J., Roulet, P., & Sara, S. J. (1999). Attenuation of emotional and nonemotional memories after their reactivation: Role of beta adrenergic receptors. *The Journal of Neuroscience*, 19(15), 6623-6628.
- Raisman, G. (1966). The connexions of the septum. *Brain*, 89(2), 317-348.
- Rajkowska, G., & Miguel Hidalgo, J. J. (2007). Gliogenesis and glial pathology in depression. *CNS & Neurological Disorders Drug Targets*, 6(3), 219-233.
- Rawlins, J. N., Feldon, J., & Gray, J. A. (1979). Septo-hippocampal connections and the hippocampal theta rhythm. *Experimental Brain Research*, 37(1), 49-63.
- Ray, Saikat Naumann, Robert Burgalossi, Andrea Tang, Qiusong Schmidt, Helene Brecht, Michael. (2014). Grid-layout and theta-modulation of layer 2 pyramidal neurons in medial entorhinal cortex. *Science*, 343(6173), 891-896.
- Reul, J. M., de Kloet, E. R., van Sluijs, F. J., Rijnberk, A., & Rothuizen, J. (1990). Binding characteristics of mineralocorticoid and glucocorticoid receptors in dog brain and pituitary. *Endocrinology*, 127(2), 907-915.
- Reul, J. M., & de Kloet, E. R. (1985). Two receptor systems for corticosterone in rat brain: Microdistribution and differential occupation. *Endocrinology*, 117(6), 2505-2511.
- Rolls, E., & Kesner, R. (2006). A computational theory of hippocampal function, and empirical tests of the theory. *Progress in Neurobiology*, 79(1), 1-48.
- Roosendaal, B., McEwen, B., & Chattarji, S. (2009). Stress, memory and the amygdala. *Nature Reviews Neuroscience*, 10(6), 423-433.
- Roosendaal, B., & McGaugh, J. (2011). Memory modulation. *Behavioral Neuroscience*, 125(6), 797-824.
- Roszkowski, M., Manuella, F., von Ziegler, L., Durán Pacheco, G., Moreau, J., Mansuy, I., et al. (2016). Rapid stress-induced transcriptomic changes in the brain depend on beta-adrenergic signaling. *Neuropharmacology*, 107, 329-338.

- Rutecki, P. A., Grossman, R. G., Armstrong, D., & Irish Loewen, S. (1989). Electrophysiological connections between the hippocampus and entorhinal cortex in patients with complex partial seizures. *Journal of Neurosurgery*, 70(5), 667-675.
- Sandi, C., Davies, H., Cordero, M. I., Rodriguez, J., Popov, V., & Stewart, M. (2003). Rapid reversal of stress induced loss of synapses in CA3 of rat hippocampus following water maze training. *European Journal of Neuroscience*, 17(11), 2447-2456.
- Sandi, C., & Pinelo Nava, M. T. (2007). Stress and memory: Behavioral effects and neurobiological mechanisms. *Neural Plasticity*, 2007, 78970-78970.
- Sandi, C., Woodson, J., Haynes, V., Park, C., Touyarot, K., Lopez Fernandez, M., et al. (2005). Acute stress-induced impairment of spatial memory is associated with decreased expression of neural cell adhesion molecule in the hippocampus and prefrontal cortex. *Biological Psychiatry*, 57(8), 856-864.
- Sandi, C. (2004). Stress, cognitive impairment and cell adhesion molecules. *Nature Reviews Neuroscience*, 5(12), 917-930.
- Sara, S. J., Roullet, P., & Przybyslawski, J. (1999). Consolidation of memory for odor-reward association: Beta-adrenergic receptor involvement in the late phase. *Learning & Memory*, 6(2), 88-96.
- Sara, S. J., & Devauges, V. (1989). Idazoxan, an alpha-2 antagonist, facilitates memory retrieval in the rat. *Behavioral and Neural Biology*, 51(3), 401-411.
- Sargolini, Francesca Fyhn, Marianne Hafting, Torkel McNaughton, Bruce Witter, Menno Moser, May-Britt Moser, Edvard. (2006). Conjunctive representation of position, direction, and velocity in entorhinal cortex. *Science*, 312(5774), 758-762.
- Scanziani, M., Gähwiler, B. H., & Thompson, S. M. (1993). Presynaptic inhibition of excitatory synaptic transmission mediated by alpha adrenergic receptors in area CA3 of the rat hippocampus in vitro. *The Journal of Neuroscience*, 13(12), 5393-5401.
- Schwartz, S. P., & Coleman, P. D. (1981). Neurons of origin of the perforant path. *Experimental Neurology*, 74(1), 305-312.
- SCOVILLE, W. B., & MILNER, B. (1957). Loss of recent memory after bilateral hippocampal lesions. *Journal of Neurology, Neurosurgery and Psychiatry*, 20(1), 11-21.

- Seckl, J. R., & Walker, B. R. (2001). Minireview: 11beta-hydroxysteroid dehydrogenase type 1- a tissue-specific amplifier of glucocorticoid action. *Endocrinology*, *142*(4), 1371-1376.
- Seckl, J. R. (1993). 11 beta-hydroxysteroid dehydrogenase isoforms and their implications for blood pressure regulation. *European Journal of Clinical Investigation*, *23*(10), 589-601.
- Sharma, Sunita Rakoczy, Sharlene Brown Borg, Holly. (2010). Assessment of spatial memory in mice. *Life Sciences*, *87*(17-18), 521-536.
- Shors, T J Thompson, R F. (1992). Acute stress impairs (or induces) synaptic long-term potentiation (LTP) but does not affect paired-pulse facilitation in the stratum radiatum of rat hippocampus. *Synapse*, *11*(3), 262-265.
- Sirviö, J., & MacDonald, E. (1999). Central alpha1-adrenoceptors: Their role in the modulation of attention and memory formation. *Pharmacology & Therapeutics*, *83*(1), 49-65.
- Smith, M. L., & Milner, B. (1981). The role of the right hippocampus in the recall of spatial location. *Neuropsychologia*, *19*(6), 781-793.
- Solstad, Trygve Boccara, Charlotte Kropff, Emilio Moser, May-Britt Moser, Edvard. (2008). Representation of geometric borders in the entorhinal cortex. *Science*, *322*(5909), 1865-1868.
- Soriano, E., Martinez, A., Farinas, I., & Frotscher, M. (1993). Chandelier cells in the hippocampal formation of the rat: The entorhinal area and subicular complex. *Journal of Comparative Neurology*, *337*(1), 151-167.
- Sousa, N., Lukoyanov, N. V., Madeira, M. D., Almeida, O. F., & Paula Barbosa, M. M. (2000). Reorganization of the morphology of hippocampal neurites and synapses after stress-induced damage correlates with behavioral improvement. *Neuroscience*, *97*(2), 253-266.
- Squire, L., Stark, C. E. L., & Clark, R. (2004). The medial temporal lobe. *Annual Review of Neuroscience*, *27*, 279-306.
- Stanton, P. K., Jones, R. S., Mody, I., & Heinemann, U. (1987). Epileptiform activity induced by lowering extracellular [Mg<sup>2+</sup>] in combined hippocampal-entorhinal cortex slices: Modulation by receptors for norepinephrine and N-methyl-D-aspartate. *Epilepsy Research*, *1*(1), 53-62.
- Steffenach, Hill-Aina Witter, Menno Moser, May-Britt Moser, Edvard. (2005). Spatial memory in the rat requires the dorsolateral band of the entorhinal cortex. *Neuron*, *45*(2), 301-313.

- Steinvorth, S., Wang, C., Ulbert, I., Schomer, D., & Halgren, E. (2010). Human entorhinal gamma and theta oscillations selective for remote autobiographical memory. *Hippocampus*, *20*(1), 166-173.
- Stensola, H., Stensola, T., Solstad, T., Frøland, K., Moser, M., & Moser, E. (2012). The entorhinal grid map is discretized. *Nature*, *492*(7427), 72-78.
- Steward, O., & Scoville, S. A. (1976). Cells of origin of entorhinal cortical afferents to the hippocampus and fascia dentata of the rat. *Journal of Comparative Neurology*, *169*(3), 347-370.
- Steward, O. (1976). Topographic organization of the projections from the entorhinal area to the hippocampal formation of the rat. *Journal of Comparative Neurology*, *167*(3), 285-314.
- Strosberg, A. D. (1993). Structure, function, and regulation of adrenergic receptors. *Protein Science*, *2*(8), 1198-1209.
- Sugawara, T., Hirasawa, A., Hashimoto, K., & Tsujimoto, G. (2002). Differences in the subcellular localization of alpha1-adrenoceptor subtypes can affect the subtype selectivity of drugs in a study with the fluorescent ligand BODIPY FL-prazosin. *Life Sciences*, *70*(18), 2113-2124.
- Suh, J., Rivest, A., Nakashiba, T., Tominaga, T., & Tonegawa, S. (2011). Entorhinal cortex layer III input to the hippocampus is crucial for temporal association memory. *Science*, *334*(6061), 1415-1420.
- Sunanda, M. S., Rao, T. R., & Raju. (1995). Effect of chronic restraint stress on dendritic spines and excrescences of hippocampal CA3 pyramidal neurons--a quantitative study. *Brain Research*, *694*(1-2), 312-317.
- Swanson Park, J. L., Coussens, C. M., Mason Parker, S. E., Raymond, C. R., Hargreaves, E. L., Dragunow, M., et al. (1999). A double dissociation within the hippocampus of dopamine D1/D5 receptor and beta-adrenergic receptor contributions to the persistence of long-term potentiation. *Neuroscience*, *92*(2), 485-497.
- Swanson, L. W., & Cowan, W. M. (1979). The connections of the septal region in the rat. *Journal of Comparative Neurology*, *186*(4), 621-655.
- Tang, Q., Burgalossi, A., Ebbesen, C., Ray, S., Naumann, R., Schmidt, H., et al. (2014). Pyramidal and stellate cell specificity of grid and border representations in layer 2 of medial entorhinal cortex. *Neuron*, *84*(6), 1191-1197.

- Tank, A. W., & Lee Wong, D. (2015). Peripheral and central effects of circulating catecholamines. *Compr Physiol*, 5(1), 1-15.
- Taube, J S Muller, R U Ranck, J B. (1990). Head-direction cells recorded from the postsubiculum in freely moving rats. II. effects of environmental manipulations. *The Journal of Neuroscience*, 10(2), 436-447.
- Taube, J. S., Muller, R. U., & Ranck, J. B. (1990). Head-direction cells recorded from the postsubiculum in freely moving rats. I. description and quantitative analysis. *The Journal of Neuroscience*, 10(2), 420-435.
- Taube, J. S. (1995). Head direction cells recorded in the anterior thalamic nuclei of freely moving rats. *The Journal of Neuroscience*, 15(1), 70-86.
- Timmermans, W., Xiong, H., Hoogenraad, C. C., & Krugers, H. J. (2013). Stress and excitatory synapses: From health to disease. *Neuroscience*, 248, 626-636.
- Torkaman Boutorabi, A., Danyali, F., Oryan, S., Ebrahimi Ghiri, M., & Zarrindast, M. (2014). Hippocampal  $\alpha$ -adrenoceptors involve in the effect of histamine on spatial learning. *Physiology & Behavior*, 129, 17-24.
- Tsigos, C., & Chrousos, G. (2002). Hypothalamic-pituitary-adrenal axis, neuroendocrine factors and stress. *Journal of Psychosomatic Research*, 53(4), 865-871.
- Tsujimoto, G., Hirasawa, A., Sugawara, T., & Awaji, T. (1998). Subtype-specific differences in subcellular localization and chlorethylclonidine inactivation of  $\alpha$ 1-adrenoceptors. *Life Sciences*, 62(17-18), 1567-1571.
- Tukker, J., Fuentealba, P., Hartwich, K., Somogyi, P., & Klausberger, T. (2007). Cell type-specific tuning of hippocampal interneuron firing during gamma oscillations in vivo. *The Journal of Neuroscience*, 27(31), 8184-8189.
- Ulrich Lai, Y., & Herman, J. (2009). Neural regulation of endocrine and autonomic stress responses. *Nature Reviews Neuroscience*, 10(6), 397-409.
- Unnerstall, J. R., Fernandez, I., & Orensanz, L. M. (1985). The  $\alpha$ -adrenergic receptor: Radiohistochemical analysis of functional characteristics and biochemical differences. *Pharmacology, Biochemistry and Behavior*, 22(5), 859-874.
- Unnerstall, J. R., Kopajtic, T. A., & Kuhar, M. J. (1984). Distribution of  $\alpha$  2 agonist binding sites in the rat and human central nervous system: Analysis of some functional, anatomic correlates of the pharmacologic effects of clonidine and related adrenergic agents. *Brain Research*, 319(1), 69-101.

- van Haeften, T., Wouterlood, F. G., & Witter, M. P. (2000). Presubicular input to the dendrites of layer-V entorhinal neurons in the rat. *Annals of the New York Academy of Sciences*, 911, 471-473.
- Van Hoesen, G. W., Hyman, B. T., & Damasio, A. R. (1991). Entorhinal cortex pathology in alzheimer's disease. *Hippocampus*, 1(1), 1-8.
- van Stegeren, A., Roozendaal, B., Kindt, M., Wolf, O., & Joëls, M. (2010). Interacting noradrenergic and corticosteroid systems shift human brain activation patterns during encoding. *Neurobiology of Learning and Memory*, 93(1), 56-65.
- Varga, Csaba Lee, Soo Soltesz, Ivan. (2010). Target-selective GABAergic control of entorhinal cortex output. *Nature Neuroscience*, 13(7), 822-824.
- Veldhuis, H. D., Van Koppen, C., Van Ittersum, M., & De Kloet, E. R. (1982). Specificity of the adrenal steroid receptor system in rat hippocampus. *Endocrinology*, 110(6), 2044-2051.
- Venero, C., Tilling, T., Hermans Borgmeyer, I., Schmidt, R., Schachner, M., & Sandi, C. (2002). Chronic stress induces opposite changes in the mRNA expression of the cell adhesion molecules NCAM and L1. *Neuroscience*, 115(4), 1211-1219.
- Venero, C., & Borrell, J. (1999). Rapid glucocorticoid effects on excitatory amino acid levels in the hippocampus: A microdialysis study in freely moving rats. *European Journal of Neuroscience*, 11(7), 2465-2473.
- Vyas, A., Pillai, A. G., & Chattarji, S. (2004). Recovery after chronic stress fails to reverse amygdaloid neuronal hypertrophy and enhanced anxiety-like behavior. *Neuroscience*, 128(4), 667-673.
- Watanabe, Y., Gould, E., & McEwen, B. S. (1992). Stress induces atrophy of apical dendrites of hippocampal CA3 pyramidal neurons. *Brain Research*, 588(2), 341-345.
- WEIL MALHERBE, H., & BONE, A. D. (1957). Intracellular distribution of catecholamines in the brain. *Nature*, 180(4594), 1050-1051.
- Wichmann, R., Fornari, R., & Roozendaal, B. (2012). Glucocorticoids interact with the noradrenergic arousal system in the nucleus accumbens shell to enhance memory consolidation of both appetitive and aversive taste learning. *Neurobiology of Learning and Memory*, 98(2), 197-205.

- Wiegert, O., Joëls, M., & Krugers, H. (2006). Timing is essential for rapid effects of corticosterone on synaptic potentiation in the mouse hippocampus. *Learning & Memory, 13*(2), 110-3.
- Winson, J. (1978). Loss of hippocampal theta rhythm results in spatial memory deficit in the rat. *Science, 201*(4351), 160-163.
- Witter, M. P., Naber, P. A., van Haeften, T., Machielsen, W. C., Rombouts, S. A., Barkhof, F., et al. (2000). Cortico-hippocampal communication by way of parallel parahippocampal-subicular pathways. *Hippocampus, 10*(4), 398-410.
- Witter, M. P., Wouterlood, F. G., Naber, P. A., & Van Haeften, T. (2000). Anatomical organization of the parahippocampal-hippocampal network. *Annals of the New York Academy of Sciences, 911*, 1-24.
- Wong, T., Howland, J., Robillard, J., Ge, Y., Yu, W., Titterness, A., et al. (2007). Hippocampal long-term depression mediates acute stress-induced spatial memory retrieval impairment. *Proceedings of the National Academy of Sciences of the United States of America, 104*(27), 11471-11476.
- Woodson, J., Macintosh, D., Fleshner, M., & Diamond, D. (2003). Emotion-induced amnesia in rats: Working memory-specific impairment, corticosterone-memory correlation, and fear versus arousal effects on memory. *Learning & Memory, 10*(5), 326-336.
- Woolley, C. S., Gould, E., Frankfurt, M., & McEwen, B. S. (1990). Naturally occurring fluctuation in dendritic spine density on adult hippocampal pyramidal neurons. *The Journal of Neuroscience, 10*(12), 4035-4039.
- Wouterlood, F. G., Härtig, W., Brückner, G., & Witter, M. P. (1995). Parvalbumin-immunoreactive neurons in the entorhinal cortex of the rat: Localization, morphology, connectivity and ultrastructure. *Journal of Neurocytology, 24*(2), 135-153.
- Xiao, Z., Deng, P., Rojanathammanee, L., Yang, C., Grisanti, L., Permpoonputtana, K., et al. (2009). Noradrenergic depression of neuronal excitability in the entorhinal cortex via activation of TREK-2 K<sup>+</sup> channels. *Journal of Biological Chemistry, 284*(16), 10980-10991.
- Yang, C., Huang, C., & Hsu, K. (2005). Behavioral stress enhances hippocampal CA1 long-term depression through the blockade of the glutamate uptake. *The Journal of Neuroscience, 25*(17), 4288-4293.
- Yaniv, S., Lucki, A., Klein, E., & Ben Shachar, D. (2010). Dexamethasone enhances the norepinephrine-induced ERK/MAPK intracellular pathway possibly via dysregulation of the alpha2-adrenergic receptor: Implications for

antidepressant drug mechanism of action. *European Journal of Cell Biology*, 89(9), 712-722.

Yartsev, M., Witter, M., & Ulanovsky, N. (2011). Grid cells without theta oscillations in the entorhinal cortex of bats. *Nature*, 479(7371), 103-107.

Zha, Q., Wang, Y., Fan, Y., & Zhu, M. (2011). Dexamethasone-induced up-regulation of the human norepinephrine transporter involves the glucocorticoid receptor and increased binding of C/EBP- $\beta$  to the proximal promoter of norepinephrine transporter. *Journal of Neurochemistry*, 119(3), 654-663.

## **BIOGRAPHY**

Jeremiah Hartner was born April 15, 1985 in Grosse Pointe, MI to Gary and Claudia Hartner. He is the youngest of three children. He graduated from L'Anse Creuse High School North in 2003. Jeremiah received his Bachelor of Science in Neuroscience from the University of Michigan in 2007. After working for four years as an intraoperative neuromonitoring clinician in Ann Arbor, MI he joined the Graduate Neuroscience Program at Tulane University in 2011. Under the direction of Dr. Laura Schrader, his doctoral research focused on synaptic signaling changes in the medial entorhinal cortex in response to stress hormones. After graduation he plans to move back to Ann Arbor, MI to raise a family of hockey players.